University of Sunderland

Adejokun, Deborah (2021) Design of a novel anti-cellulite treatment, an evidence based approach. Doctoral thesis, University of Sunderland.

DESIGN OF A NOVEL ANTI-CELLULITE TREATMENT - AN EVIDENCE BASED APPROACH.

DEBORAH ADEFUNKE ADEJOKUN

A Thesis Submitted in Partial Fulfilment of the

Requirements of the University of Sunderland for the

Degree of

Doctor of Philosophy in Cosmetic Science.

March 2022

Director of Study: Dr Kalliopi Dodou

ABSTRACT

Cellulite is an aesthetic defect on the skin of the buttocks and upper thighs. It affects 80-90% of women & it can influence their quality of life. There are no treatments for cellulite however there are various interventions that claim to be effective.

The purpose of this research was: (a) to conduct a user-trial investigating the most effective treatment of cellulite among 3 non-invasive interventions (dry brushing, exercise and cream); (b) the evidence-based design of a novel topical anti-cellulite cream using active-containing nanocarriers; and (c) the *in vitro* and *in vivo* evaluation of the safety and efficacy of the novel anti-cellulite cream.

The user trial was conducted in 9 volunteers as part of the BBC1 study "The truth about looking good". Photonumeric evaluation before & after five weeks of intervention showed a total average improvement of 25.8% in the dry brushing group, 12.7% in exercise and 14.7% in the cream group. It was therefore concluded that for the short-term treatment of cellulite, dry brushing was the most effective amongst the 3 interventions.

Four 100g each oil-in-water creams and their controls (without active) were formulated; the first, labelled model I (1:1 of jojoba and baobab oil) contained a water phase of 80%w/w, oil phase (10%w/w), emulsifier (5%w/w) and active (5%w/w) while the remaining three had an equal % composition of water phase (78%w/w), oil phase (12%w/w), emulsifier (5%w/w) and active (5%w/w), labelled II (1:1 of jojoba and baobab oil), III (1:1 of jojoba and coconut oil) and IV (1:1 of baobab and coconut oil). Short-term stability studies on the creams were performed after 8, 14 and 28 days, under three different storage temperature conditions (4°C, 25°C and 40°C) and at ambient relative humidity.

Quantitative sensory evaluation was performed in three stages; (a) Pick-up – compression/spreadability and stringiness/stretchability (b) Rub-out – spreadability (c) Appearance – skin hydration and viscosity/opaqueness using an original method to directly determine the refractive index. A novel protocol was developed for the correlation of the rheological measurements with the sensorial properties of semisolid formulations. The microbial challenge results revealed the creams were capable of inhibiting bacterial, yeast and fungal growth. The phase separation resistance, pH, microscopic size analysis, globule size and surface charge, suggests that creams containing jojoba with baobab oil may have good shelf-life, especially with samples stored at room temperature, over the period of measurement.

A new method was devised for the long-term stability of the creams using Dynamic Vapour Sorption (DVS), which demonstrated that creams with jojoba/baobab oil combinations showed good long-term stability compared to creams containing jojoba with coconut oil, and baobab with coconut oil. This observation was in agreement with the results from the short-term stability studies. Preliminary blind user-trial studies on 12 volunteers were promising; the active-containing cream was

compared against its control and a popular commercial anti-cellulite cream. The best product in terms of quality and efficacy, chosen by the volunteers, was the novel active-containing anti-cellulite cream.

ACKNOWLEDGEMENT

CONTENTS

LIST OF FIGURES AND TABLES

LIST OF ABBREVIATIONS

BMI   Body Mass Index

BF   Body Fat

Kg   Kilograms

lbs   Pounds

cm   Centimetres

m   Metres

mm   Millimetres

PN   Photo-numeric

R0   Skin Firmness

R2   Gross Elasticity

R3   Maximum Amplitude of Final Curve

R5   Net Elasticity

R7   Elastic Portion

R9   Fatique

Uf   Complete Elastic Curve

Ua   Relaxation Distance

Ur   Elastic Portion of the Suction Phase

Ue   Elastic Portion of the Relaxation Phase

SE$_R$ Skin Evaluation Roughness

SE$_{sm}$ Skin Evaluation Smoothness

SE$_w$ Skin Evaluation Wrinkles

SE$_{sc}$ Skin Evaluation Scaliness/Desquamation

Linf   Number of Pixels

Fax   Average Number of Horizontal wrinkles

Fay   Average Number of vertical wrinkles

Co-Cu   Average Width of Histogram

Fmx   Average Width of Horizontal wrinkles

Fmy   Average Width of Vertical wrinkles

RH   Relative Humidity

DVS   Dynamic Vapour Sorption

RI   Refractive Index

UV   Ultraviolent

λ   Wavelength

CHAPTER 1
INTRODUCTION

1.1. THE HUMAN INTEGUMENTARY SYSTEM (SKIN)

The human skin is a vital as well as the largest single organ of the body [1]. The skin consists of different layers, Figure 1.1, performing several complex functions; It serves to protect against micro-organisms, chemicals and radiations, variations in temperature, and mechanical forces by acting as a barrier [2]. It also acts as a regulatory organ, regulating body temperature through hair and sweat, changes in peripheral microvascular circulation and fluid equilibrium through sweat, and serve as a depot for Vitamin D synthesis [3]. The skin is made up of sensory cells, making it serve as an organ of sensation, detecting changes in the environment (i.e. temperature, itching, pressure, pain and touch) by transmitting information through free nerve endings to the brain, as electrical impulses. Sometimes, damages to these cells occur resulting in a loss of feeling or sensation, a condition known as Neuropathy, here, patients are at an increased risk of acute wounding [4][5][6].

1.2. STRUCTURE OF THE INTEGUMENT

The integumentary system has a total surface area of 2 square meters in adults and weighs about 5Kg, it is made up of two main layers varying in thickness from each region of the body (from 0.5mm on the back - 4.0mm on the soles of the feet and palm of the hand) [7]: The epidermis (outer) layer – Its surface consists of irregular characters that creates a unique pattern in every individual, specifically on the fingers, producing exclusive fingerprints for individual identification. The dermis (deep) layer – There is a sharp boundary between the dermis and epidermis, divided by epidermal ridges. However, the fibrous connective tissue of the dermis is intertwined with the beneath hypodermis or subcutis (loose connective tissue) [7][8]. The structure of the skin is similar to most organs, having an epithelium that lies directly above a layer of connective tissue, containing blood and lymph vessels, nerve endings, wondering cells for fighting infections, and probably glandular tissues [9].
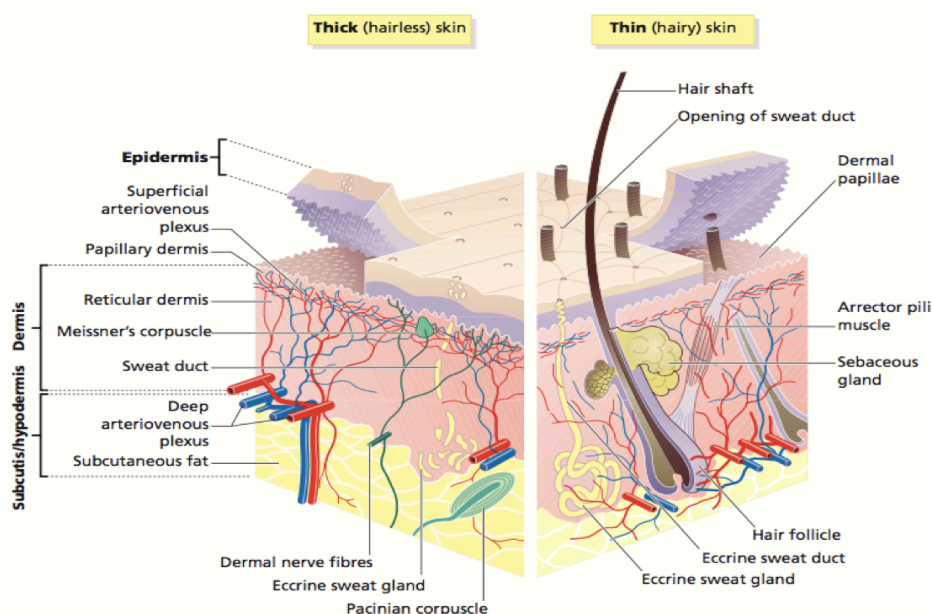
Figure 1.1. A 3-Dimensional Structure of the Human Skin with a Hair Follicle [10].

1.2.1. EPIDERMIS

The epithelial layer of the integument, Figure 1.2, is made up of five different layers (depending on the region of the body), they include stratum germinativum (basale), stratum spinosum, stratum granulosum, stratum lucidum, and stratum corneum [11]. These layers are a representation of cells in various phases of keratinization, a process by which the outer epidermal cells die, and their cytoplasm is replaced by keratin [12].
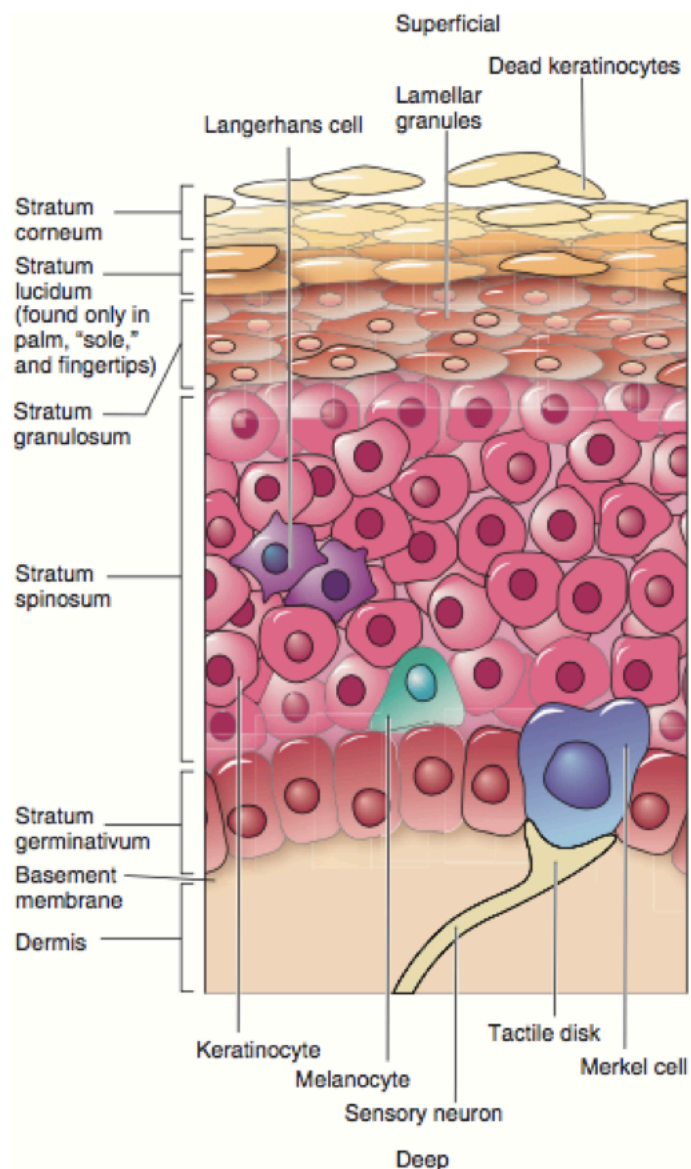
Figure 1.2. The Structure of the Epidermis and its Layers [13].

1.2.1.1. STRATUM GERMINATIVUM (BASALE)

The stratum germinativum is the deepest layer of the epidermis, consisting of a single layer of cells arranged in columns which are connected to the dermis layer beneath, through the tonofibrils in their cytoplasm, passing towards the basement membrane [14][15]. Here, cells (melanocytes) are

12

responsible for the production of melanin, giving the skin its characteristic color. It is also responsible for the production of new cells (keratinocytes) which are constantly dividing and multiplying. The newly formed cells move to the stratum corneum to replace keratinized or desquamated cells [15]. Other cells of the stratum germinativum include the merkel cells, they are present in large amounts in touch sensitive sites (i.e. fingertips and lips) and are closely related to cutaneous nerves, explaining their involvement in light touch sensation [16].

1.2.1.2. STRATUM SPINOSUM

The stratum spinosum consists of many layers of polyhedral cells having exquisite interlocking "spines" projecting from their surface, which helps prevent surface bacteria from entering as well as providing support to the layer [17]. Inside the cells of the stratum spinosum is the synthesis of active protein, indicating the generation of new cells through constant cell division and growth. Some newly formed cells move to replace desquamated cells on the surface [17][18].

1.2.1.3. STRATUM GRANULOSUM

Stratum granulosum (granular layer) consists of 3 to 5 rows of layered non-dividing, flattened keratinocytes (keratinocytes that migrated from layers below), containing tonofibrils, lamellar granules and granular protein called keratinohyalin - helps organises keratin into thicker bundles [19]. Lamellar granules releases lipid-rich secretion into spaces between cells, acting as a sealant to slow body fluid loss. As keratinocytes continue to produce keratinohyalin and loose cell components, they begin to change in structure (becoming flatter and thinner with thicker cell membranes that prevents skin permeability to water), providing protection against pathogens [13][20].

1.2.1.4. STRATUM LUCIDUM

The stratum lucidum is immediately below the stratum corneum. It is made up of flat, translucent layers of dead cells containing a protein called eleidin. This layer helps provide protection against the ultraviolet (UV) radiation of the sun. The stratum granulosum and stratum lucidum are well defined in the palms and soles region of the skin [21].

1.2.1.5. STRATUM CORNEUM

The stratum corneum (also called horny layer) is the outermost layer of the epidermis, possessing a dynamic structure with cells migrating from the deep layers of the epidermis to the surface direction as they mature, this takes a period of 1 to 2 weeks. Stratum corneum, SC is made up 15 layers of corneocytes (depending on the region), it takes about a day to form a single layer, and 15 days for the complete renewal of the SC [22].

The transition of granular cells to corneocytes represents a late stage of epidermal differentiation. These cells of the SC are embedded in a multilamellar, lipid-rich extracellular matrix. Each corneocyte is enveloped by a 10nm thick peripheral protein, known as the cornified envelope

(made up of structural proteins i.e. involucrin and loricrin) - having an interior surface that is connected to bundles of keratin fibres, helping to fill the intracellular space of the corneocytes, and an exterior surface covalently linked to omega-hydroxyceramides, called the corneocyte lipid-bound envelope [23]. This complex, multiple layers of the corneocytes of SC allows it to function as a critical protective barrier, preventing excess water loss and protection against antigens [24].

1.2.2. DERMIS

The dermis (also called corium or true skin) is mainly composed of tough, irregular, flexible connective tissue that includes collagen and elastin fibers, Figure 3. Other components of the dermis include lymphatic vessels, nerve endings, hair follicles, sebaceous glands, sweat glands, and numerous cells - fibroblasts, adipocytes and macrophages [25][26]. The dermis can be divided into the papillary - the outer layer is made up of loosely arranged fibers and expands into the epidermis to supply it with vessels. Papillary ridges constitute lines of the hands, providing us fingerprints; and reticular layer - is denser and extends into the subcutis. Its fibers are irregularly arranged and resists stretching [26].

1.2.2.1. PAPILLARY LAYER (STARTUM PAPILLAROSUM)

This superficial layer of the dermis is made up of a loosed network of collagen and elastin fibers, projecting into the stratum germinativum layer of the epidermis to form finger-like dermal papillae. The papillary layer consists of fibroblasts, small amounts of adipocytes, numerous tiny blood vessels, lymphatic drainage, nerve fibers and touch receptors (meissner corpuscles). The presence of phagocytes and other defensive cells in this layer prevents microorganisms from further breaching the skin [27].

1.2.2.2. RETICULAR LAYER (STRATUM RETICULAROSUM)

The reticular layer is the thicker and deeper layer of the dermis, consisting of denser and regularly arranged strong, flexible web of collagen and elastin fibers. Strands of collagen extends into the papillary region and the hypodermis. This layer has numerous sensory nerve supply and is extremely distensible, preventing the skin from being torn, which is apparent in pregnant women and obese individuals. Restoration of a constrained dermal region results in stretch marks [28][29][30].

1.2.2.3. COLLAGEN AND ELASTIN FIBERS

Collagen in the dermis is mainly produced by fibroblasts and makes up 95% of the human skin, together with the elastin fibers, they form a dense network of extracellular matrix throughout the layer. It contains several nonessential and essential amino acids, including proline (makes up 15% of collagen and serve to protect blood vessels), glycine (constitute one-third of collagen and ensures proper cell function), glutamine and arginine [31][32]. Fibroblasts are cells of the connective tissue responsible for the synthesis of collagen through two different mechanisms that induce fibroblast activation and proliferation - A chemical mechanism dependent on small ligands binding to their receptors on the

surface (lock and key); and a physical mechanism involving direct interaction of fibroblasts and collagen [32].

Collagen and elastin fibers are responsible for the structural strength, elasticity and firmness of the dermis, giving the skin its ability to resist deformation. Collagen fibres are arranged in many different directions, nevertheless, some are arranged in a few directions than others, resulting in cleavage or tension lines in the skin. Any incision made across or parallel to these lines produce damage or scar to the tissue. If the skin is overstrained, the structure of these fibers in dermis maybe disrupted, leaving lines that are apparent through the epidermis [33].
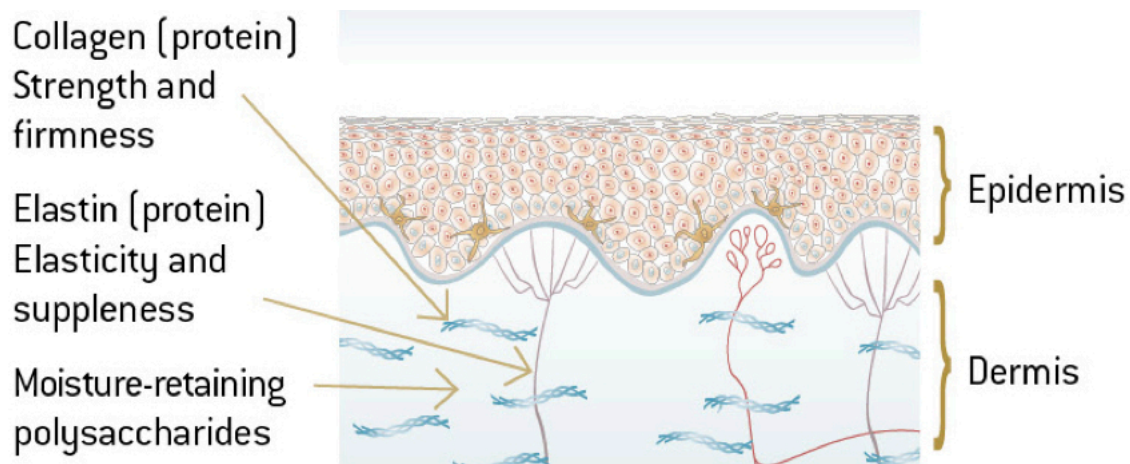
Figure 1.3. Structure of the Skin Revealing the Collagen and Elastin Fibers of the Dermis [34].

1.2.2.4. **AUXILIARIES OF THE DERMIS**

GLANDS

This includes sweat glands and sebaceous glands. Sweat or sudoriferous glands can be divided into two; (a) Eccrine glands - are small simple sweat glands widely distributed throughout the body except for the border of the lips, nail bed, eardrums, tip of the penis and the inner lips of the vulva. They are richly found in the soles, palms and fingers where they respond to psychological stress [35]. Eccrine glands have coiled secretory portions in the dermis but, straightens as it reaches the epidermis. They serve to secret sweat by a physiological process called perspiration, thereby, regulating body temperature when external temperature increases or during exercise by evaporation [36] (b) Apocrine or odiferous glands - they are larger and more deeply situated than the eccrine glands and are richly located under the arm, outer ear (as ceruminous glands), around the nipples (as mammary glands), the eyelid (as moll's glands), outer lip of the vulva, genital and anal regions [36][37]. Unlike the eccrine glands, they secret pheromones (often referred to as body odour), do not function before puberty onset and are not responsive to heat, rather they respond to stress during physical activities including sex. They serve to produce breast milk during pregnancy and lactation, ear wax to prevent substances from penetrating the inner ear [37].

Sebaceous or oil glands are ducts present throughout the body except for the palm and sole. They open into hair follicles, secreting sebum (by the breakdown of their interior cells) to provide heat insulation, inhibit the growth of bacteria and lubricate the skin and hair, preventing the skin from drying out [38][39]. The sebum secreted contains a mixture of squalene, cholesterol esters, free cholesterol and triglyceride. An increased sebum production is associated with the pathophysiology of acne, while a loss of function can result in scarring alopecia [39].

HAIR FOLLICLES

Hair follicles are referred to as a complex mini organ with many distinct cell populations which are unique depending on the region, protein expression and function. Its matured structure, Figure 1.4, consists of a dermal papilla with a fiber sheath and an epithelial portion with transient cells of the hair matrix enveloping the dermal papilla, a bulge at the insertion region of the arrestor pili muscle, a connected sebaceous gland, hair shaft, an outer root sheath which is a direct continuation of the epidermal layer and inner root sheath [40][41]. Hair follicles are a vital component of the skin, thick scalp hair function to provide protection against actinic damage, eyebrows, eyelashes, ears, nasal, anus and vagina hairs provide protection from the environment. They also play an important role in sensory activity and thermoregulation [42].
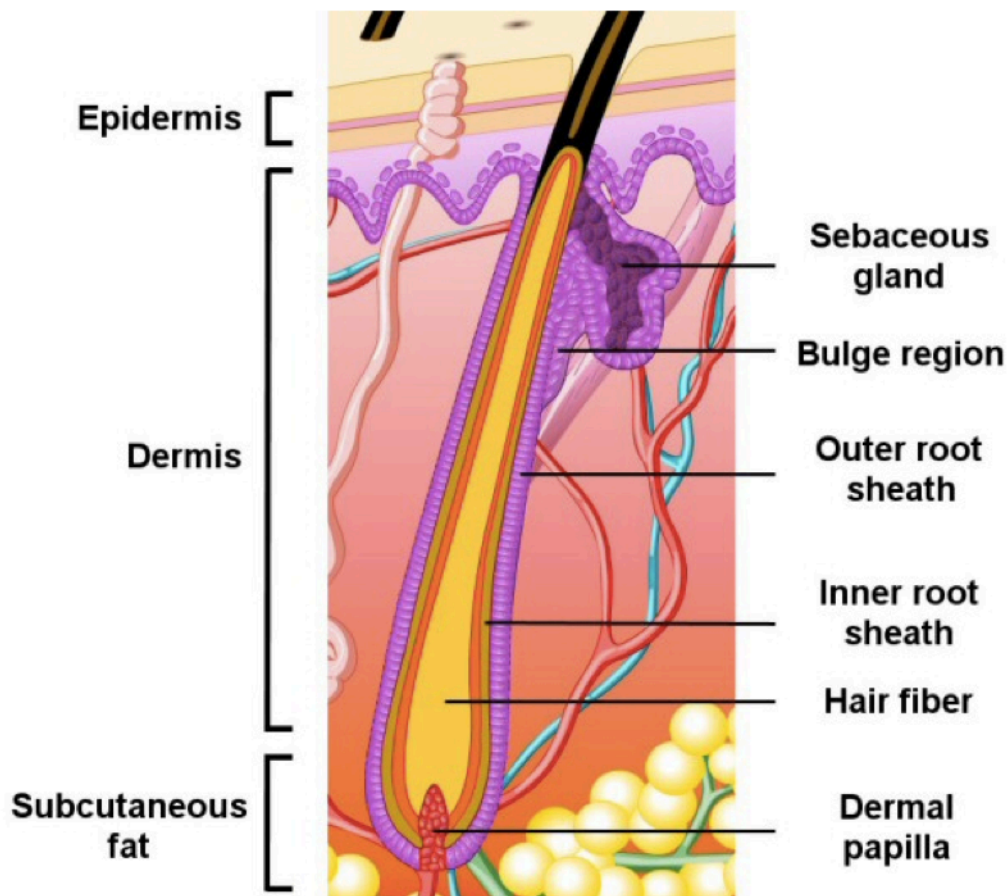
Figure 1.4. The Structure of a Hair Follicle [43].

16

BLOOD AND LYMPHATIC VESSELS

Blood and lymphatic (unidirectional) vessels transport defence cells, remove wastes, supply nutrients, such as oxygen and other substances throughout the cells of the dermis and the stratum germinativum of the epidermal layer - by a process called diffusion due to their lack of blood and lymphatic drainage system [44][45]. Blood vasculature is arranged from the bottom horizontal plexus to a superficial horizontal plexus with the appearance of capillaries in the latter one. The lymphatic drainage system is also organised in two plexuses surrounding that of the blood vessels. The lymphatic superficial plexus expands into the papillary layer of the dermis and plummet into large lymphatic vessels in the reticular layer [46]. Tiny small blood vessels are known as arterioles, having smooth muscle in their interior linen which allows them close (constrict) or open (dilate). Thereby serving a thermoregulatory function, as the blood carries heat in form of energy. In hot temperatures, the arterioles dilate, increasing blood flow through the dermis which releases heat to the external environment. While in cold temperatures, the arterioles constrict to conserve body heat, lowering blood flow in the dermis [47].

Blood and lymphatic vasculature respond to inflammatory mediators. Lymphatic drainages are unidirectional vessels, connected to the extracellular matrix (ECM) at one end through anchoring filaments, enabling them respond to changes in nearby interstitial fluid pressure and inflammation of the ECM due to edema move these filaments opening the inter endothelial junctions. If prolonged pressure is applied on the skin, lymphatic vessels in the dermis becomes damaged or "leaky" and its fluid leak out into surrounding tissues, this may result in lymphedema, adipose deposition and eventually, fibrosis [48].

NERVOUS SYSTEM

The dermis consists of an extensive network of autonomic nerve - controls blood flow and glandular secretion such as sweat; and sensory nerve fiber - containing free nerve endings or mechanoreceptors i.e. tactile, merkel, ruffini and lamellar corpuscles, and krause end bulbs for sensations (touch, pressure, pain, temperature, itching) [49]. Tactile corpuscles are found in some region of dermal papilla, they respond to light touch and have the highest level of sensitivity. Merkel corpuscles are found in the epidermal region and are responsive to touch. Ruffini and lamellar corpuscles are found throughout the dermal papilla and respond to vibration and pressure. While krause end bulbs respond to cold temperatures [50].

1.2.3.   HYPODERMIS (SUBCUTIS)

The Hypodermis, also called subcutaneous or subcutis or fat layer or superficial fascia, is composed of looser connective (areolar) and adipose tissue, connecting the dermis to the deep fascia i.e. envelopes of the muscle [51]. Although not classified as a skin layer, it is 4 to 9 mm thick and

provides cushion for the underlying organs against shocks and bumps, storage as well as insulating the body. It contains a vast network of nerves and vascular system. Subcutis adipose tissue varies in mass depending on the location (it is rare on the ears, eye lids, nose, clitoris and penis), age, sex and nutrition. Women have 8% thicker fat layer than their male counterparts [52][53].

The body has three main adipose deposition sites, two of which are superficial (in the skin) - the upper fat layer (superficial fascia) of the hypodermis anchoring the dermis, accommodates more fat tissue than other layers due to their ability to expand, causing cellulite appearance; deep fascia - this is the lower fat layer of the hypodermis that envelopes the muscle; and the subserous or visceral fascia - enveloping the internal organs, although not part of the hypodermis [54][55]. Adipose deposition and accumulation in the subcutis changes as the body mature, it is dependent on hormonal (i.e. oestrogen, testosterone, glucagon, insulin and leptin) and genetic factors. In women, fat is stored in the thighs, buttocks, hips and breast region of the skin. While in men, it is stored in the neck, arms, abdomen and lower back [56].
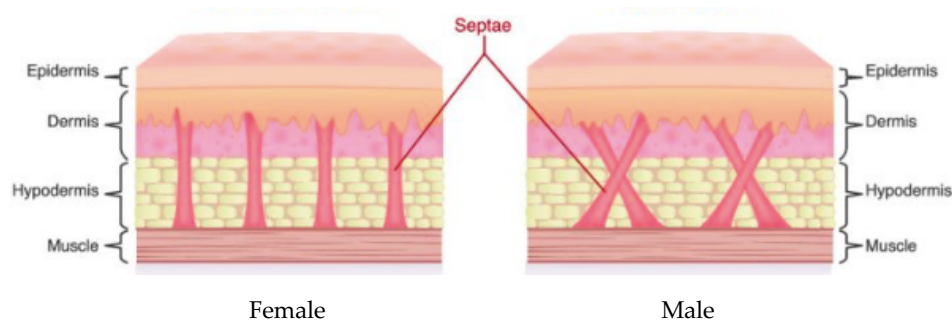
Figure 1.5. Female and Male Fat Cell Arrangement in the Subcutis [57].

1.3. THE CONDITIONS OF THE SKIN

The large amount of annual revenue generated by the cosmetic industry is indicative of how much importance is placed on the psychosocial role of the nails, hair, and skin by most the entire world population. The physical state of the skin can be influenced by various internal and external factors such as irritants, allergic reaction to drugs or non-drug components, genetics, issues related to the immune system, and certain disease conditions [58].

1.3.1.   ACNE VULGARIS

Acne is a common skin condition caused when blocked skin follicles from a plug caused by oil from glands, bacteria, and dead cells clump together and swell. Acne usually begins in puberty in conjunction with sex hormones. Sebum and dead skin cells plug the pores, which leads to outbreaks of lesions, commonly called pimples or zits. The outbreaks often occur on the face but can also appear on the back, chest, and shoulders. For most people, acne tends to go away by the time they reach their thirties, but some people in their forties and fifties continue to have this skin problem [58][59].

1.3.2.   ALOPECEA AREATA

It is a condition that attacks the hair follicles that make hair. In most cases, hair falls out in small, round patches about the size of a quarter, producing a few bare patches. It is an autoimmune disease that can lead to total hair loss. Immune dysregulation results in the hair follicles being attacked by inflammatory T-lymphocytes. Hair loss is more widespread in some people. In rarer cases, the disease can cause total loss of hair on the head, referred to as *alopecia areata totalis*, or the entire body, known as *alopecia areata universalis*. Doctors cannot predict if hair loss will end at some point, or whether it will grow back. The individual may continue to lose hair, or hair loss may stop [58][60].

1.3.3.   ATOPIC DERMATITIS

Often referred to as eczema, it is a chronic skin disease that causes inflammation, redness, and irritation of the skin. It is a common condition that usually begins in childhood however, anyone can get the disease. Atopic dermatitis is not contagious. It causes the skin to become extremely itchy. Scratching leads to redness, swelling, cracking, weeping clear fluid, crusting, and scaling. It is not clear what causes atopic dermatitis, however genes, immune system, and the environment may play a role in the disease. Depending on the severity and location of the symptoms, living with atopic dermatitis can be hard. Treatment can help control symptoms. In many people, atopic dermatitis improves by adulthood, but for some, it can be a lifelong illness [58][61].

1.3.4.   CICATRICIAL ALOPECIA

It is a group of rare disorders that destroy hair follicles. Hair follicles are the part of the skin where the hair grows. It is also called scarring alopecia. The follicles are replaced with scar tissue, causing permanent hair loss. Cicatricial alopecia is not contagious and can affect anyone, however it is not common in children. It can either be caused by white blood cells destroying hair follicles or when the hair follicle is destroyed by certain situations such as a burn, infection, radiation, or a tumor. Medications are used to treat cicatricial alopecia, surgery might be an option. The disease may come back, even after treatment [62].

1.3.5.   EPIDERMOLYSIS BULLOSA

It is a group of rare diseases causing painful blisters to form on the skin. The skin becomes fragile and blisters easily. Tears, sores, and blisters in the skin happen when friction or quick impacts occur anywhere on the body. These blisters can cause problems if they become infected. In severe cases, blisters may also develop inside the body, such as in the mouth, esophagus, stomach, intestines, upper airway, bladder, and genitals. Most people who have epidermolysis bullosa inherit a mutated gene. The gene mutation changes how the body makes proteins that help the skin bind together and remain strong. The symptoms of the disease usually begin at birth or during infancy and range from mild to severe. There is no cure for the disease, doctors may try to treat the symptoms, such as managing pain, treating wounds caused by the blisters and tears, and helping you cope with the disease [63].

1.3.6. HIDRADENITIS SUPPURATIVA

Hidradenitis suppurativa (HS) also known as acne in-versa is a chronic, noncontagious, inflammatory condition characterized by pimple-like bumps or boils and tunnels or tracts on and under the skin. Pus-filled bumps on the skin or hard bumps beneath the skin can progress to painful, inflamed lesions with chronic drainage. It starts in the hair follicle in the skin. In most cases, the cause of the disease is unknown, although a combination of genetic, hormonal, and environmental factors is likely playing a role in its development [64].

1.3.7. ICHTHYOSIS

It is a disorder that causes dry, thickened skin that appears scaly, rough, and red. The symptoms can range from mild to severe. Ichthyosis can affect only the skin, but some forms of the disease can affect internal organs as well. Most people inherit ichthyosis from their parents through a mutated gene. However, some people develop a form of acquired ichthyosis from another medical disorder or certain medications. There is no cure for ichthyosis, treatments are available to help manage the symptoms [65].

1.3.8. LICHEN SCLEROSUS

Lichen sclerosus is a long-term condition that usually affects the skin in the genital and anal areas. It causes white spots or patches on skin of the genital and anal areas, but can appear elsewhere such as the upper body, breasts, and upper arms. Itchiness, pain, and bleeding are common. The disease does not cause skin cancer but may increase the likelihood of developing it, if the skin is scarred [66].

1.3.9. PACHYONYCHIA CONGENITA

It is a rare genetic disorder causing overgrowth, thick nails and painful calluses on the bottoms of the feet. In some cases, blisters also form on the palms of the hand. The disorder is usually seen starting at birth or early in life, and it affects people of both sexes and all racial and ethnic groups. It is caused by mutations in one of at least five genes that help produce keratins. These mutations change keratin structure so that nails thicken, and skin cells are more sensitive to minor stress such as walking. There is no cure or medicine to treat pachyonychia congenital. Over-the-counter medications are commonly used to treat pain associated with symptoms [67].

1.3.10. PEMPHIGUS

It is a rare disease where the immune system attacks healthy cells in the top layer of skin and the mucous membranes, resulting in blistering of the skin and inside the mouth, nose, throat, eyes, and genitals. Pemphigus is not contagious. It occurs when the immune system produces antibodies against desmoglein, a protein that normally forms the "glue" to keep skin cells attached. Skin cells separate from each other. Fluid may collect between the layers of skin, forming blisters that do not heal. In some

cases, these blisters can cover a large area of skin. The disease can be controlled with medications that can eventually be completely discontinued due to serious side effects [68].

1.3.11. PSORIASIS

It is a chronic skin disease in which the immune system becomes overactive, causing skin cells to multiply too quickly. Patches of skin become scaly and inflamed, most often on the scalp, elbows, or knees, but other parts of the body can be affected as well. Psoriasis is caused by a mix of genetics and environmental factors. The symptoms of psoriasis can sometimes go through cycles, flaring for a while followed by periods when they subside. Most forms of psoriasis are mild or moderate and can be treated with creams or ointments. Managing common triggers, such as stress and skin injuries, can also help keep the symptoms under control. Having psoriasis carries the risk of getting other serious conditions, such as, psoriatic arthritis, cardiovascular disease, mental health problems, cancers, crohn's disease, diabetes, metabolic syndrome, obesity, osteoporosis, uveitis, liver, and kidney disease [58][69].

1.3.12. REYNAUD'S PHENOMENON

It is a disease that affects blood vessels. It causes the body to not send enough blood to the hands and feet for a period of time also known as vasospasms. This usually happens when one is cold or feeling stressed. During vasospasms, the fingers and toes feel very cold or numb and may change color. Individuals may experience three phases of skin color change - typically from white to blue to red in the fingers and toes. During vasospasms, blood flow to the skin will remain low until the skin is rewarmed. After warming, it usually takes 15 minutes to recover normal blood flow to the skin. Prognosis often depends on existing underlying health condition. Many people with Raynaud's phenomenon have mild symptoms that do not cause any blood vessel or tissue damage. These symptoms are easily managed, often without medicines [70].

1.3.13. ROSACEA

It is a long-term condition that causes reddened skin and pimples, usually on the face. It can also make the skin thicker and cause eye problems. There is no cure for rosacea but management can make the skin look and feel better. It mostly affects middle-aged and older adults and is most apparent in people with fair skin. The redness of the skin usually occurs around the center of the face, as well as the forehead, nose, cheeks and chin. The skin may also feel swollen or burning sensation. In advanced stages, the skin may become thicker and can also cause eye problems. The eyes may become red, dry, itchy, burning or watery. The eyelids can become inflamed and swollen. Individuals may also have blurred vision or some other kind of vision problem or be more sensitive to light. Rosacea rarely affects other parts of the body [58][71].

1.3.14. SCLERODERMA

It is an autoimmune connective tissue and rheumatic disease that causes inflammation in the skin and other areas of the body. When an immune response tricks tissues into thinking they are injured, it causes inflammation, and the body makes too much collagen, leading to scleroderma which causes patches of tight, hard skin, which can also harm blood vessels and organs. There are two major types of scleroderma: localized scleroderma which only affects the skin and the structures directly under the skin, and systemic scleroderma which affects many systems of the body. It can damage the blood vessels and internal organs, such as the heart, lungs, and kidneys. There is no cure for scleroderma. The goal of treatment is to relieve symptoms and stop the progression of the disease [72].

1.3.15. VITILIGO

It is a chronic disorder that causes patches of skin to lose pigment. It happens because cells that make pigment in the skin (melanocytes) are destroyed, causing the skin to turn a milky-white color. There are two types of vitiligo: generalized vitiligo which happens when the white patches appear symmetrically on both sides of the body, such as on both hands or both knees, it is the most common type of vitiligo and segmental vitiligo which happens when the white patches are only on one segment of the body such as a leg, arm or one side of the face, this type of vitiligo often begins at an early age and progresses for about 1 to 2 years and then usually stops. The cause of vitiligo is unknown, but research suggests that it is an autoimmune disease. There is no cure for vitiligo, but treatment may help skin tone appear more even [73].

1.3.16. SKIN AGING

Skin aging is a progressive process in which environmental damage superimposed on aging skin determines the ultimate skin appearance. There are two distinct types of aging. Aging caused by the genes we inherit and depending on the passage of time per se is called chronological or intrinsic aging. The other type of aging is known as extrinsic aging and is caused by environmental factors such as sun exposure. Age is not the determining factor in the condition of mature skin. Environmental factors that influence aging of the skin play a central role. Tone, elasticity, and epidermal regeneration capacity do not decline until advanced age in areas not exposed to light, whereas they do so prematurely in areas exposed to light [74].

1.3.17. SUNBURN

It is a condition that is caused by too much exposure to ultraviolet light from sunshine or artificial sources, such as sunlamps resulting in red, irritated, and painful skin that feels hot to the touch. Repeated UV light exposure that results in sunburn increases the risk of other skin damages, such as dark spots, rough spots, and dry or wrinkled skin. It also raises the risk of photoaging and skin cancers such as melanoma. Sunburn symptoms, involving changes in skin tone, pain, tenderness, swelling, small fluid-filled blisters, headache, fever, nausea, and fatigue, usually appear within a few hours after

sun exposure. However, it may take a day or two to know its severity. Home remedies can usually provide sunburn relief, but sunburn may take days to fade [75].

1.3.18. CELLULITIS

This is a common bacteria (*Staphylococcus* and *Streptococci aureus*) infection of the dermis and subcutis layers of the skin and can result in life-threatening complications when left untreated. It occurs anywhere in the body (mostly, the face and legs), causing redness, soreness, erythema, inflammation, and localized lymphadenopathy. Patients with cellulitis make-up about 1 to 14% emergency room visits and 4 to 7% of clinical admissions. Although, the severity of cellulitis is still very controversial due to its variation from one patient to the other, and the absence of population-based data [76].

1.3.19. GYNOID LIPODYSTROPHY

Gynoid lipodystrophy otherwise known as Cellulite (not to be mistaken for cellulitis – a skin condition causing redness and swelling brought about by a bacteria infection) affects 80-90% of the total population of women worldwide [77][78], from puberty onset and increases during menstruation, pregnancy, and nursing [79]. Yet its pathogenesis is not still clear [80]. It presents relief alterations i.e. depression and bulging of the skin topography, especially on the abdomen, buttocks and thighs, imitating the appearance of an orange peel, mattress or cottage cheese. These depressions and bulges are produced by underlying thick fibrous septa resulting in recantation of the skin and projection of adipocytes to the surface, respectively [81][82][83]. Women are more prone to cellulite than their male counterpart, as a result of the longitudinal arrangement of connective tissue bands (fibrous septa separating adipose tissue into channels) linking the deep fascia to the dermis. This arrangement allows easy projection of fat to the skin surface as the subcutis continues to stretch (an over expansion of the subcutis leads to an increase in ectopic fat accumulation, promoting metabolic disorder), making the surface rough [84][85]. While in men, bands of connective tissue in their buttocks and thighs have an interwoven architecture, making it almost impossible for the projection of fat to the surface. Asides from the structural factor mentioned above, other factors affecting cellulite include biochemical (e.g. hormones), inflammatory and morphological factors [85].

Cellulite is a multifactorial disease, although not entirely understood, causes adipose tissue degradation through stages of altering the interstitial matrix, micro-circulatory harmony, fat cell hypertrophy and hyperplasia, thereby, giving rise to blood and lymphatic vessel restriction and also the breakdown of elastin and collagen network [86][87]. When left untreated, cellulite can progress into a more severe form and may result in oedema, and eventually fibrosis [87]. It also causes feelings of insecurities and low self-esteem due to its unattractive nature, reducing the quality of life of patients Although numerous medical devices and cosmetic products aiming to treat cellulite are on the market

23

today, they seem to provide little to no clinical evidence to support their claims and none has been seen to produce a long-term effect or effectively manage the condition

1.3.19.1. FACTORS INFLUENCING CELLULITE APPEARANCE

Cellulite appearance is unattractive and reduces the quality of life of patients so, the need for a safe, affordable, and effective treatment is essential [88][89]. Numerous medical devices and cosmetic products aimed at cellulite reduction exists. Nevertheless, they show little to no clinical evidence to support their claims, and none has been seen to produce a long-term effect or effectively manage the condition [89]. Extensively understanding the molecular mechanisms involved in the pathophysiology of cellulite will result in its successful treatment. Currently, it is suggested that the following influences cellulite occurrence; (a) Hormone - females are most likely to have cellulite than men because, the oestrogen hormone promotes lipogenesis while inhibiting lipolysis, which leads to adipocyte hypertrophy and hyperplasia. (b) Genetic predisposition - this has been linked to specific polymorphism in the angiotensin converting enzyme, ACE rs1799752 (promotes ACE activity and disrupts tissue oxygenation by inactivating the protein bradykinin, a vasodilator, thereby increasing blood pressure and reducing blood flow to tissues e.g. the dermal layer) and hypoxia inducible factor 1A gene, HIF1A rs11549465 (a potent hypoxia sensor and regulator of inflammatory and microhypoxic tissue responses in the subcutis, through the up-regulation of genes responsible for angiogenesis – blood vessels formation, therefore, preventing fibro-inflammation) [90]. (c) Microvascular circulation and lymphatic drainage - oedema, vascular congestion, loss in capillary network and tissue hypoxia occurs as a result of changes in arteriole sphincters allowing uncontrolled capillary permeability and glycosaminoglycan, GAG build-up in capillary walls increasing fluid concentration. (d) Other factors influencing cellulite development include weight gain, lifestyle i.e. smoking and inflammatory factors [90].

1.3.19.2. TREATMENT OF CELLULITE

Various medical devices aimed at improving the appearance of cellulite on the skin have been investigated. One of such study involves a three-step cellulite treatment with the use of 1440-nm Nd:YAG wavelength laser with side firing fibre on 57 patients. The novel technology was able to provide targeted delivery of laser energy to the cellulite affected area. The effectiveness of the treatment was monitored for at least 12 months during a follow-up period [91]. Although this procedure may be effective but, known to cause adverse effects such as pain, swelling, numbness, bruising and itching in patients following treatment [92]. Another study involved the use of high-resolution ultrasound (before and after therapy) and low-energy extracorporeal shock wave device to target lateral thigh (cellulite affected area) in 21 female volunteers, twice a week for six weeks; the results showed an improvement in the treated area. However, this procedure presented limited evidence to its claims, the device

produced sounds causing irritation to the ear, participants reported that the therapy caused some level of physical pain and a reoccurrence of cellulite was also reported in some subjects after a 2 months follow-up study [93].

Several topical formulations containing caffeine (methylxanthine) and other natural plant extracts (i.e., green tea, verbena, fennel, marjoram, ivy, algae etc) for the treatment of cellulite are on the market today. However, a placebo controlled, double blind study was carried out by Nasrollahi and others on 12 healthy females, involving the use of an anti-cellulite cream containing the active ingredients Coenyme A, caffeine (known to cause adipocyte hydrolysis into free fatty acids) and L-Carnitine, the placebo was an identical cream lacking these active ingredients. The result showed no significant difference between active and placebo treatment [94]. This means that the characteristics of caffeine to inhibit phosphodiesterase enzymes and promote lipolysis is too low to be associated with desirable results. A formulation study revealed methylxanthine anti-cellulite cream (such as caffeine and aminophylline) failure to demonstrate dermal reconstruction despite evidence of its ability to cause lipolysis can be attributed to poor delivery to the appropriate subcutaneous layer, proving encapsulated methylxanthines in carriers delivers a much higher concentration to the site of action [95]. The delivery of hydrophilic actives in the aqueous core of a carrier vesicle (e.g. liposomes and niosomes) presents a promising potential for topical anti-cellulite formulation [96].

Vitamin A (retinols) is another active ingredient that serve as an antioxidant and have found its application in topical anticellulite treatment through the increase of fibroblast proliferation, promoting collagen synthesis and inhibiting collagenases – they cleave or digest collagen. In a study performed by Kligman and others on 19 volunteers showed an improvement in the skin condition in 63.2% of all test subjects, demonstrating the ability of retinols to bring about collagen and elastin fibre synthesis and reconstruction of their networks. However, another study carried out by Pierard-Franchimont and others observed increased skin elasticity but, no difference in skin surface appearance [97][98]. Other actives used for the treatment of cellulite include peroxisome proliferator-activated receptor (PPAR) agonists such as monosaturated and polysaturated fatty acids are known to activate the enzymes glucocerebrosidase and keratinocyte serine palmitoyl transferase thereby, increasing epidermal barrier synthesis, extracellular matrix components and promoting epidermal cell differentiation while decreasing inflammation. This action results in the synthesis of proteins such as collagen and elastin fibre. Similarly, alphahydroxyacids, especially lactic acids, are antioxidants that are thought to cause collagen synthesis and repair photodamaged skins, however, evidence of this have not yet been reported [99][100].

The purpose of this study, using an evidence-based approach to design a novel anticellulite cream without any adverse effects, involves encapsulating a new hydrophilic active (methylene blue)

25

ingredient into niosome vesicles using the thin-film hydration technique for targeted delivery, and characterisation studies such as microscopic examination, size and zeta measurement, separation, and entrapment efficiency analysis, to determine the lead niosomal formulation to be incorporated into the cream base. Designing a novel oil in water topical formulation and investigating the safety and quality.

Methylene blue is proposed to have antioxidant and free radical scavenging activities by targeting cellular mitochondria [101]. Free radicals are responsible for increasing collagen and elastin degradation while decreasing its synthesis by promoting matrix metalloproteinase (MMP) expression (also called collagenases – they cleave or digest collagen), and eventually result to dermal network alteration. In order to reverse this process, localized application of antioxidants to the skin surface can help reduce the production or accumulation of free radicals or neutralize its effect [102][103]. This active was entrapped in niosomal vesicles for delivering a much higher concentration to the site of action. The cream was formulated using jojoba and baobab oil possessing antioxidant properties that helps reduce fine lines and wrinkles, stimulating collagen synthesis and eventually skin healing and rejuvenation of epithelial cells [104].

REFERENCE

1. *De Sousa Crespo J*. Human Tissue Hyperelastic Analysis. Instituto Superior Tecnico, Universidade Tecnica de Lisboa. 2009.

2. Thiele FA, Malten KE. Evaluation of skin damage. I. *British Journal of Dermatology*. 1973 Oct 1;89(4):373-82.

3. Freinkel, Ruth K., and David T. Woodley, editors. *The biology of the skin*. CRC Press, 2001 Mar 15.

4. Melzack R, Casey KL. Sensory, motivational and central control determinants of pain: a new conceptual model. Skin Senses, 1. 1968.

5. Roosterman D, Goerge T, Schneider SW, Bunnett NW, Steinhoff M. Neuronal Control of Skin Function: The Skin as a Neuroimmunoendocrine Organ. *Physiological Reviews*. 2006 Oct 1;86(4):1309–79.

6. Montagna W. The Structure and Function of Skin. 24/28 Oval Road, London NW1: Academic Press, INC. (London) LTD.; 2012. 448: 157-163.

7. Fowler I. Human Anatomy, 1st ed. Belmont, California 94002: Wadsworth Publishing Company 9780534027469 - Anybook Ltd. 1984. 88-96.

8. Fox S. Human Physiology. 13th ed. New York, NY 10020: McGraw-Hill Publishing Company; 2012. 832 p.

9. SEER Training Modules. SEER Training:Anatomy of the Skin [Internet]. National Institute of Health, National Cancer institute. 2008. Available online: https://training.seer.cancer.gov/melanoma/anatomy/ (accessed on 10 June 2017).

10. Themes UFO. The Function and Structure of the Skin [Internet]. Plastic Surgery Key. 2016. Available online: https://plasticsurgerykey.com/the-function-and-structure-of-the-skin/ (accessed on 10 June 2017).

11. Shimizu H. Shimizu's textbook of dermatology. JA KUBU. Hokkaido University Press, Nakayama Shoten Publishers; 2007.

12. Davis BO, Holtz N, Davis JC. Conceptual human physiology. Columbus, Ohio 43216: C.E. Merrill Pub. Co; 1985. 507-508 p.

13. Premkumar K. The massage connection: anatomy and physiology. Baltimore, Maryland 21201-2436 USA: Lippincott Williams & Wilkins; 2004. 58 p.

14. Cunningham DJ. Cunningham's Textbook of Anatomy. 12th ed. New York, NY: Oxford medical publications, Oxford University Press; 1981. 830-831 p.

15. Archambeau JO, Pezner R, Wasserman T. Pathophysiology of irradiated skin and breast. *International Journal of Radiation Oncology Biology Physics*. 1995;31(5):1171–1185.

16. Bensouilah J, Buck P. Aromadermatology: Aromatherapy in the Treatment and Care of Common Skin Conditions. Radcliffe Publishing Company; 2006.

17. Wynsberghe D, Carola R, Noback C. Human anatomy and physiology. 3rd ed. London: McGraw-Hill; 1995.

18. Menon GK. Skin Basics; Structure and Function. In: Pappas A, editor. Lipids and Skin Health. Cham: Springer International Publishing; 2015. 9–23 p.

19. Shukla A, Nandi P, Ranjan M. Acellular dermis as a dermal matrix of tissue engineered skin substitute for burns treatment. Ann Public Health Res. 2015;2(3):1023.

20. Williams AC. Transdermal and Topical Drug Delivery. Vol. 272. *The Pharmaceutical Journal. London*; 2003. 242 p.

21. Assefa N, Tsige Y. Human Anatomy and Physiology. Diakses Dari - Ethiopia Public Health Training Initiative, The Carter Center, Ethiopia Ministry of Health and Education. 2003; 17:43–9.

22. Gupchup GV, Zatz JL. Skin and Nail; Barrier function, structure and anatomy consideration for drug delivery. J CosmetSci. 1999; 50:363-85.1.

23. Madison KC. Barrier Function of the Skin: 'La Raison d'Être' of the Epidermis. Journal of Investigative Dermatology. 2003 Aug 1; 121(2):231–41. doi: 10.1046/j.1523-1747.2003.12359.x.

24. Mizutani Y, Mitsutake S, Tsuji K, Kihara A, Igarashi Y. Ceramide biosynthesis in keratinocyte and its role in skin function. Biochimie, (Lipids for the future). 2009 Jun 1;91(6):784–90. doi: 10.1016/j.biochi.2009.04.001.

25. Wilkin D, Brainard J. Human Biology. 3430 W. Bayshore Rd., Suite 101 Palo Alto, CA 94303: FlexBook Foundation; 2015.

26. Baroni A, Buommino E, De Gregorio V, Ruocco E, Ruocco V, Wolf R. Structure and function of the epidermis related to barrier properties. Clinics in Dermatology. (Epidermal Barrier Function: Clinical Implications and Therapeutic Relevance). 2012 May 1;30(3):257–62. doi: 10.1016/j.clindermatol.2011.08.007.

27. Betts JG, Desaix P, Johnson E, Johnson JE, Korol O, Kruse D, et al. Anatomy & physiology. 6100 Main Street MS-375 Houston, Texas 77005: Rice University; 2016. 178(1426). 978-1-938168-13-0.

28. Ratcliffe NA. Integumentary System (Skin). In: Practical Illustrated Histology. Macmillan Education UK; 1982. 85–9. 10.1007/978-1-349-86060-9_9.

29. Paxton S, Peckham M, Adele K, Paxton S, Adele K, Peckham M. The Leeds Histology Guide. 2003. Available online: http://www.histology.leeds.ac.uk/skin/skin_layers.php/ (accessed on 30 June 2017).

30. McLafferty E, Hendry C, Farley A. The integumentary system: anatomy, physiology and function of skin. Nursing Standard. 2012 Sep 19;27(3):35–42. doi: 10.7748/ns2012.09.27.3.35.c9299.

31. Ricard-Blum S. The collagen family. Cold Spring Harbor perspectives in biology. 2011 Jan 1;3(1):a004978.

32. Krieg T, Aumailley M. The extracellular matrix of the dermis: flexible structures with dynamic functions: Extracellular matrix of the dermis. Experimental Dermatology. 2011 Aug;20(8):689–95. doi: 10.1111/j.1600-0625.2011.01313.x.

33. VanPutte C, Regan J, Russo A. Seeley's Essentials of Anatomy and Physiology. 9th Edition. 2 Penn Plaza, New York, NY 10121: McGraw-Hill Education; 2016. 96 p. 978-0-07-809732-4.

34. Imedeen. Skin and ageing. 2014. Available online: http://www.imedeen.com.sg/your-skin/skin-and-ageing/ (accessed on 5 July 2017).

35. Bovell D. The Human Eccrine Sweat Gland: Structure, Function and Disorders. Bloomsbury Qatar Found Journals. (Bovell. Journal of Local and Global Health Science). 2015;(10.5339).

36. Amirlak B, Shahabi L. Skin Anatomy: Overview, Epidermis, Dermis. American Society of Plastic Surgeons; 2017 Mar 9.

37. Lupi O. Ancient adaptations of human skin: why do we retain sebaceous and apocrine glands?. International Journal of Dermatology, 2008;47(7), 651-654.

38. Cottle DL, Kretzschmar K, Schweiger PJ, Quist SR, Gollnick HP, Natsuga K, et al. c-MYC-Induced Sebaceous Gland Differentiation Is Controlled by an Androgen Receptor/p53 Axis. Cell Rep. 2013 Feb 21;3(2):427–41.

39. Zouboulis CC. Acne and sebaceous gland function. Clin Dermatol. 2004 Sep 1;22(5):360–366. doi: 10.1016/j.clindermatol.2004.03.004.

40. Rishikaysh P, Dev K, Diaz D, Qureshi W, Filip S, Mokry J. Signaling Involved in Hair Follicle Morphogenesis and Development. Int J Mol Sci. 2014 Jan 22;15(1):1647–1670.

41. Brajac I, Vičić M, Periša D, Kaštelan M. Human hair follicle: an update on biology and perspectives in hair growth disorders treatment. Hair therapy and transplantation. 2014 Jan 1;4:3-6.

42. Powell BA, Crocker LE, Rogers GE. Hair follicle differentiation: expression, structure and evolutionary conservation of the hair type II keratin intermediate filament gene family. Development. 1992 Feb 1;114(2):417-33.

43. Stovall G. Hair Follicle Structure. Biological Science Picture Directory – Pulpbits.net. 2013. Available online: http://pulpbits.net/8-structure-hair-follicle-pictures/hair-follicle-structure/ (accessed on 1 July 2017).

44. Tuchin VV. Optical Clearing of Tissues and Blood. 1000 20th Street, Bellingham, WA 98227-0010 USA: SPIE; 2005. doi: 10.1117/3.637760.

45. Boundless. Blood Supply to the Epidermis. Boundless [Internet]. 2016. Available online: /physiology/textbooks/boundless-anatomy-and-physiology-textbook/integumentary-system-5/functions-of-the-integumentary-system-66/blood-supply-to-the-epidermis-405-5030/ (accessed on 1 July 2017).

46. Zgraggen S, Ochsenbein AM, Detmar M. An Important Role of Blood and Lymphatic Vessels in Inflammation and Allergy. J Allergy. 2013;2013:1–9.

47. Scanlon VC, Sanders T. Essentials of anatomy and physiology. 5th ed. Philadelphia: F.A. Davis Co; 2007. 603 p.

48. Lund AW, Medler TR, Leachman SA, Coussens LM. Lymphatic Vessels, Inflammation, and Immunity in Skin Cancer. Cancer Discov. 2016 Jan;6(1):22. doi: 10.1158/2159-8290.CD-15-0023.

49. Maceo AV. Anatomy and physiology of adult friction ridge skin. Fingerpr Sourceb. 2011. Available online: https://evolveforensics.com/wp-content/uploads/2015/07/Maceo-Alice.-Anatomy-and-Physiology-of-Adult-Friction-Skin.pdf/ (accessed on 1 July 2017).

50. Spellman, Frank R. *Biology for nonbiologists*. Vol. 2. Government Institutes, 2007.

51. Igarashi T, Nishino K, Nayar SK. The appearance of human skin: A survey. Foundations and Trends® in Computer Graphics and Vision. 2007 Nov 5;3(1):1-95.

52. Flowers FP, Adrian W. Transdermal and Topical Drug Delivery: From Theory to Clinical Practice. Ann Pharmacother. 2004 Apr; 38(4):726–7. doi: 10.1345/aph.1D555.

53. Arda, O., Göksügür, N., & Tüzün, Y. Basic histological structure and functions of facial skin. Clin Dermatol. 2014 Jan;32(1):3–13. doi: 10.1016/j.clindermatol.2013.05.021.

54. Liposuction. Fat Cells and Your Anatomy. Liposuction4You. 2013. Available from: http://www.liposuction4you.com/anatomy.htm/ (accessed on 1 July 2017).

55. Martini FH, Bartholomew EF. Essentials of anatomy and physiology, ed 5, New York, 2009.

56. Betts, J. G., P. Desaix, J. E. Johnson, O. Korol, D. Kruse, B. Poe, J. Wise, M. D. Womble, and K. A. Young. "OpenStax College, et al. Anatomy and Physiology." 2013; 787-846.

57. Vanish Unsightly Cellulite | Painless, Effectively & Naturally | Ensoul Body Clinic [Internet]. Ensoulbodyclinic.com. 2020 [cited 1 December 2020]. Available from: https://ensoulbodyclinic.com/treatment-solutions/cellulite-reduction/

58. Shenefelt PD. Psychological interventions in the management of common skin conditions. Psychology research and behaviour management. 2010; 3:51.

59. Health topics. Acne [Internet]. National Institute of Arthritis and Musculoskeletal and Skin Diseases. 2020 [cited 16 December 2020]. Available from: https://www.niams.nih.gov/health-topics/acne/advanced

60. Health Topics. Alopecia Areata [Internet]. National Institute of Arthritis and Musculoskeletal and Skin Diseases. 2020 [cited 16 December 2020]. Available from: https://www.niams.nih.gov/health-topics/alopecia-areata/advanced

61. Health Topics. Atopic Dermatitis [Internet]. National Institute of Arthritis and Musculoskeletal and Skin Diseases. 2020 [cited 16 December 2020]. Available from: https://www.niams.nih.gov/health-topics/atopic-dermatitis/advanced

62. Health Topics. Cicatricial Alopecia [Internet]. National Institute of Arthritis and Musculoskeletal and Skin Diseases. 2020 [cited 17 December 2020]. Available from: https://www.niams.nih.gov/health-topics/cicatricial-alopecia/advanced

63. Health Topics. Epidermolysis Bullosa [Internet]. National Institute of Arthritis and Musculoskeletal and Skin Diseases. 2020 [cited 16 December 2020]. Available from: https://www.niams.nih.gov/health-topics/epidermolysis-bullosa/advanced

64. Health Topics. Hidradenitis Suppurativa (HS) [Internet]. National Institute of Arthritis and Musculoskeletal and Skin Diseases. 2020 [cited 16 December 2020]. Available from: https://www.niams.nih.gov/health-topics/hidradenitis-suppurativa-hs/advanced

65. Health Topics. Ichthyosis [Internet]. National Institute of Arthritis and Musculoskeletal and Skin Diseases. 2020 [cited 16 December 2020]. Available from: https://www.niams.nih.gov/health-topics/ichthyosis/advanced

66. Health Topics H. Lichen Sclerosus [Internet]. National Institute of Arthritis and Musculoskeletal and Skin Diseases. 2020 [cited 17 December 2020]. Available from: https://www.niams.nih.gov/health-topics/lichen-sclerosus/advanced

67. Health Topics. Pachyonychia Congenita [Internet]. National Institute of Arthritis and Musculoskeletal and Skin Diseases. 2020 [cited 17 December 2020]. Available from: https://www.niams.nih.gov/health-topics/pachyonychia-congenita/advanced

68. Health Topics. Pemphigus [Internet]. National Institute of Arthritis and Musculoskeletal and Skin Diseases. 2020 [cited 17 December 2020]. Available from: https://www.niams.nih.gov/health-topics/pemphigus/advanced

69. Health Topics. Psoriasis [Internet]. National Institute of Arthritis and Musculoskeletal and Skin Diseases. 2020 [cited 17 December 2020]. Available from: https://www.niams.nih.gov/health-topics/psoriasis/advanced

70. Health Topics. Raynaud's Phenomenon [Internet]. National Institute of Arthritis and Musculoskeletal and Skin Diseases. 2020 [cited 17 December 2020]. Available from: https://www.niams.nih.gov/health-topics/raynauds-phenomenon/advanced

71. Health Topics. Rosacea [Internet]. National Institute of Arthritis and Musculoskeletal and Skin Diseases. 2020 [cited 17 December 2020]. Available from: https://www.niams.nih.gov/health-topics/rosacea/advanced

72. Health Topics. Scleroderma [Internet]. National Institute of Arthritis and Musculoskeletal and Skin Diseases. 2020 [cited 17 December 2020]. Available from: https://www.niams.nih.gov/health-topics/scleroderma/advanced

73. Health Topics. Vitiligo [Internet]. National Institute of Arthritis and Musculoskeletal and Skin Diseases. 2020 [cited 17 December 2020]. Available from: https://www.niams.nih.gov/health-topics/vitiligo/advanced

74. Sjerobabski-Masnec I, Šitum M. Skin aging. Acta Clinica Croatica. 2010 Dec 20;49(4):515-8.

75. Sunburn - Symptoms and causes [Internet]. Mayo Clinic. 2020 [cited 17 December 2020]. Available from: https://www.mayoclinic.org/diseases-conditions/sunburn/symptoms-causes/syc-20355922

76. Simonsen SE, Van Orman ER, Hatch BE, Jones SS, Gren LH, Hegmann KT, Lyon JL. Cellulitis incidence in a defined population. Epidemiology & Infection. 2006 Apr;134(2):293-299.

77. Pianez LR, Custódio FS, Guidi RM, de Freitas JN, Sant'Ana E. Effectiveness of carboxytherapy in the treatment of cellulite in healthy women: a pilot study. Clinical, cosmetic and investigational dermatology. 2016;9:183.

78. DiBernardo BE, Sasaki GH, Katz BE, Hunstad JP, Petti C, Burns AJ. A multicenter study for cellulite treatment using a 1440-nm Nd: YAG wavelength laser with side-firing fiber. Aesthetic surgery journal. 2016 Feb 18;36(3):335-43.

79. Peterson JD, Goldman MP. Laser, light, and energy devices for cellulite and lipodystrophy. Clinics in plastic surgery. 2011 Jul 31;38(3):463-74.

80. Milani GB, Natal Filho AD, João SM. Correlation between lumbar lordosis angle and degree of gynoid lipodystrophy (cellulite) in asymptomatic women. Clinics. 2008;63(4):503-8.

81. Yosipovitch G, Devore A, Dawn A. Obeisity and the skin: skin physiology and skin manifestations of obesity. Journal of the American Academy of Dermatology. 2007 Jun 30;56(6):901-16.

82. Hexsel DM, Dal'Forno T, Hexsel CL. A validated photonumeric cellulite severity scale. Journal of the European Academy of Dermatology and Venereology. 2009 May 1;23(5):523-8.

83. Hexsel DM, Mazzuco R. Subcision: a treatment for cellulite. International journal of dermatology. 2000 Jul 1;39(7):539-44.

84. Letter, A. and Roden, M. Ectopic fat and insulin resistance. Current diabetes reports. 2008 Jun 1;8(3), pp. 185-191.

85. Hexsel D, Soirefmann M. Cosmeceuticals for cellulite. InSeminars in cutaneous medicine and surgery 2011 Sep 1 (Vol. 30, No. 3, pp. 167-170). Frontline Medical Communications.

86. Soares IJ, Cristina doAmaral T, Miranda deAraújo DD, Sales deMelo V, Valentim daSilva RM, Meyer PF. Effects of combined therapy in celullitis: controlled clinical trial, randomized and blind. Manual Therapy, Posturology & Rehabilitation Journal= Revista Manual Therapy. 2016;14.

87. Naves JM, Soares C, Svezzia VD, Cussolim FD, Mendonça AC. Correlation between pelvic alignment and cellulitis. Fisioterapia e Pesquisa. 2017 Mar;24(1):40-5.

88. Purim KS, Titski AC, and Leite N. Dermatological aspects influencing the practice of physical activities by obese individuals. Fisioterapia em Movement. 2015 Dec;28(4):837-50.

89. Costa A, Alves RT, Pegas Pereira ES, Martins Cruz FA, Fidelis MC, Marega Frigerio R, Montagner S, de Medeiros VL. Gynoid Lipodystrophy and clinical therapy: critical analysis of available scientific publications. Surgical & Cosmetic Dermatology. 2012; 4 (1).

90. Friedmann DP, Vick GL, Mishra V. Cellulite: a review with a focus on subcision. Clinical, cosmetic and investigational dermatology. 2017;10:17.

91. DiBernardo BE, Sasaki GH, Katz BE, Hunstad JP, Petti C, Burns AJ. A multicenter study for cellulite treatment using a 1440-nm Nd: YAG wavelength laser with side-firing fiber. Aesthetic surgery journal. 2016 Feb 18;36(3):335-43.

92. Sasaki GH. Single treatment of grades II and III cellulite using a minimally invasive 1,440-nm pulsed Nd: YAG laser and side-firing fiber: an institutional review board-approved study with a 24-month follow-up period. Aesthetic plastic surgery. 2013 Dec 1;37(6):1073-89.

93. Angehrn F, Kuhn C, Voss A. Can cellulite be treated with low-energy extracorporeal shock wave therapy?. Clinical interventions in aging. 2007 Dec;2(4):623.

94. Nasrollahi SA, Hasanzadeh H, Ajami M, Ameri S, Variji Z, Komeili A, Firooz A. Assessment of an anti-cellulite cream: A randomized, double-blind, placebo controlled, right-left comparison, clinical trial. Iranian Journal of Dermatology. 2015;18(4):145-50.

95. LUEDER M, MOREL J, TIEDTKE DJ, MARKS DO. Anti-Cellulite actives, dream or reality?. Cosmetics Today. Suplemento to chimica oggi/Chemistry Today. 2004:45-8.

96. Vyas LK, Tapar KK, Nema RK, Parashar AK. Development and characterization of topical liposomal gel formulation for anti-cellulite activity. measurement. 2013;15:18.

97. Kligman AM, Pagnoni A, Stoudemayer T. Topical retinol improves cellulite. Journal of Dermatological Treatment. 1999;10(2):119-25.

98. Piérard-Franchimont C, Piérard GE, Henry F, Vroome V, Cauwenbergh G. A randomized, placebo-controlled trial of topical retinol in the treatment of cellulite. American journal of clinical dermatology. 2000;1(6):369-74.

99. Wahli W. Peroxisome proliferator-activated receptors (PPARs): from metabolic control to epidermal wound healing. Swiss medical weekly. 2002;132(7-8):83-91.

100. Rawlings AV, Davies A, Carlomusto M, Pillai S, Zhang K, Kosturko R, Verdejo P, Feinberg C, Nguyen L, Chandar P. Effect of lactic acid isomers on keratinocyte ceramide synthesis, stratum corneum lipid levels and stratum corneum barrier function. Archives of dermatological research. 1996;288(7):383-90.

101. Marimuthu M, Praveen Kumar B, Mariya Salomi L, Veerapandian M, Balamurugan K. Methylene blue-fortified molybdenum trioxide nanoparticles: harnessing radical scavenging property. ACS applied materials & interfaces. 2018; 10(50):43429-38.

102. Rinnerthaler M, Bischof J, Streubel MK, Trost A, Richter K. Oxidative stress in aging human skin. Biomolecules. 2015; 5(2):545-89.

103. Masaki H. Role of antioxidants in the skin: anti-aging effects. Journal of dermatological science. 2010; 58(2):85-90.

104. Adejokun DA, Dodou K. A Novel Method for the Evaluation of the Long-Term Stability of Cream Formulations Containing Natural Oils. Cosmetics. 2020 Dec;7(4):86.

CHAPTER 2

RESEARCH GOALS AND OBJECTIVES

2.1. RESEARCH GOALS

The purpose of this research was to investigate the best intervention for cellulite (dry brushing, exercise and cream) based on efficacy studies involving 9 adult female volunteers, encapsulating the new active ingredient into niosome vesicles using the thin-film hydration technique, and characterisation studies such as microscopic examination, size and zeta measurement, separation and entrapment efficiency studies, to determine the lead niosomal formulation to be incorporated into the cream base. Designing a novel oil in water cream formulation and investigating the safety and quality. The criteria for progression were based on short- to long-term stability and resistance to microbial contamination (safety evaluation), flow behavior and sensory profile or attributes (quality evaluation). Lastly, the efficacy study involving 12 adult female volunteers was performed using individual perception, the cutometer, visioscan and the visiometer to evaluate changes in skin topography after cream application.

2.2. Hypothesis

The hypothesis of this study is the improvement in cellulite appearance using a novel anti-cellulite cream containing active niosomes observed by user perception, the cutometer, visioscan, and visiometer technique.

2.3. Aims/Objectives

This research aims to examine the effect of a non-invasive topical anti-cellulite treatment in relation to the user perception. The specific aims are clearly stated below,

Chapter 3 - Evaluating the reduction in cellulite appearance through non-invasive means such as exercise, dry brushing and a topical cream formulation.

Chapter 4 – To design and characterize a novel cream formulation containing active-loaded niosomes.

Chapter 5 – To explore the correlation of the rheological parameters of semisolid formulations with their sensorial attributes such as pourability, firmness, elasticity and stickiness.

Chapter 6 - Short- to long-term stability studies on the novel formulations.

Chapter 7 – To investigate the user perception on the efficacy of the novel cream on 12 healthy female volunteers.

CHAPTER 3

PRELIMINARY STUDY: *IN VIVO* INVESTIGATION OF THE EFFICACY OF ANTI-CELLULITE TREATMENTS

3.1. INTRODUCTION

The human skin (integument) has a total area of 2 m² in adults and weighs about 5Kg, it is a vital as well as the biggest organ of the body [1]. The skin is made up of different layers performing several complex functions, these layers consists of:

(a) The epidermis (outer) layer – Its surface consists of irregular texture that creates a unique pattern in every individual, specifically on the fingers, producing exclusive fingerprints for individual identification. This layer is made up of five different layers with varying thickness (depending on the region of the body), representing cells in various phases of keratinization, a process by which the outer epidermal cells die, and their cytoplasm is replaced by keratin [2][3][4][5].

(b) The dermis (deep) layer – This layer is mainly made up of tightly collagen and elastin fibers. There is a sharp boundary between the dermis and epidermis, divided by epidermal ridges. However, the fibrous elements of the dermis is intertwined with the beneath hypodermis (loose connective tissue) [5].

(c) The Hypodermis - Is composed of looser connective and adipose tissue. It is divided into two main layers - the upper fat layer (superficial fascia) of the hypodermis anchoring the dermis, accommodates more fat tissue than other layers due to their ability to expand, causing cellulite appearance on the skin surface; and deep fascia - this is the lower fat layer of the hypodermis that envelopes the muscle [6].

Cellulite affects 80-90% of the total female population worldwide [7][8], starting from puberty and increasing during menstruation, pregnancy, and nursing [9]. Yet its pathogenesis is not apparent [10]. It presents relief alterations i.e. depression and bulging of the skin topography, especially on the abdomen, buttocks and thighs, imitating the appearance of an orange peel or cottage cheese. These depressions and bulges are produced by underlying thick fibrous septa resulting in retraction of the skin and projection of adipocytes to the surface, respectively [11][12][13]. Women are more prone to cellulite than men as a result of the longitudinal arrangement of connective tissue bands (fibrous septa separating adipose tissue into channels) linking the deep fascia to the dermis. This arrangement allows easy projection of fat to the skin surface as the subcutis continues to stretch (an over expansion of the subcutis could lead to an increase in ectopic fat accumulation, promoting metabolic disorder), making the surface rough [14][15]. While in men, bands of connective tissue in their buttocks and thighs have an interwoven architecture, making it almost impossible for the projection of fat to the surface [15].

Cellulite is believed to be a multifactorial condition, although not entirely understood, causing adipose tissue degradation through stages of altering the interstitial matrix, micro-circulatory harmony, fat cell hypertrophy and hyperplasia, thereby, giving rise to blood and lymphatic vessel restriction and also the breakdown of elastin and collagen network [16][17]. When left untreated, cellulite can progress into a more severe form and may result in edema, and eventually fibrosis [17]. It also causes feelings of

insecurity and low self-esteem due to its unattractive nature, reducing the quality of life of patients [18] [19]. Although numerous medical devices and cosmetic products aiming to treat cellulite are on the market today, they seem to provide little to no clinical evidence to support their claims and none has been seen to produce a long-term effect or effectively manage the condition [19].

In this study, the *in vivo* efficacy of three most used anti-cellulite interventions was evaluated: (a) Dry Brushing. A technique used to massage the skin surface topography promoting lymphatic drainage and microvascular circulation, (b) Exercise. As millions of women spend thousands on gym memberships each year to try lower body fat and improve skin tone so, it only makes sense that the effectiveness of this intervention is evaluated, (c) Cream. The last intervention assessed was an anti-cellulite cream, providing the following claims "2-IN-1 BODY MOISTURISER + TONING CREAM" formulated with green coffee and Indian forskolin to inhibit lipogenesis and promote lipolysis.

This study was performed in collaboration with British Broadcasting Corporation (BBC) One, as part of a TV series entitled "The Truth About Looking Good"

3.2. MATERIALS AND METHODS

3.2.1. Participants/Volunteers

A total of nine (n = 9) healthy Caucasian female participants with varying cellulite grade (I-III) were enrolled into this randomized single blinded study via the BBC. Their age and weight range were between 29 to 64 years and 57.85 to 85.5 Kg, respectively. The inclusion criteria used was the presence of cellulite, no history of related surgical procedure and absence of pregnancy or any disease condition. Prior to the investigation, all 9 participants were well informed about the procedures involved and signed a consent form.

Recruitment of participants was performed by the BBC. BBC was also responsible for any ethical procedures involved in this study, as well as participant consent and medical clearance.

3.2.2. Study Design

All participants were equally assigned into 3 groups on their arrival. Group 1 was given the dry brushing therapy, group 2 exercise and finally, group 3 was appointed the cream intervention.

Theory of Interventions

- Dry Brushing. As cellulite is said to be mainly due to fluid retention containing toxic waste, causes dimpling and bulging on the skin surface. This cosmetic tool brush claims to stimulate lymph drainage, thus, eliminating lymph fluids in small vesicles in the dermal layer [20][21]. The participants in the first group were assigned this intervention for 5 weeks.

- Exercise. Another main cause of skin surface dimpling and bulging is fat accumulation and expansion in the subcutis [21]. A daily exercise routine (such as skaters, lunges, squats) that directly burns fat cells in the thighs and legs was appropriately chosen for group two throughout the period of study.

- Cream. Participants in the third group were assigned the test cream - an anti-cellulite cream containing 2 active ingredients, (a) Indian Forskolin. Its principal mode of action is elevating intracellular assembly of cyclic adenosine monophosphate (cAMP) and its associated functions by activating the enzyme adenylate cyclase [22]. High assembly of cAMP results in the activation of protein kinase enzyme. Ultimately, active protein kinase (PKA) enzyme stimulates another enzyme known as the hormone sensitive lipase, resulting in the disintegration of triglycerides (TG - the building block of adipose tissue) - causing fat burn in the subcutis [22][23]. (b) Caffeine. This also elevates cellular level of cAMP through the inhibition of the enzyme phosphodiesterase (which degrades intracellular cAMP) in the subcutis and skeletal muscles, in turn activating hormone sensitive lipase resulting in lipolysis [24][25].

The study was carried out over a period of 5 weeks, during which the participants were asked not to apply any other moisturizer or cellulite reducing products to their right posterior lateral thigh (beneath the buttocks), the human participant test site with the exception of those in group 3 who were assigned the test cream. Two skin measurements were taken, the first at the start of the experiment, time zero (t_0) before any intervention was employed and the second measurement was taken at the end of the experiment, 5 weeks (t_5).

3.2.3. Measurement of Skin Elasticity and Firmness

The Cutometer® dual MPA 580, (Courage - Khazaka electronics, Cologne, Germany) is a dermal elasticity meter that determine the degree of skin firmness and elasticity. It is also used in efficacy testing, providing claim support for a wide range of cosmetic products. The principle of operation of the Cutometer is based on suction, whereby, the device produces a negative pressure and an area of the skin in which the probe is placed is pulled into the small circular opening. As an optical measuring system, it is equipped with a light source, two prisms opposite one another that project the light generated to a receiver. The distance (mm) of skin penetration determines the brightness of the light, allowing the assessment of the following parameters,

- R0 (mm) – The lower the value (<0.5), the firmer the skin and vice versa

  R0 = Uf,   Where R0 is firmness and Uf is the complete elastic curve or the highest point (maximum amplitude) of the curve.

- R2 (%) – The adjacent the value is to 1 or 100% (>0.9 or 90%), the more elastic the skin.

  R2 = Ua/Uf,   Where R2 is the gross elasticity, Uf the maximum amplitude and Ua the relaxation distance.

- R5 (%) – The adjacent the value is to 1 or 100% (>0.9 or 90%), the more elastic the skin.

  R5 = Ur/Ue,   Where R5 is net elasticity, Ur is the elastic portion of the suction phase and Ue the elastic portion of the relaxation phase.

- R7 (%) – The adjacent the value is to 1 or 100% (>0.9 or 90%), the more elastic the skin.

R7 = Ur/Uf, Where R7 is the elastic portion, Ur is the elastic portion of the suction phase and Uf is the complete elastic curve.

- R9 (mm) - The adjacent the value is to 0, the firmer the skin (measured in mm).

R9 = R3 – R0, Where R9 is the fatigue or tiring effect, R3 is the maximum amplitude of the final curve and R0 is the maximum amplitude of the initial curve.

3.2.4. Measurement of Skin Surface Texture Parameters

3.2.4.1. Visioscan

To evaluate skin surface texture (roughness and micro-relief), the Visioscan was used - A black and white high resolution video sensor camera with a UVA light generator, illuminating the skin. The device which uses an arbitrary unit, produces an explicit assessment of the stratum corneum without protruding into the deeper layers of the epidermis based on the following,

- SE_R – The smaller the value (<5.0), the rougher the skin.

SE_R = 10 x Linf / [(Fax + Fay)/2], Where SE_R is the roughness, Linf is the number of pixels, Fax and Fay is the average number of horizontal and vertical wrinkles, respectively.

- SE_{SM} - The smaller the value, the smoother the skin (<100).

SE_{SM} = 100/ [(Co - Cu)^x(Fmx + Fmy)], Where SE_{SM} is the Smoothness, Co – Cu is the average width of the histogram, Fmx is the average width of wrinkles in x direction and Fmy is the average width of wrinkles in y direction.

- Desquamation, SE_{SC} (%) – The smaller the value, the more the scaling of the stratum corneum (<0.5). It corresponds to skin moisture.

- Wrinkles, SE_W – The higher the value, the more apparent the wrinkles (>70).

SE_W = (Fmx + Fmy) x 100/ (Fax +Fay), Where Fmx is the average width of wrinkles in x direction, Fmy is the average width of wrinkles in y direction, Fax and Fay is the average number of horizontal and vertical wrinkles, respectively.

3.2.4.2. Visiometer

The Visiometer is more or less like the Visioscan, except that it uses a blue silicone dye to produce skin replicas for surface texture measurements. It is based on the principle of Lambert's and Beer law where, the amount of light absorbed is equivalent to the thickness of replica produced. To assess the skin surface texture, the following parameters (measured in μm) are important,

- Energy – Young, elastic and hydrated skin shows increased energy value (>0.1) than a rough or aged skin.

- Variance – Highly rough skin gives elevated variance values.

- Contrast – A smooth or even skin gives a low contrast value (<0.5) compared to a rough skin.

- Entropy – A smooth or even skin gives low entropy value (<0.5) than rough skin.

- Homogeneity – An elastic and hydrated skin gives an elevated homogeneity value (>2.0).

3.2.5. **Photonumeric Assessment of Cellulite Severity**

High-definition photographs of the women's thigh area were taken before, t_0 and after treatment, t_5 at the medical photography unit at the Sunderland Royal Hospital (SRH). The number of bulging and depressions was inspected and scored by 2 independent health professionals, after which a comparison of pre- and post-photographs for each volunteer was made. The criteria used in scoring cellulite severity were developed and validated by Hexsel Table 3.1, (please see appendix for full details) [12].

The volunteers also had the pre- and post-photographs taken of their right posterior thigh by an expert using an ultrasound system (method not shown in this report), in order to observe changes in their body fat.

Table 3.1. Cellulite Severity Scoring and Classification.

Score	Severity Scale	Classification
0	0	Absent
1	1-5	Mild
2	6-10	Moderate
3	11-15	Severe

3.2.6. **Statistical Analysis**

All data-set analysis during the course of study was performed using IBM SPSS statistical software version 23.0, to assess the correlation of data obtained at t0 and t5 i.e. how statistically significant ($p < 0.05$) the three interventions are likely to cause a change or difference in cellulite appearance from the initial measurement (without treatment) to the final measurement (with treatment application for 5 weeks). The two factor ANOVA-mixed design method was employed, due to its ability to compare the difference of repeated measures (2 or more time points), presenting the p-value in a table of 'Mauchly's test of Sphericity' (if the assumption of Sphericity is not yet met) or as 'Tests within-Subject Effects' (when the assumption of Sphericity can be made). A 'Pairwise Comparisons' was also produced by the test consisting of severally paired t-tests with Bonferroni correction (to help minimize overall error), as well as calculating the mean difference value.

P-value < 0.001 or 0.05 is classified as a statistically significant value i.e. there is a 99.9% or 95% possibility the relationship is less than likely to have occurred by chance.

3.3. **RESULTS AND DISCUSSION**

3.3.1. Participants/Volunteers

The characteristics of the 9 healthy Caucasian female participants with varying cellulite grade (I-III) were summarized in Table 3.2. Their mean age and pre-weight were 47.3 years and 72.5 Kg, respectively. At the end of the 5 weeks treatment, the mean weight value was 72.02 Kg.

Table 3.2. Pre- and Post-Treatment Weight Assessment.

Volunteer No	Age	Height (m)	Pre-Weight (Kg)	Post-Weight (Kg)	Intervention
1	36	1.65	81.05	82.15	Dry Brushing
2	51	1.55	57.85	57.05	Dry Brushing
3	64	1.59	85.05	86.48	Dry Brushing
4	45	1.63	59.25	58.75	Exercise
5	29	1.68	85.5	84.05	Exercise
6	38	1.61	69.55	69.75	Exercise
7	62	1.55	59.4	57.55	Cream
8	51	1.68	84.5	80.85	Cream
9	50	1.66	71	71.55	Cream

3.3.2. Measurement of Skin Elasticity and Firmness

The measurement of skin firmness and elasticity was repeated in triplicate (n = 3) for each participant and their individual mean was taken. As seen in Table 3.3, five individuals had high R0 value of more than 0.5, four were seen to show low R2 value (<0.90), four also showed low R5 values of <0.90. Most of the volunteers (n = 8) showed low R7 values of <0.90 while an overall low R9 value was observed. In comparison, the four individuals who had low R2 values were also seen to have low R5 and R7 values.

Out of the 3 interventions, exercise showed the highest improvement in firmness (an average total of 52.8%), followed by the dry brushing (an average total of 48.6%) and the cream showed the least firmness average increase (an average total of 32.5%, however, the highest individual increase in firmness was seen in this group, volunteer 7). Total elasticity average was highest in the dry brushing group (7.8%), followed by the cream group (6%) and the least was seen in the exercise group (3.2%). However, in comparing the three interventions, the cream showed improvement in all elasticity parameters, R2, R5 and R7 of the subjects with volunteer 8 having an increased R2 by 5.1%, R5 increased by 5% and an increase in R7 by 2.8%. In volunteer 9, R2 increased by 6.6%, R5 by 8.5% and an increase in R7 by 7.8%, this makes the cream have the only increase in R5. Nevertheless, dry brushing showed the highest percentage improvement in R2 by 18.1% in volunteer 3, compared to others.

However, R2, R5, and R7 in all volunteers showed no statistical significance (P value > 0.05) at the end of the 5 weeks study, with the exception of R0 showing a significant difference $p = 0.026$ (Table 2.5), which means that statistically, the interventions involved in the study were only able to improve firmness by an average 0.538 and not skin elasticity. Results obtained from statistical analysis is influenced by the sample size as a larger sample size makes the analysis strong and more reliable, therefore, the disparity seen in the statistical data compared to the actual data could be as a result of the small number of volunteers involved in the study.

Table 3.3. Pre- and Post-Treatment Measurement for Firmness and Elasticity.

Volunteer No	Treatment	R0	R2	R5	R7	Intervention
1	Before	0.3586	0.8526	0.8256	0.7181	Dry Brushing
	After	0.3563	0.8815	0.8186	0.7317	
2	Before	0.9593	0.9841	0.9033	0.8365	Dry Brushing
	After	0.2873	0.9062	0.8039	0.7311	
3	Before	1.4367	0.7382	0.7631	0.6344	Dry Brushing
	After	0.3590	0.8720	0.6879	0.6047	
4	Before	0.4347	0.9019	0.9140	0.7660	Exercise
	After	0.3206	0.9366	0.8384	0.7860	
5	Before	1.1970	0.9712	1.0093	0.9375	Exercise
	After	0.3803	0.9332	0.9471	0.8445	
6	Before	1.5120	0.9468	0.9821	0.8787	Exercise
	After	0.5436	0.9234	0.9066	0.8104	
7	Before	1.4646	0.9251	0.9065	0.8195	Cream
	After	0.3400	0.8254	0.7691	0.6661	
8	Before	0.3867	0.8767	0.7437	0.6754	Cream
	After	0.3513	0.9211	0.7809	0.6941	
9	Before	0.2803	0.8822	0.8682	0.7485	Cream
	After	0.248	0.9400	0.9422	0.8068	

Where; (a) Firmness, R0 (mm) – The lower the value (<0.5), the firmer the skin. (b) Gross Elasticity, R2 (%) – The adjacent the value is to 1 or 100% (>0.9 or 90%), the more elastic the skin. (c) Net Elasticity, R5 (%) – The adjacent the value is to 1 or 100% (>0.9 or 90%), the more elastic the skin. (d) Elastic Portion, R7 (%) – The adjacent the value is to 1 or 100% (>0.9 or 90%), the more elastic the skin.

Table 3.4. Percentage (%) Change in Skin Firmness and Elasticity

Volunteer No	R0 (%)	R2 (%)	R5 (%)	R7 (%)	Intervention
1	**0.64**	**3.4**	-0.85	**1.9**	Dry Brushing
2	**70.1**	-7.9	-11	-12.6	Dry Brushing
3	**75**	**18.1**	-9.9	-4.7	Dry Brushing
4	**26.2**	**3.8**	-8.3	**2.6**	Exercise
5	**68.2**	-3.9	-6.2	-9.92	Exercise
6	**64**	-2.5	-7.7	-7.8	Exercise
7	**76.8**	-10.8	-15.2	-18.7	Cream
8	**9.2**	**5.1**	5	**2.8**	Cream
9	**11.5**	**6.6**	8.5	7.8	Cream

The above % change was calculated using the formula; (final value – original value)/original value X 100, where the original value is the initial/before measurement and the final value is the after measurement
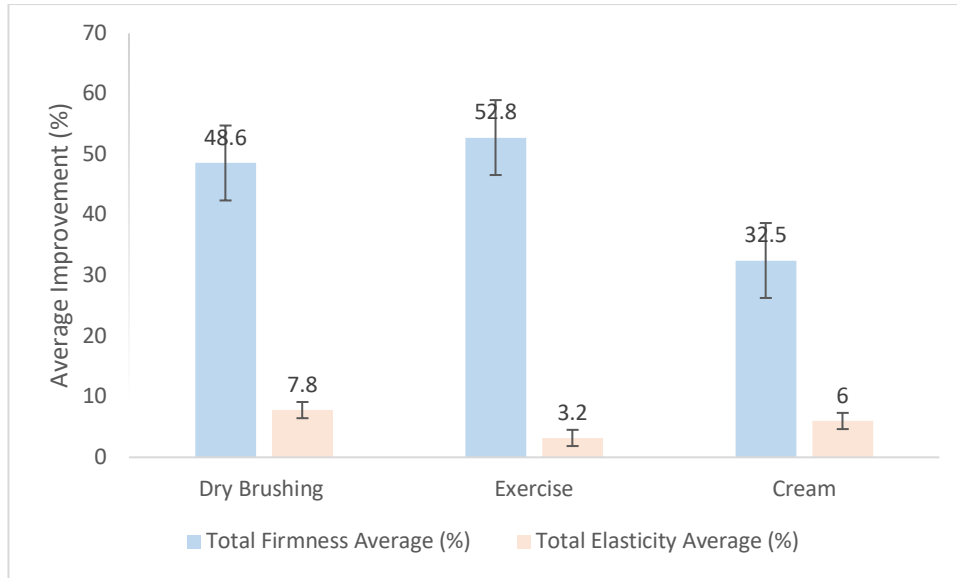
Figure 3.1. Total Firmness and Elasticity Average Improvement.

Table 3.5. Correlations/Relationships of Pre- and Post-Treatment for all Three Groups

ANOVA Test	R0	R2	R5	R7
Mean Difference of t_0 and t_5	±.538[*]	±.007	±.047	±.214
Significance	**.026**	.814	.095	.038

3.3.3. Measurement of Skin Surface Texture Parameters

3.3.3.1. Visioscan

For measurement of skin topographical area using the Visioscan (Table 3.6), the cream group showed the highest overall improvement in the roughness parameters, SE_R 20.5%, SE_{sc} 49% SE_w -52%, SE_{sm} -16.7%. All three interventions exhibited a significant improvement in SE_{SM}, however, the lowest average improvement was observed in the cream group (-16.7%). Also, dry brushing, exercise and cream were able to reduce the appearance of fine lines by 25%, 31.1% and 52% respectively.

Table 3.6. Percentage (%) Change in Surface Topography Visioscan Measurement.

Volunteer No	SE_R %	SE_{sm} %	SE_{sc} %	SE_w %	Intervention
1	5.4	-29.2	-11.9	-37.8	Dry Brushing
2	-29.2	-6.2	33.3	-12.6	Dry Brushing
3	-8	-25.4	-29	-24.7	Dry Brushing
4	-41.1	-13.5	25.6	-32.6	Exercise
5	-26.5	-32.1	25.5	-33.8	Exercise
6	-77.9	-30.2	-10.5	-26.9	Exercise
7	4.9	-20.9	3.6	-13.5	Cream
8	48.9	-27.9	70	-92.2	Cream
9	7.9	-1.5	73.4	-50.3	Cream

Where; (a) Roughness, SE_R – The smaller the value (<5.0), the rougher the skin. (b) Smoothness, SE_{SM} - The smaller the value, the smoother the skin (<100). (c) Desquamation, SE_{SC} (%) – The smaller the value, the more the scaling of the stratum corneum (>0.5). It corresponds to skin moisture. (d) Wrinkles, SE_W – The higher the value, the more appearent the wrinkles (>70).

Table 3.7. Correlations/Relationships of Pre- and Post-Treatment.

ANOVA Test	SE_R	SE_{sm}	SE_{Sc}	SE_w
Mean Difference of t_0 and t_5	±.833	±45.363*	±.379	±28.995*
Significance	.115	**.003**	.085	**.004**

There was a significant difference in pre- and post-treatment measurement of skin smoothness, $p = 0.003$ and wrinkles $p = 0.004$. Skin smoothness improved by an average of 45.363 while wrinkles had a mean reduction of 28.995. Although, no significant reduction was observed in skin roughness, $p = 0.115$ and scaliness, $p = 0.085$.

Volunteer 1: Before / After

Volunteer 2: Before / After

| Volunteer 3: Before | After |
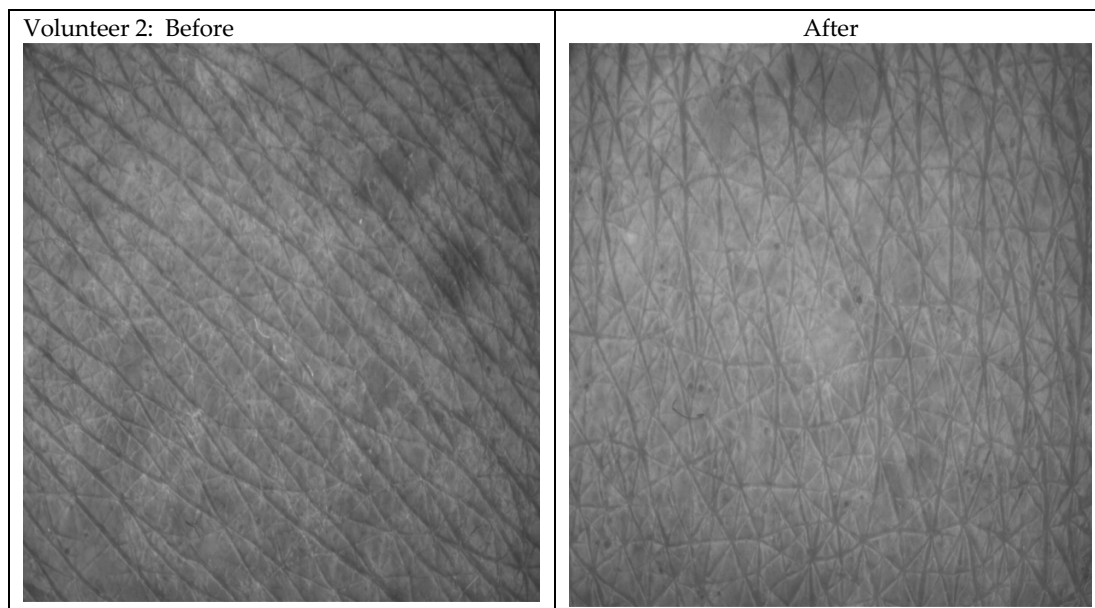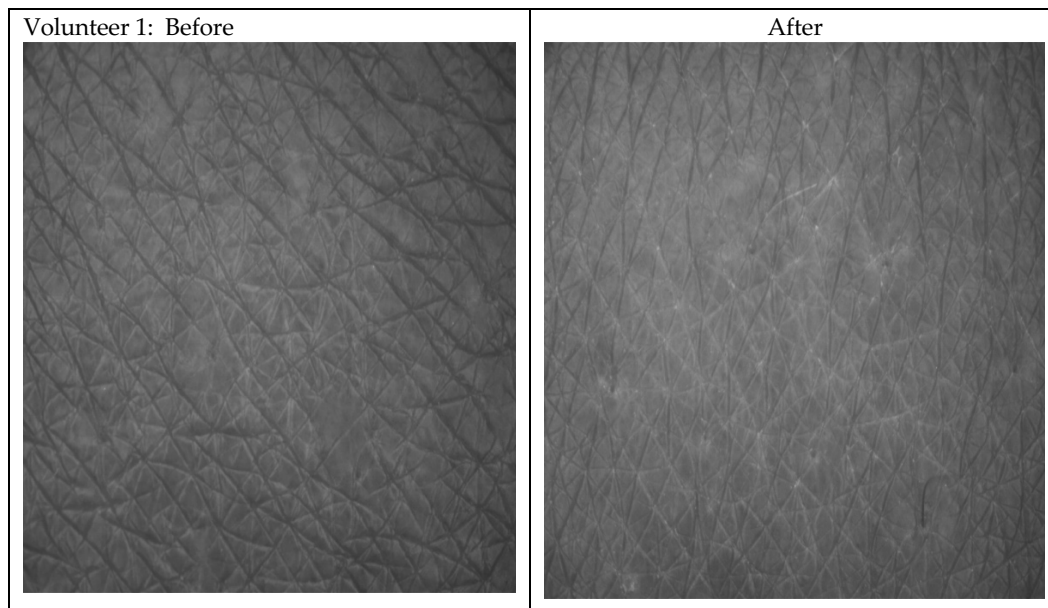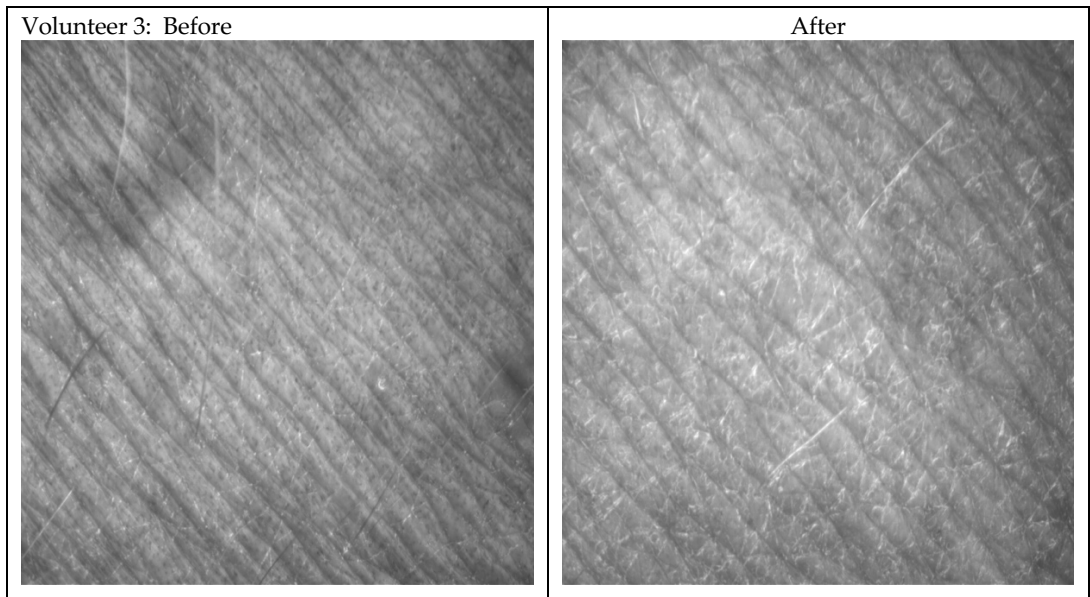
Figure 3.2. Before and After Treatment Skin-Visioscan Images for the Dry Brushing group. The post-photographs, in relation to the pre-photographs, showed a tremendous reduction in fine lines, showing improved surface smoothness or firmness, however, dryness increased as the skin appeared whitish. The increase in dryness was expected, due to the friction produced from rubbing the cosmetic tool brush against the skin, ridding the surface of its moisture content. Also, due to the fact that the volunteers were not allowed to apply any form of moisturisers or anti-cellulite products on their right posterior lateral thigh during the course of study.

| Volunteer 4: Before | After |
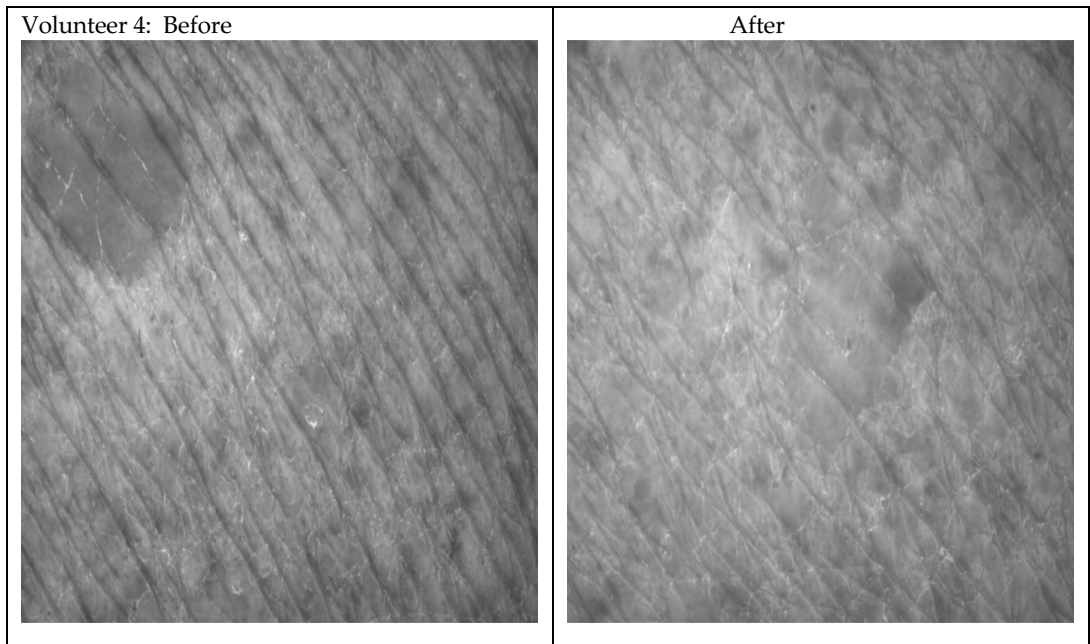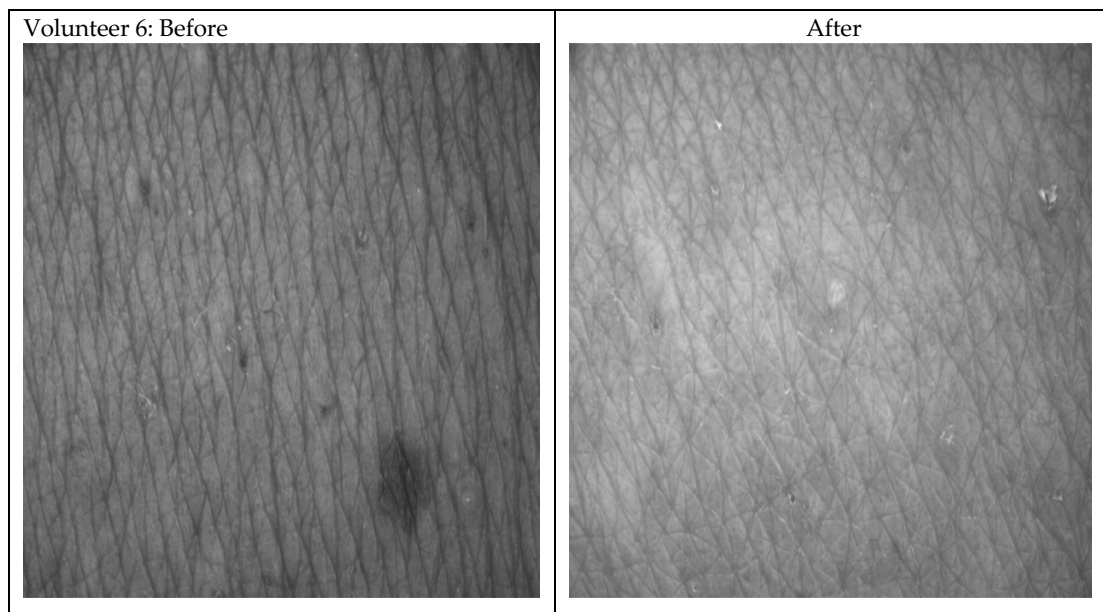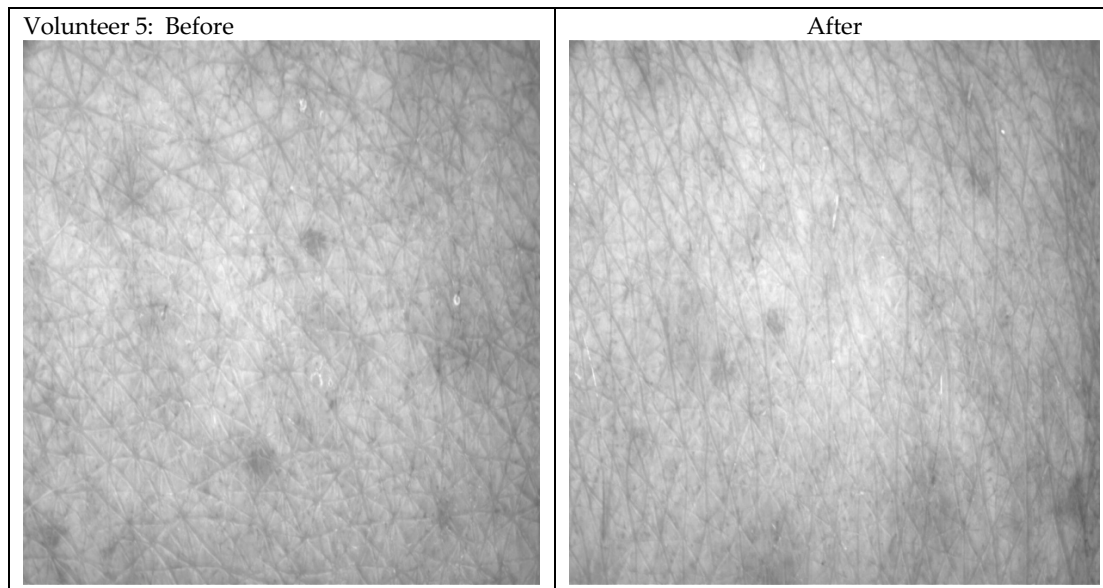
Figure 3.3. Before and After Treatment Skin-Visioscan Images for the Exercise group. When comparing the pre- and post-photographs, the fine lines were less visible in the post-photographs indicating increased firmness or smoothness, however, the skin had a whitish appearance, indicating an increase in dryness. The increase in dryness is also expected in this group, as volunteers were asked not to apply any moisturisers or anti-cellulite products on their right posterior lateral thigh during the course of study.
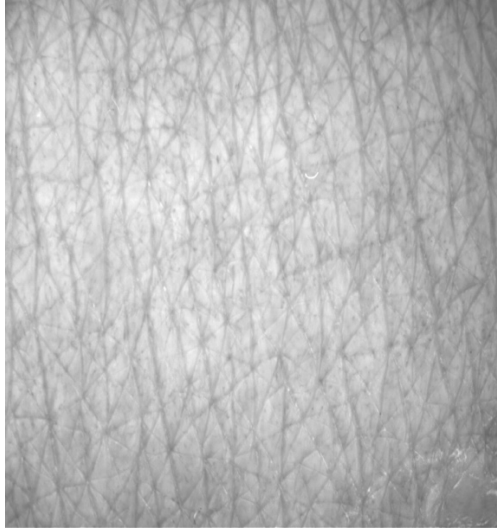
Volunteer 7: Before	After
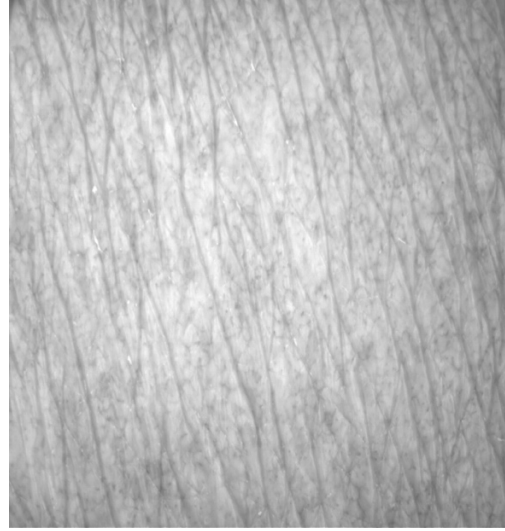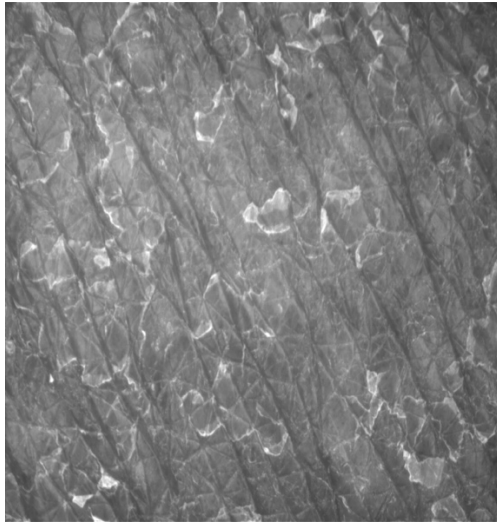
Volunteer 8: Before	After
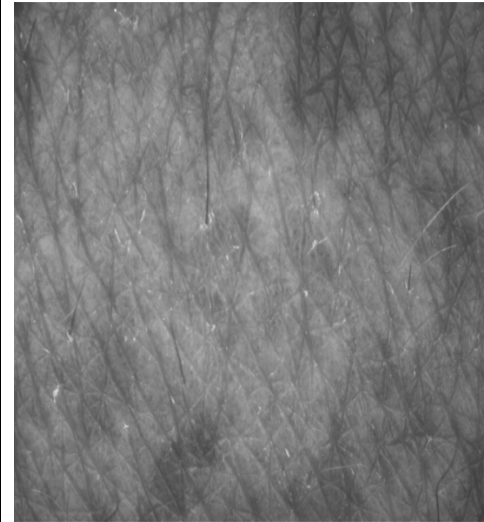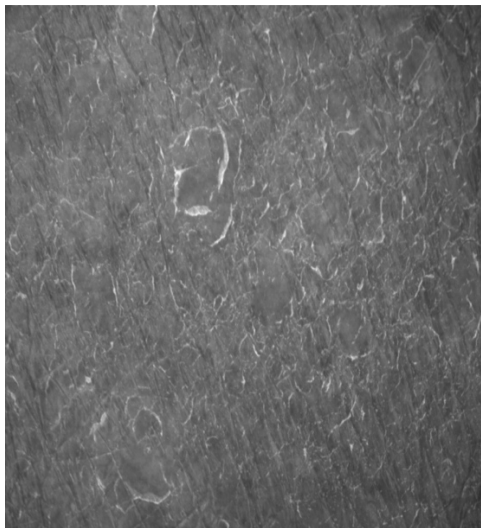
Volunteer 9: Before	After

Figure 3.4. Before and After Treatment Skin-Visioscan images for the Cream group. When comparing each set of photographs, the post-treatment photographs appeared to have fewer fine lines and the white residues or patches illustrating dry skin (as seen in the initial photographs) vanished. This means that the cream considerably hydrated the skin as claimed and improved smoothness or firmness.

Table 3.8. Percentage (%) Change in Skin Topography Visiometer Measurement.

| Volunteer No	Energy %	Contrast %	Var %	Ent %	Hom %	Intervention
1	-6.3	-7.7	0.86	1	-0.8	Dry Brushing
2	-6.25	3.6	11	0.5	0.25	Dry Brushing
3	7.4	-10.6	-0.74	-0.07	-1.1	Dry Brushing
4	32.1	15.2	12.2	-2.8	0.8	Exercise
5	-10.3	-1.5	1.8	0.8	-0.3	Exercise
6	-17.8	-0.2	-1.6	1.6	-0.3	Exercise
7	-12.5	-4.8	-2.1	1.3	-0.4	Cream
8	51.9	46.8	32.3	-5	4.7	Cream
9	20.8	50.2	35.2	-3.2	5.2	Cream

Where; (a) Energy – Young, elastic and hydrated skin shows increased energy value (>0.1) than a rough or aged skin. (b) Variance, Var – Highly rough skin gives elevated variance values. (c) Contrast, Con – A smooth or even skin gives a low contrast value (<0.5) compared to a rough skin. (d) Entropy, Ent – A smooth or even skin gives low entropy value (<0.5) than rough skin. (e) Homogeneity, Hom – An elastic and hydrated skin gives an elevated homogeneity value (>2.0).

3.3.3.2. Visiometer

In Table 3.8, the cream group showed the highest overall improvement in the texture parameters, energy 20.1%, entropy -2.3% and homogeneity 3.2%, however, the lowest improvement in contrast 30.7% and variance 21.8% was observed. Dry brushing showed the highest improvement in comparison to the cream and exercise group, showing a total improvement in energy of -1.7%, contrast -4.9%, variance 3.7%, entropy 0.47% and homogeneity -0.55%. The least improvement was seen in the exercise group which gave a total improvement in energy by 1.3%, contrast 4.5%, variance 4.1%, homogeneity 0.06%, and entropy -0.13%.

3.3.4. Photonumeric Assessment of Cellulite Severity

In Table 3.9, the exercise group showed the least average percentage improvement of 12.7% in photo-numeric (PN) scale but, the highest total percentage improvement in body fat, 5.5%, when compared to other groups. Dry brushing was seen to have a total percentage improvement of 3.5% in body fat and the highest average percentage improvement in photo-numeric scale, 25.8% in relation to other groups. The cream showed an average percentage improvement of photo-numeric scale by 14.7% but, the least total percentage improvement in body fat, 1% was observed.

Table 3.9. Pre- and Post-Treatment Body Fat and Photonumeric Assessment.

Volunteer No	Pre-BF	Post-BF	%Change in BF	Pre-PN	Pre-PN	PN % Change	Intervention
1	39.2	39.1	0.3	11	8	27.3	Dry Brushing
2	34.2	33.4	2.3	13	8.5	34.6	Dry Brushing

3	44.9	44.5	0.9	9.5	8	15.7	Dry Brushing
4	30.03	29.7	1.1	8	7	12.5	Exercise
5	38.3	36.6	4.4	9.5	8	15.8	Exercise
6	38.3	38.5	-0.5	10	9	10	Exercise
7	34.9	35.4	-1.4	10.5	9	14.3	Cream
8	38.5	38.1	1.0	8	8	0	Cream
9	34	34.5	-1.5	10	7	30	Cream

Where, PN stands for Photo-numeric; and BF stands for Body Fat.

Table 3.10. Correlations/Relationships of Pre- and Post-Treatment.

ANOVA Test	Energy	Contrast	Var	Ent	Hom	PN
Mean Difference of t_0 and t_5	±.001	±.103	±.388	±.010	±.013	±1.889*
Significance	.623	.127	.066	.456	.217	**.004**

The ANOVA statistical analysis from the table above showed no significant difference ($p>0.05$) in the visiometer measurement after 5 weeks of treatment. However, a strong statistical significance, $p = 0.004$ was observed between the pre- and post-photonumeric measurement. This means that there is a clear difference between the two time points and an average reduction in cellulite by 1.889.
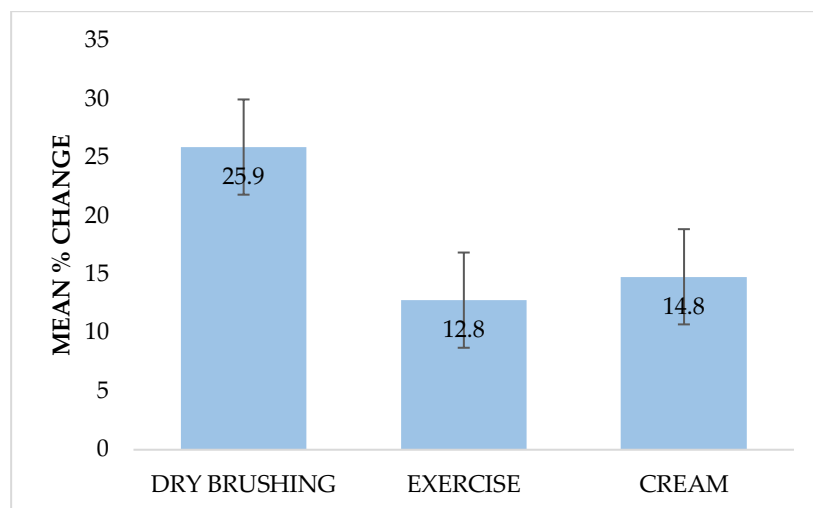
Figure 2.5. Average Percentage (%) Photo-numeric Change

3.4.   CONCLUSION

Cellulite affects most of the entire female population, it is said to be a multifactorial condition caused by stages of morphological, inflammatory, structural and biochemical changes, making it difficult to abolish [26]. The current experiment investigates the best method of eliminating cellulite in a group of female volunteers for a period of 5 weeks. The elasticity data from this study proved dry brushing to be the best treatment for cellulite among the 3 interventions evaluated presumably improved skin elasticity through elastin fibre synthesis and reconstruction, since the appearance of cellulite is said to cause a reduction or breakdown of elastin and collagen network [16][17]. In order to obtain an optimal effect from the dry brushing treatment, the instructions for brushing must be

carefully and closely followed, as volunteer 3 showed the highest possible improvement in gross elasticity compared to the rest in the same group. This could only mean that the method of brushing can determine the end result of the treatment. All 3 interventions brought about skin firmness or tightening, although exercise proved to be the best among the three treatments for skin firmness.

Results obtained from the measurement of skin texture using the Visioscan proved that all three interventions improved skin smoothness, the cream was the only intervention to show an overall improvement in roughness parameters. This implies that the cream is capable of reducing skin surface dimpling and bulging through skin hydration, the action of Indian forskolin and caffeine causing the reduction of adipocyte hypertrophy [22][23][24][25], allowing elastin and collagen network reconstruction. At the end of the study, it was not unusual that dry brushing will cause skin desquamation and dehydrating as the process produces abrasion on the skin when rubbing the brush against its surface. Similarly, the Visiometer measurement also showed the cream intervention to be the best treatment for rough and dehydrated skin. While dry brushing proved to promote even or smooth skin but, it was shown to cause dehydration.

The post-treatment photographs of the thigh area presented decreased number of visible bulging and depressions on the surface in all groups, with dry brushing proving to be the best anti-cellulite treatment (Figure 3.5). Although exercise significantly reduced body fat (as it demonstrated the highest total percentage improvement in body fat by 5.5% among the 3 interventions), it does not effectively improve cellulite. The body fat measurement proved that the action of Indian forskolin and caffeine to burn fat was very low, however, improved cellulite appearance. The development of a novel formulation that would help transport these actives through the tough barrier of the stratum corneum, delivered to the targeted site, would lead to a better management of cellulite.

The ability of dry brushing and anti-cellulite cream to produce a long-term effect is uncertain, this presents a constraint to the study, another limitation is the small sample size involved and the lack of diversity in selected volunteers. As cellulite is affected by various intrinsic and extrinsic factors, future studies should investigate their degree of influence on treatment outcomes as well as treatment combinatory approach for effectiveness. Also, further studies should assess the molecular mechanisms (current suggestions includes the following factors, structural, inflammatory, morphological and biochemical alterations) involved in the pathophysiology of the condition for a better understanding of cellulite and ultimately, its successful treatment.

REFERENCE

1. WebMD Boots. (2017). *Picture of the skin*. [online] Available at: http://www.webmd.boots.com/skin-problems-and-treatments/guide/picture-of-the-skin [Accessed 10 Jun. 2017].

2. Melzack, R. and Casey, K.L., 1968. Sensory, motivational and central control determinants of pain: a new conceptual model. *The skin senses, 1*.

3. Roosterman, D., Goerge, T., Schneider, S.W., Bunnett, N.W. and Steinhoff, M., 2006. Neuronal control of skin function: the skin as a neuroimmunoendocrine organ. *Physiological reviews, 86*(4), pp.1309-1379.

4. Montagna, W., 2012. The structure and function of skin. Elsevier.

5. Fowler, I. (1984). Human Anatomy. 1st ed. Belmont, California 94002: Wadsworth Publishing Company, pp.88-96.

6. Martini FH, Bartholomew EF. Essentials of anatomy and physiology, ed 5, New York, 2009.

7. Pianez LR, Custódio FS, Guidi RM, de Freitas JN, Sant'Ana E. Effectiveness of carboxytherapy in the treatment of cellulite in healthy women: a pilot study. Clinical, cosmetic and investigational dermatology. 2016;9:183.

8. DiBernardo BE, Sasaki GH, Katz BE, Hunstad JP, Petti C, Burns AJ. A multicenter study for cellulite treatment using a 1440-nm Nd: YAG wavelength laser with side-firing fiber. Aesthetic surgery journal. 2016 Feb 18;36(3):335-43.

9. Peterson JD, Goldman MP. Laser, light, and energy devices for cellulite and lipodystrophy. Clinics in plastic surgery. 2011 Jul 31;38(3):463-74.

10. Milani GB, Natal Filho AD, João SM. Correlation between lumbar lordosis angle and degree of gynoid lipodystrophy (cellulite) in asymptomatic women. Clinics. 2008;63(4):503-8.

11. Yosipovitch G, Devore A, Dawn A. Obeisity and the skin: skin physiology and skin manifestations of obesity. Journal of the American Academy of Dermatology. 2007 Jun 30;56(6):901-16.

12. Hexsel DM, Dal'Forno T, Hexsel CL. A validated photonumeric cellulite severity scale. Journal of the European Academy of Dermatology and Venereology. 2009 May 1;23(5):523-8.

13. Hexsel DM, Mazzuco R. Subcision: a treatment for cellulite. International journal of dermatology. 2000 Jul 1;39(7):539-44.

14. Letter, A. and Roden, M. Ectopic fat and insulin resistance. Current diabetes reports. 2008 Jun 1;8(3), pp. 185-191.

15. Hexsel D, Soirefmann M. Cosmeceuticals for cellulite. InSeminars in cutaneous medicine and surgery 2011 Sep 1 (Vol. 30, No. 3, pp. 167-170). Frontline Medical Communications.

16. Soares IJ, Cristina doAmaral T, Miranda deAraújo DD, Sales deMelo V, Valentim daSilva RM, Meyer PF. Effects of combined therapy in celullitis: controlled clinical trial, randomized and blind. Manual Therapy, Posturology & Rehabilitation Journal= Revista Manual Therapy. 2016;14.

17. Naves JM, Soares C, Svezzia VD, Cussolim FD, Mendonça AC. Correlation between pelvic alignment and cellulitis. Fisioterapia e Pesquisa. 2017 Mar;24(1):40-5.

18. Purim KS, Titski AC, and Leite N. Dermatological aspects influencing the practice of physical activities by obese individuals. Fisioterapia em Movement. 2015 Dec;28(4):837-50.

19. Costa A, Alves RT, Pegas Pereira ES, Martins Cruz FA, Fidelis MC, Marega Frigerio R, Montagner S, de Medeiros VL. Gynoid Lipodystrophy and clinical therapy: critical analysis of available scientific publications. Surgical & Cosmetic Dermatology. 2012; 4 (1).

20. Shellman JJ, inventor; Shellman Jeremy J, assignee. Method for administering phototherapy as a cellulite firming treatment. United States patent US 7,101,385. 2006 Sep 5.

21. Smith E, Oblong J, Samuel J, Bissett D, Bascom C, Kelm G, inventors; Procter, Gamble Co, assignee. Method, kit and device for the treatment of cosmetic skin conditions. United States patent application US 10/132,045. 2003 Apr 10.

22. Wagh VD, Patil PN, Surana SJ, Wagh KV. Forskolin: upcoming antiglaucoma molecule. Journal of postgraduate medicine. 2012 Jul 1;58(3):199.

23. Ding X, Staudinger JL. Induction of drug metabolism by forskolin: the role of the pregnane X receptor and the protein kinase a signal transduction pathway. Journal of Pharmacology and Experimental Therapeutics. 2005 Feb 1;312(2):849-56.

24. Dulloo AG, Seydoux J, Girardier L, Chantre P, Vandermander J. Green tea and thermogenesis: interactions between catechin-polyphenols, caffeine and sympathetic activity. International journal of obesity. 2000 Feb;24(2):252.

25. Dulloo AG, Duret C, Rohrer D, Girardier L, Mensi N, Fathi M, Chantre P, Vandermander J. Efficacy of a green tea extract rich in catechin polyphenols and caffeine in increasing 24-h energy expenditure and fat oxidation in humans–. The American journal of clinical nutrition. 1999 Dec 1;70(6):1040-5.

26. Schonvvetter B, Soares JL, Bagatin E. Longitudinal evaluation of manual lymphatic drainage for the treatment of gynoid lipodystrophy. Anais brasileiros de dermatologia. 2014 Oct;89(5):712-8.

CHAPTER 4

NIOSOMAL FORMULATION AND CHARACTERIZATION STUDIES

4.1. INTRODUCTION

In the 1970's, the formation of non-ionic surfactants into vesicles was first proposed by cosmetic scientists [1]. Non-ionic surfactant vesicles or niosomes are microscopic drug carriers used for targeted drug delivery to desired tissues, sustained drug release and reduced toxicities or adverse reactions due to their ability to alter biodistribution and pharmacokinetics. Niosomes produce unilamellar and multilamellar spheres and are able to encapsulate a wide range of drugs or actives. The structure of niosomes allows for hydrophilic drug molecules to be entrapped within the aqueous compartment while the lipophilic drugs are present in the matrix bilayer, Figure 4.1 [2][3]. They can be formulated using the following techniques: thin layer evaporation or thin film method, ether injection, melted amphiphile injection, miscellar solutions or enzymes, transmembrane pH gradient, microfluidization, bubbling of nitrogen, reversed phase evaporation and hot water method. Niosomes possess very similar physical characteristics and *in vivo* behavior to liposomes but, are more cost effective when compared [4][5].

Furthermore, niosomes do not possess the phospholipids present in liposomes, these phospholipids are highly prone to oxidative degradation, producing instability. The phospholipids in liposomes require comprehensive purification and variable purity due to their natural origin. Niosomes show extensive photostability and intrinsic skin penetration (due to its low molecular weight and ability to passively diffuse through membranes), as well as increasing drug concentration in the superficial strata of the skin. Liposomes need to be stored in an inert nitrogen environment to help maintain stability, whereas this is not required for niosomes [6][7][8][9]. These advantages of niosomes over liposomes presents a more feasible tool for topical and transdermal drug delivery [9].
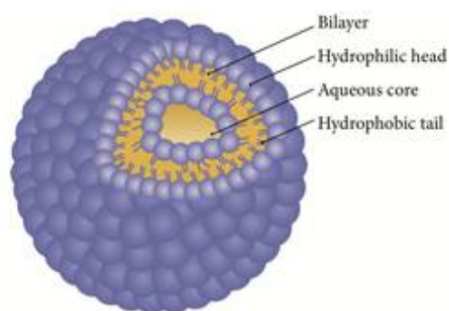
Figure 4.1. The Structure of Non-ionic surfactant vesicle (NSV) [10].

The mechanism of niosomes with cells interaction involves [11][12]: (a) Intermembrane transfer – Lipid transfer occurs upon close passage of niosomal lipid membrane to cell membrane phospholipids. Niosomes can interact with lipoproteins and may result in the destruction of the niosomal membrane. (b) Contact release – Aqueous components of the niosomes can be released when they come in contact with cells, resulting to increased noisomal membrane permeability. (c) Adsorption - Niosomes can be absorbed into cells through specific cell receptors to niosomal ligand binding or by

physical attractive forces. (d) Fusion – Fusion of cell membranes and niosomes may occur upon close passage by diffusion process, resulting in total mixture of drug molecules into the cytoplasm. (e) Endocytosis – Engulfment of niosomes into the cell, where it is degraded in the cytoplasm by lysozymes, releasing the encapsulated drug [11][12].

Methylene blue is a tricyclic thiazine drug soluble in both water and organic solvents. Methylene blue (MB) is a blue cation subjected to redox catalysis – MB produces leucomethyleneblue (an uncharged colorless compound) after reduction by thioredoxin or nicotinamide adenine dinucleotide phosphate (NADPH). LeucoMB can be reoxidized in the presence of O_2 or $2Fe^{2+}$ back to MB. This redox cycle enables mitochondrial electron transport, reducing superoxide production. The excretion of MB occurs via the urine in a mixture of demethylated metabolies, leucoMB and finally MB, here the urine appears to have a clear blue color but vanishes after a few days [13][14]. MB has been used to treat hepatopulmonary syndrome, septic shock, malaria, methemoglobinemia, cancer, ifosfamide neurotoxicity, as a heparin neutralizer in protamine allergy, priapism, alzheimers, resistance plague psoriasis and microbial infections [14][15]. In a study performed by Marimuthu *et al*., MB was seen to demonstrate antioxidant and free radical scavenging activities by targeting cellular mitochondria [16]. These free radicals are responsible for increasing collagen and elastin degradation while decreasing its synthesis by promoting matrix metalloproteinase (MMP) expression, and eventually result to dermal network alteration. In order to reverse this process, localized application of antioxidants to the skin surface can help reduce the production or accumulation of free radicals or neutralize its effect [17][18].

This research aims to formulate niosomal encapsulated MB for the repair of dermal matrix through collagen and elastin fiber synthesis in cellulite prone skin. Also, characterization studies such as microscopic examination, size, polydispersity index and zeta measurement, purification or separation studies and drug entrapment efficiency of the newly entrapped MB were conducted for the determination of the lead active niosomes to be incorporated into the cream base.

4.2 MATERIALS AND METHODS

4.2.1. Materials

Methylene blue (MB), cholesterol, span 65, solutol-HS 15 were obtained from Sigma-Aldrich, Inc. United Kingdom. Tris buffer solutions were of analytical grade.

4.2.2. Methods

4.2.2.1. Niosome Preparation

Five niosomal formulations were prepared using the thin-film hydration technique, with Phospholipid - cholesterol (45%); Surfactant - span 65 (45%); Cosurfactant - solutol-HS 15 (10%) each dissolved in 4mL organic solvent (chloroform) in a 250mL round bottom flask, for the manufacture of

300µmol of vesicles. The chloroform was removed using a rotary evaporator at 60℃, 40rpm and a vacuum of 464 ± 10 mbar by placing the 250mL flask at the interface of the H_2O in the bath, the pressure was allowed to drop until no chloroform was left and a thin film of the mix was formed on the flask wall (Figure 4.2). 5mL of Tris buffer pH 7.4 with 0.01mL or 10µL of the active, methylene blue (i.e. total drug concentration added is 0.002 v/v) was added to hydrate the lipid films, followed by gentle agitation – enabling formation of multi-lamellar vesicles and the entrapment of the actives in the vesicles. The mix was intermittently incubated at 60℃ for a period of 10 minutes while shaking to allow complete detachment of the lipid film, encouraging more drug entrapment. After which, the newly prepared niosomes were separated via sephadex G-50 column chromatography and characterized before incorporating the loaded vesicles into the cream base. Note, during the period of characterization, the prepared niosomes were stored at 4℃.
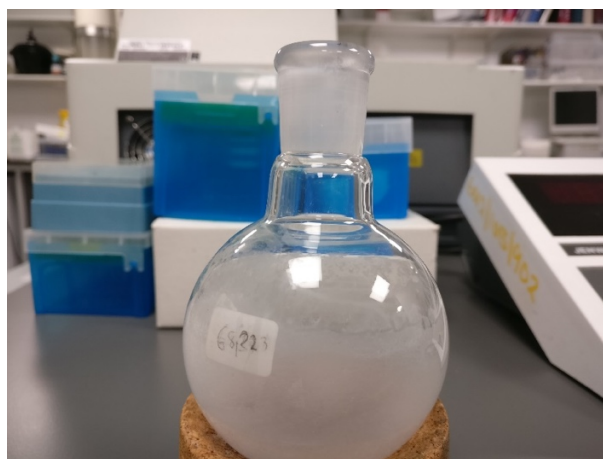
Figure 4.2. A photographic image of the thin film formed around the flask wall.

4.2.2.2. Total Drug Concentration

0.01mL of MB in 5mL of water to obtain the total concentration of the drug in % w/v, the below formula was used; Conc. = Amount/Volume

0.01mL/5mL = 0.002 v/v = 0.002 x 100 = 0.2% v/v

Therefore, the total amount of active to be present in added in 100mL cream formulation is 0.2% v/v.

4.2.2.3. Characterization Studies

Microscopic Examination

The microscopic studies were conducted before column separation using the Olympus microscope, AxioVision® Rel. software version 4.4. This was done by transferring 10µL of each product to a glass slide and viewed at angle 90, M100 magnification.

Size and Zetapotential (Charge) Measurement

Particle size of the prepared niosomal dispersions were performed using the photon correlation principle of the Malvern® ZETASIZER NANO Instrument (Malvern, UK) by adding 10µL of each model

to 990μL of distilled H_2O (100x dilution) in a cuvette cell. Also, particle charge analysis for stability of emulsion was also performed using the same instrument by mixing 10μL of each model with 990μL of distilled H_2O and injecting the mix into a double folded capillary cell through one of the two openings of the cell, while the other opening remained closed. All measurement was done in triplicate and at 25°C.

Purification/Separation Studies

In order to separate the free drug from the encapsulated or entrapped drug, the sephadex G-50 gel filtration was employed. The method was used to separate small volumes of the prepared niosomes by allowing 4 g of G50 powder to swell for 48 hours in a 60 mL 30 mM tris buffer (the mixture was gently stirred to avoid the particles breaking into very fine dust), each gram of the powder swells to approximately 10 mL gel so, the mix produced a 40 mL gel. The gel was gently stirred again and transferred into the column using a dropper, additional buffer was carefully added to the column as soon as the gel bed was formed. The prepared niosomes were individually added to the column without any disruption to the gel bed, once all the noisome sample had been absorbed into the gel, excess buffer was gently added to the column to prevent drying out. The entrapped drug eluted first and collected into a measuring cylinder, leaving the free drug in the gel.

Entrapment Efficiency

The amount of active drug, methylene blue encapsulated in the niosomes was determined at 665 nm using a systronic ultraviolet spectrophotometer to evaluate the eluent derived from the gel filtration column. The difference between the amount of active measured during formulation and amount eluted from the column was used to determine the entrapment efficiency.

The entrapped drug was then diluted 1:1000 (X1000) and calibrated, the standard solutions was performed in triplicate, repeated thrice and the mean data was used to produce the calibration curve. This was done to obtain the actual drug concentration.

4.3. RESULTS AND DISCUSSION

Microscopic Examination

The microscopic examination of the formulated niosomes were performed using the Olympus microscope, AxioVision® Rel. software version 4.4 showed the niosomes prepared by thin film hydration method were small in size (<1μm in diameter), spherical in shape, and unilamellar. Model B, C, and D observed at angle 90, M100 magnification were seen to have separate vesicles without aggregation or any irregularities. However, model A had visible levels of aggregation and model E had slight irregularities. Although, all models were formulated with the same excipients and concentrations, the variations observed can be attributed to mechanical stress (hand shaking or mixing) and/or heating interval during niosomal preparation.

Size and Zeta Potential Measurement

The mean particle size of a standard niosome varies from 50 to 1000nm [19]. A zeta potential value of +25 or -25 mV for a nanoparticle is said to be electrostatically stable while the values between +25 and -25 mV have electrostatic instability [20][21]. Zeta potential influences the movement of nanoparticles through a specific membrane, charges between +10 and -10 are considered neutral while those above +10 and -10 are said to be cationic and anionic, respectively. Strong cationic nanoparticles (i.e. >+30mV), due to their charge, have the tendency to disrupt cell walls and therefore are toxic to most biological membranes [22].

Particle size and charge of the dispersed niosome models using the Malvern® ZETASIZER NANO Instrument (Malvern, UK) at 25°C was shown in the Table 4.1.

Table 4.1. Particle Size and Zetapotential Measurement of Entrapped Actives.

Repeat	Size (d.nm)	Zetapotential (mV)	Conductive (mS/cm)	Temperature (°C)
1	763.8	-4.94	0.0138	25
2	656.3	-3.53	0.00875	25
3	592	-49.2	0.115	25
4	601	-34.5	0.0857	25
5	730	-3.64	0.0112	25

The table above showed the particle size ranged from 601 d.nm to 763.8 d.nm and 0.333 to 0.914, respectively. Repeats 2, 3, 4 and 5 proved to have more uniform niosomal dispersion size compared to model 1, which gave a high polydispersity index i.e. 0.914, showing the niosomal dispersion to be too heterogeneous or non-uniform in terms of its molecular mass and shape. This could imply that the formulation is not very stable.

A negatively charged dispersion was observed in all repeats from the zetapotential analysis (Figure 3), ranged from -3.53 to -49.2mV. Interestingly, repeats 3 and 4 showed good electrostatic stability -49.2 and -34.5mV, respectively. This means that repeats 3 and 4 are extremely stable against the formation of aggregates, rapid coagulation or flocculation, showing very low toxicity due to their strongly anionic nature. While repeats 1, 2 and 5 had neutral zeta values of -4.94, -3.53 and -3.64, respectively, indicating electrostatic instability.

Although, all repeats contained the same excipients and concentrations, the differences observed can be attributed to mechanical stress (hand shaking or mixing) and/or heating interval during niosomal preparation.

Repeat 1	
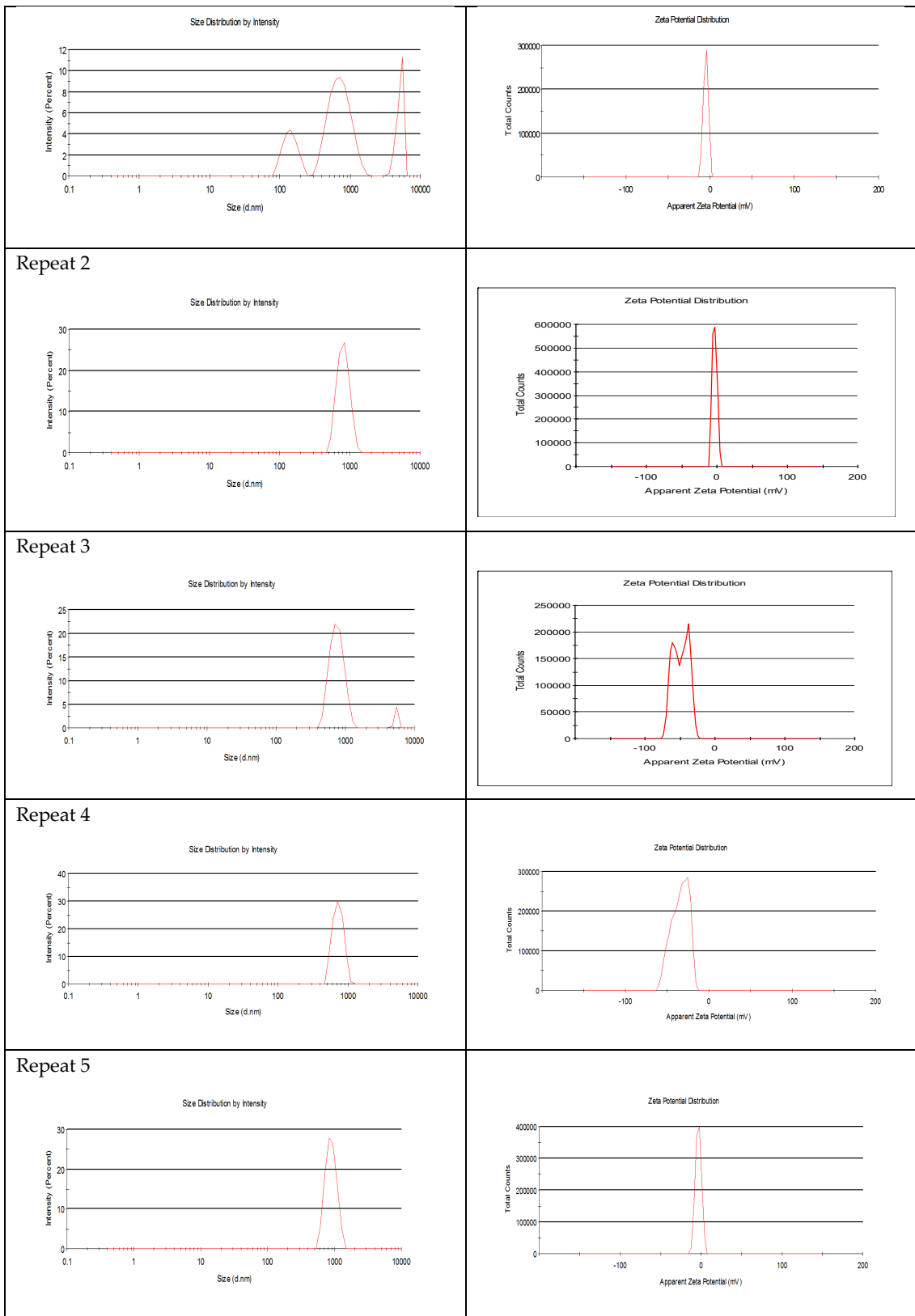
Figure 4.3. A Graphical Representation of Size (left) and Zetapotential (right) Measurement of the Niosomes.

Separation Studies

The entrapped drug (Methylene Blue) initially eluted out of the column was collected (about 10 mL each) into a measuring cylinder, appeared to be cloudy with a light blue shade compared to the unentrapped drug (final eluent) which gave a transparent blue appearance Figure 4.4. The entrapped drug from each model collected was then used to calculate the entrapment efficiency.
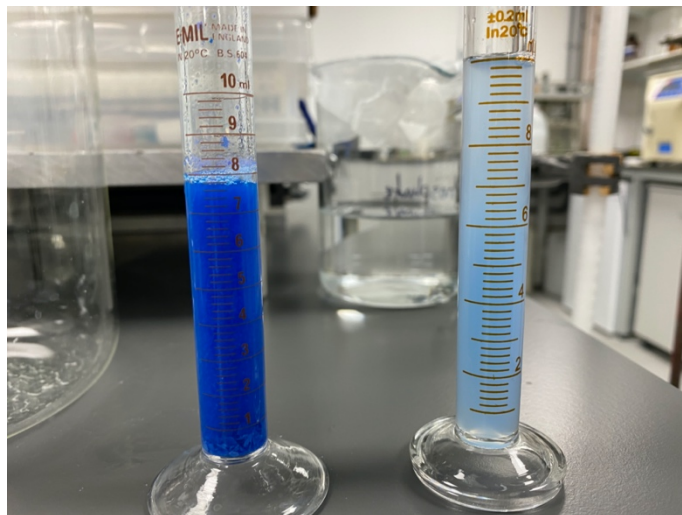
Figure 4.4. A Photographic Image of Unentrapped (left) and Entrapped (right) Active after Separation.

Entrapment Efficiency

The amount of active drug, methylene blue encapsulated in the niosomes was determined from the calibration curve by measuring the absorbance of dilution concentration (0.1 – 1.75 µg/mL) at 665 nm using a systronic ultraviolet spectrophotometer to evaluate the eluent derived from the gel filtration column. The difference between the amount of active drug added during niosomal formulation and amount eluted from the column was used to determine the entrapment efficiency i.e. EE = (EDC/TDA) X 100.

Table 4.2. Methylene Blue Concentration and Absorbance Values

Concentration (µg/mL)	Absorbance 1	Absorbance 2	Absorbance 3	Mean Absorbance
0.100	0.035	0.035	0.034	0.0347
	0.038	0.037	0.038	0.0377
	0.038	0.038	0.037	0.0377
0.250	0.035	0.035	0.036	0.0353
	0.039	0.039	0.039	0.0390
	0.038	0.039	0.040	0.0390
0.380	0.037	0.036	0.036	0.0363
	0.040	0.041	0.041	0.0407
	0.040	0.041	0.040	0.0403
0.500	0.036	0.036	0.036	0.0360
	0.042	0.043	0.043	0.0427
	0.042	0.041	0.042	0.0417
0.750	0.037	0.038	0.038	0.0377
	0.045	0.045	0.045	0.0450
	0.043	0.044	0.044	0.0437
1.000	0.038	0.038	0.038	0.0380
	0.045	0.046	0.046	0.0457

	0.046	0.046	0.047	0.0463
1.250	0.038	0.038	0.039	0.0383
	0.047	0.048	0.048	0.0477
	0.048	0.048	0.049	0.0483
1.500	0.039	0.039	0.040	0.0393
	0.049	0.050	0.049	0.0493
	0.049	0.049	0.050	0.0493
1.750	0.040	0.040	0.041	0.0403
	0.055	0.056	0.056	0.0557
	0.057	0.055	0.055	0.0557
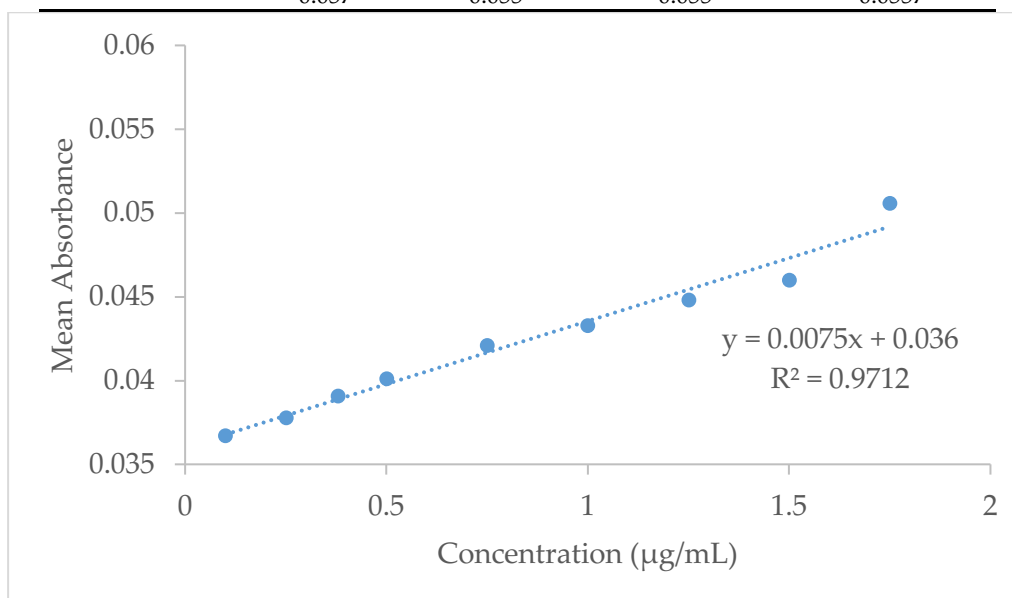
Figure 4.5. Calibration Curve of Mean Absorbance against Concentration (µg/mL).

Using the equation of a straight line, y = mx + c, where y = y-intercept (any value on the y axis), m = gradient or slope of the graph, x = x-intercept and c = the point where the straight line crosses the y-axis.

From the graph above,

y = 0.0075x + 0.036, where y = 0.046 and x = unknown concentration

0.046 = 0.0075x + 0.036

0.046 – 0.036= 0.0075x

0.01/0.0075 = 0.0075x /0.0075

x = 1.33 µg/mL

Therefore, the unknown concentration of drug (methylene blue) entrapped or encapsulated   is 1.33µg/mL.

1.33µg/mL is represented as 0.133mL in 100mL of solvent, i.e. 1.33/1000 x 100 = 0.133mL

Converting to % v/v, if 0.133mL of the active drug is present in 100mL, then

(0.144/100) x 100 = 0.133 % v/v

To calculate the entrapment or encapsulation efficiency percentage, the equation below was used,

EE = (EDC/TDA) X 100, where EE = Encapsulation Efficiency (%), EDC = Entrapped Drug

Concentration (0.133% v/v), and TDA = Total Drug Added (0.2% v/v)

Encapsulation Efficiency = (0.133/0.2) x 100

Encapsulation Efficiency (Repeat 3) = 66.5%

Lead Niosomal Formulation

Based on the results obtained from the characterization studies performed on all 5 niosomal repeats, 3 and 4 proven to be of excellent quality (in terms of shape, size, charge, and entrapment studies), were considered lead formulations and incorporated into the cream base via manual mixing. Further characterization studies were then performed on the cream, such as size analysis, sensorial, rheological, stability and diffusion studies.

4.4. CONCLUSION

MB has played an essential role in medicine for the treatment of many ailments and in microbiology as a staining dye [23]. To improve skin delivery and eliminate the staining blue color effect of MB, encapsulation of the drug into niosomal vesicles was performed using the thin-film hydration method. The characterization studies adapted to determine the lead active niosomal formulation – microscopic examination, purification, size, polydispersity index and zeta measurement.

Repeat 1 had visible levels of aggregation and repeat 5 had slight irregularities when observed under the microscope. repeats 2, 3, 4 and 5 proved to have more uniform niosomal dispersed size compared to repeat 1. Repeats 3 and 4 showed stability against the formation of aggregates, rapid coagulation or flocculation, showing very low toxicity due to their strongly anionic nature. Repeats 1, 2 and 5 had neutral zeta values of -4.94, -3.53 and -3.64, respectively, indicating electrostatic instability. Therefore, the lead active niosomal formulations incorporated into the cream base was models 3 and 4. Although, all repeats contained the same excipients and concentrations, the differences observed can be attributed to mechanical stress (hand shaking or mixing) and/or heating interval during niosomal preparation.

REFERENCE

1. Uchegbu IF, Vyas SP. Non-ionic surfactant based vesicles (niosomes) in drug delivery. International journal of pharmaceutics. 1998; 172(1-2):33-70.

2. Ruckmani K, Sankar V. Formulation and optimization of zidovudine niosomes. Aaps Pharmscitech. 2010; 11(3):1119-27.

3. Moghassemi S, Hadjizadeh A. Nano-niosomes as nanoscale drug delivery systems: an illustrated review. Journal of controlled release. 2014; 185:22-36.

4. Alhaique F, Esposito S, Carafa M. Niosomes from 80s to present: The state of the art. Advances in Colloid and Interface Science. 2014; 205:187-206.

5. Sahin NO. Niosomes as nanocarrier systems. InNanomaterials and nanosystems for biomedical applications 2007 (pp. 67-81). Springer, Dordrecht.

6. Singh P, Ansari H, Dabre S. Niosomes-a novel tool for anti-ageing cosmeceuticals. Journal of Pharmaceutical Research. 2016; 6(10).

7. Choi MJ, Maibach HI. Liposomes and niosomes as topical drug delivery systems. Skin pharmacology and physiology. 2005; 18(5):209-19.

8. Schreier H, Bouwstra J. Liposomes and niosomes as topical drug carriers: dermal and transdermal drug delivery. Journal of controlled release. 1994; 30(1):1-5.

9. Manconi M, Sinico C, Valenti D, Loy G, Fadda AM. Niosomes as carriers for tretinoin. I. Preparation and properties. International journal of pharmaceutics. 2002; 234(1-2):237-48.

10. Ultrasonic Formulation of Niosomes - Hielscher Ultrasound Technology [Internet]. Hielscher Ultrasound Technology. 2020 [cited 1 December 2020]. Available from: https://www.hielscher.com/ultrasonic-formulation-of-niosomes.htm

11. Mujoriya RZ, Bodla R. Niosomes–challenge in preparation for pharmaceutical scientist. Int J App Pharm. 2011; 3(3):11-5.

12. Yadav D, Sandeep K, Pandey D, Dutta RK. Liposomes for drug delivery. J. Biotechnol. Biomater. 2017; 7:276.

13. Schirmer RH, Adler H, Pickhardt M, Mandelkow E. Lest we forget you—methylene blue…. Neurobiology of aging. 2011; 32(12):2325-e7.

14. Oz M, Lorke DE, Petroianu GA. Methylene blue and Alzheimer's disease. Biochemical pharmacology. 2009 Oct 15;78(8):927-32.

15. Ginimuge PR, Jyothi SD. Methylene blue: revisited. Journal of anaesthesiology, clinical pharmacology. 2010; 26(4):517.

16. Marimuthu M, Praveen Kumar B, Mariya Salomi L, Veerapandian M, Balamurugan K. Methylene blue-fortified molybdenum trioxide nanoparticles: harnessing radical scavenging property. ACS applied materials & interfaces. 2018; 10(50):43429-38.

17. Rinnerthaler M, Bischof J, Streubel MK, Trost A, Richter K. Oxidative stress in aging human skin. Biomolecules. 2015; 5(2):545-89.

18. Masaki H. Role of antioxidants in the skin: anti-aging effects. Journal of dermatological science. 2010; 58(2):85-90.

19. Ahmad MU. NaNotechNology: emergiNg iNterest, opportuNities, aNd challeNges. InLipids in Nanotechnology 2012 (pp. 1-14). AOCS Press.

20. Cdn.shopify.com. (2012). *ZETA POTENTIAL ANALYSIS OF NANOPARTICLES*. [internet]. 2012 [cited 21 January 2019] Available from: https://cdn.shopify.com/s/files/1/0257/8237/files/nanoComposix_Guidelines_for_Zeta_Potential_Analysis_of_Nanoparticles.

21. Ag Seleci D, Seleci M, Walter JG, Stahl F, Scheper T. Niosomes as nanoparticular drug carriers: fundamentals and recent applications. Journal of nanomaterials. 2016.

22. Clogston JD, Patri AK. Zeta potential measurement. In Characterization of nanoparticles intended for drug delivery 2011 (pp. 63-70). Humana Press.

23. Tardivo JP, Del Giglio A, De Oliveira CS, Gabrielli DS, Junqueira HC, Tada DB, Severino D, de Fátima Turchiello R, Baptista MS. Methylene blue in photodynamic therapy: From basic mechanisms to clinical applications. Photodiagnosis and photodynamic therapy. 2005; 2(3):175-91.

CHAPTER 5

QUANTITATIVE SENSORY INTERPRETATION OF RHEOLOGICAL

PARAMETERS OF A CREAM FORMULATION

AVAILABLE ONLINE:

https://www.mdpi.com/2079-9284/7/1/2/htm

5.1. INTRODUCTION

The success of a cosmetic product on the market is largely dependent on the consumers' perception and the organoleptic profile of the product [1][2]. Therefore, sensory analysis of such a product is a mandatory process that determines market approval [2]. In 1979, sensory analysis was invented in France by Gonnet and Vache using conventional methods; these methods were later developed in Italy into a more sophisticated protocol involving extensive training, selection of panelists and sensory descriptive terms, before being absorbed by other European countries [3][4][5][6][7]. A general guidance for sensory analysis was then set up by the International Organization of Standardization, Geneva, ISO [8].

The sensory assessment method outlined by the ISO standard allows the qualitative and quantitative description of the attributes of a cosmetic product, hence providing accurate measurements [9]. It is a widely used tool during the product development stage, involving the adoption of a simple descriptive lexicon, a controlled environment, and 10–20 extensively trained panelists or judges that qualify the products provided based on their honest verbal perceptions (i.e., feel, fragrance and appearance), as well as quantifying the test products by assigning scores to each perception or attribute on a scale. A statistical (ANOVA) tool is then applied to compare the attributed scores and performance evaluation of the individual judges to assess data reproducibility and quality, respectively [9][10].

Sensory evaluation study performed by Gilbert et al., on eight oil-in-water cosmetic creams, using a set of panelists, successfully described perception terminology in three different stages of simple descriptive lexicons—appearance, pick-up and rub-out—to help provide information on the identity and quality of the creams [11]. Another study performed by Montenegro et al., used the standard ISO and three-stage simple descriptive lexicon method to assess sensory attributes, however, the result showed a number of variations in the data obtained from panelists; for example, 50% of the panelists labelled three test products as oily, while the other 50% labelled the same products as non-oily [12]. The difference proved that the existing sensory method is not 100% accurate due to individual preferences (i.e., differences in individual opinions or expectations) and/or limitations in sensory skills e.g., some are able to perceive odour better than others. Other limitations include the lack of adequate analytical information to back claims. It is also extensively time consuming (ranges from 10 to 120 hours based on sample nature), and expensive to acquire and maintain well-trained judges for both small and big companies and for academic research purposes, wherein time luxury and the availability of funds cannot be accorded [13]. Therefore, the need for an inexpensive, less time consuming and a more quantitative approach is essential.

The rheometer is a laboratory equipment that provides quantitative information on a product's

attributes and/or qualities, by measuring flow (viscometry test, i.e., yield stress) and deformation (oscillatory test, i.e., strain/stress amplitude sweep and frequency sweep) behavior of a sample [14]. Yield stress is an important rheological parameter that allows the investigation of the critical value or amount of applied force needed to cause the structured cream to flow out of a plastic tube or be dispensed from a bottle, i.e., stress required to trigger flow. Beneath this critical value, the cream is said to deform elastically, like a solid, but flows like a liquid above the critical value [15][16][17][18].

An oscillatory rheological test that measures the degree of linearity of the formulation is the strain (stress) amplitude sweep test, a good first step in determining the viscoelastic characteristic of the cream. The linear viscoelastic region (LVR), which is the region in which a sample is capable of maintaining its structure when force is applied (the line perpendicular to the shear strain axis), gives information on cream structure/firmness, i.e., the longer the LVR, the more firm/structured the cream, while the shorter the LVR, the less firm it appears [19]. Another oscillatory rheological test is the frequency sweep test, providing structural identity, i.e., is the cream more elastic/bouncy, just like a solid or viscous like thin oil/water. The identity of the cream at a strain below the critical strain allows the assessment of the effect of colloidal forces, as well as particles and droplets interaction; the dispersed particles and/or globules are expected to float and not form sediment when the elastic (storage) modulus, G′, is greater than viscous (loss) modulus, G″, at a low frequency [20][21]. A structured or solid-like cream shows an elastic modulus or component, G′, nearly independent of frequency, while the more dependent G′ is on frequency, the more liquid the cream. The cream is said to be non-sticky when there is no crossover of the elastic G′ and viscous G″ moduli, and sticky in nature when a crossover occurs [21]. The association between rheological measurements and the adhesive ability (tackiness) of pressure-sensitive adhesives on the skin is well-known [19] and evidences that there is a correlation between user trial data with rheological measurements.

The objective of this study was to expand this association to a wider range of sensorial attributes by developing a standard, simple and reliable method for the quantitative assessment of the sensorial attributes of O/W cream formulations by correlating simple sensory lexicons to viscometry (yield stress) and oscillatory (amplitude and frequency sweep) rheological parameters.

5.2. MATERIALS AND METHODS

5.2.1. Materials

The active ingredient (X), cholesterol, span65 and solutol HS-15 were obtained from Sigma-Aldrich, Inc. (Gillingham, UK). Baobab oil was purchased from Aromatic Natural Skin Care (Forres, UK), Jojoba and Coconut oil from SouthernCross Botanicals (Knockrow, Australia). The Emulsifying Wax was obtained from CRODA International Plc (Goole, East Yorkshire, UK). Other excipients of the cream and Tris buffer solutions were of analytical grade.

5.2.2. Methods

5.2.2.1. Preparation of Niosomes

Five (5) niosome formulations, labelled A to E, were prepared using the thin-film hydration technique, with cholesterol (45%), span 65 (45%), solutol-HS 15 (10%) each dissolved in 4 mL organic solvent (chloroform) in a 250 mL round bottom flask, for the manufacture of 300 μmol of vesicles. The chloroform was removed using a rotary evaporator at 60 °C, 40 rpm and a vacuum of 464 ± 10 mbar. After placing the 250 mL flask at the interface of the H_2O in the bath, the pressure was allowed to drop until no chloroform was left and a thin film of the mix formed on the flask wall (Figure 5.1). A total of 5 mL of Tris buffer pH 7.4 with 0.01 mL or 10 μL of the active, X (i.e., total active concentration added was 0.002 v/v) was added to hydrate the lipid films, followed by gentle agitation—enabling the formation of unilamellar vesicles and the entrapment of the active in the vesicles. The mix was intermittently incubated at 60 °C for a period of 10 minutes while shaking to allow for the complete detachment of the lipid film, encouraging more entrapment. After this, the newly prepared niosomes were separated via sephadex G-50 column chromatography and characterized. According to results obtained from characterization studies on all five niosomal formulations, models C and D were proven to be of excellent quality (i.e., sizes of 592 and 601 nm and -49.2 and -34.5 mV surface charge, respectively) following the characterisation studies and were therefore considered lead formulations and incorporated into the cream base via manual mixing.
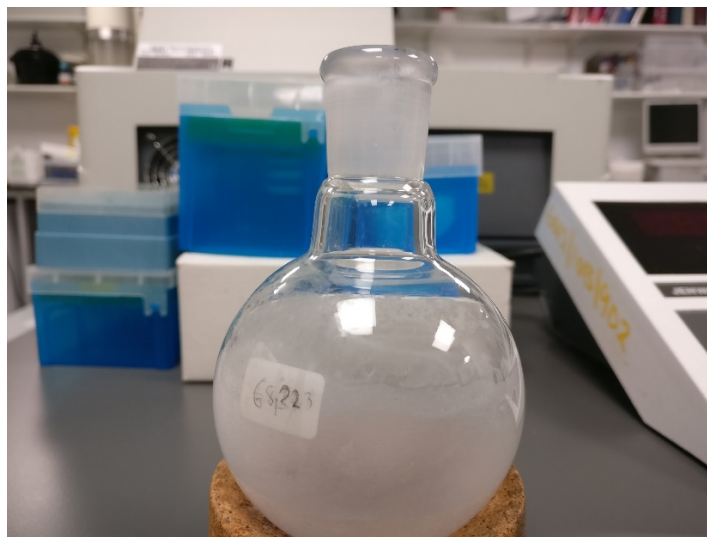
Figure 5.1. A photographic image of the thin film formed around the flask wall.

5.2.2.2. Preparation of Creams

Four (4) 100 g O/W model creams containing active-loaded niosomes (labelled as model IA-IVA), and their baselines without niosomes (labelled as model IB-IVB), were prepared with the formulas stated in Table 5.1, according to the following method: the oil phase and water phase ingredients were weighed in two separate beakers. After heating the oil phase and water phase to 75

°C, both phases were mixed together for 18 minutes at 9500 rpm using the Silverson L5M electric homogenizer to obtain a uniform mix. At a cool down temperature of 40 °C, 5% of the active niosomes suspended in water were added to each cream model in batch "A" and further mixed manually with a glass stirrer for two minutes, to avoid disruption of the vesicles. The newly formulated products were collected into eight (8) separate 100 g glass jars with plastic caps, labelled IA-IVA and IB-IVB, with and without actives, respectively. The first, labelled model I (1:1 of jojoba and baobab oil) contained a water phase of 85%, oil phase (10%) and emulsifier (5%) while the remaining three had an equal % composition of water phase (83%), oil phase (12%) and emulsifier (5%), labelled II (1:1 of jojoba and baobab oil), III (1:1 of jojoba and coconut oil) and IV (1:1 of baobab and coconut oil). All models were formulated within the standard concentration range for a cream formulation.

Table 5.1. Ingredient and amount variables in 100 g of each cream formulation.

Phase	INCI	Composition (%)	IA	IB	IIA	IIB	IIIA	IIIB	IVA	IVB
Oil	Stearyl Alcohol	Stearyl Alcohol					1	1	1	1
	Simmondsia Chinensis Seed Oil	Jojoba Oil	4	4	5	5	5	5		
	Adansonia Digitata Seed Oil	Baobab Oil	4	4	5	5			5	5
	Cocos nucifera	Coconut Oil					5	5	5	5
Water	Glycerin	Glycerine	5	5			5	5	5	5
	Propylene Glycol	Propylene Glycol			5	5				
	Aqua	Water	73.7	78.7	71.7	76.7	71.7	76.7	71.7	76.7
Active	-	Entrapped Active	5		5		5		5	

5.2.2.3. Sensory Lexicons and Definitions

A sensory lexicon was devised in three different stages [11][12], for all formulated oil-in-water products: (a) appearance—pourability (b) pick-up—firmness and elasticity/stretchability (c) rub-out—spreadability and stickiness. Each stage was correlated with rheological parameters, as shown in Table 5.2, to help provide information on the identity and quality of the test products.

Table 5.2. Proposed protocol of rheological parameters–sensory attribute pairs, and their description.

Stage of Usage Sensorial Attribute Description Rheological Parameter.

Stage of usage	Sensorial attribute	Description	Rheological parameter
Appearance	Pourability	Ability of a product to flow or be pumped out of the container when a force is applied.	Viscometry; Yield Stress
Pick-up	Firmness	The degree to which the product is able to hold its shape or structure in the presence of force.	Oscillatory; Amplitude Sweep
	Elasticity/ Stretchability	It is the ability of the product to deform or expand (strain) by resisting an external force (stress).	Oscillatory; Frequency Sweep
Rub-out	Spreadability	The force required to cause flow of the product.	Viscometry; Yield Stress

| Stickiness | Ability of product to attach to the skin, yielding a sticky skin feel. | Oscillatory; Frequency Sweep |

5.2.2.4. Instrumental Rheology and Sensory Characterization

To obtain the rheological measurements of the cream models, a Kinexus lab+ Rotational Rheometer (Malvern Panalytical Instruments, Malvern, UK) was used with a stainless-steel parallel plate of 20 mm diameter at a constant temperature of 32 ± 1 °C, a gap size of 0.25 mm, and a humidity of 33%. All measurements were performed in triplicate (n = 3)

1. Yield Stress: pourability and spreadability—a stress range of 0.001 Pa to 10,000 Pa at a ramp time of 2 min and a decade of 10 was applied.

2. Strain Amplitude Sweep with LVR Determination: firmness—the samples were oscillated over a shear stress range of 0.001 Pa to 10,000 Pa, at a frequency of 1 Hz and a decade of 10.

3. Frequency Sweep: stickiness and elasticity or stretchability—the samples were oscillated over a frequency range of 50 to 0.05 Hz, at a % strain within the LVR.

5.2.2.5. Statistical Analysis

Statistical evaluation of results obtained for the formulated creams was achieved using the SPSS software (SPSS UK Ltd, IBM, Woking, UK). To indicate whether any significant correlations ($p < 0.05$) exist between the rheological data obtained on all eight O/Wcreams, Pearson's Chi-square test was conducted.

5.3. RESULTS AND DISCUSSION

5.3.1. Rheology and Sensory Characterization

5.3.1.1. Yield Stress: Pourability and Spreadability

This is an important parameter as it allows the investigation of the amount or critical value of applied force needed to cause the structured cream to flow out of a plastic tube or be dispensed from a bottle, i.e., the stress required to trigger pumping through a pipeline. Beneath this critical value, the cream is said to deform elastically like a solid, but it flows like a liquid above the critical value [15][16]. Therefore, two types of information on the pourability (yield stress value) and spreadability (viscosity value) of the measured product, where 0 signified the least pourable or spreadable score and 9 indicated the most pourable or spreadable score are reported in Table 5.3. The scale ranges of 0–9 (Table 5.3) and 0–3 (Table 5.4) were carefully selected to provide distinct groups of similar values that would be statistically significant from each other.

Table 5.3. Correlation of the range of yield stress, viscosity values and amplitude sweep to pourability, spreadability and firmness scores (0–9).

Score	Yield Stress Values (Pa)	Viscosity/Thickness (Pa S)	Strain Amplitude Sweep (Pa)

0	181 - 200	171000 – 190000	<0.010
1	161 – 180	151000 – 170000	0.011 - 0.020
2	141 - 160	131000 – 150000	0.021 – 0.040
3	121 - 140	111000 – 130000	0.041 – 0.060
4	101 - 120	91000 – 110000	0.061 – 0.080
5	81 - 100	71000 – 90000	0.081 – 0.100
6	61 - 80	51000 – 70000	0.101 – 0.200
7	41 - 60	31000 – 50000	0.201 – 0.400
8	21 - 40	11000 - 30000	0.401 – 0.600
9	0 - 20	<10000	0.601 – 0.800

Table 5.4. Correlation of the range of yield stress, viscosity values and amplitude sweep to pourability, spreadability and firmness scores (0–3).

Score	Yield Stress Values (Pa)	Viscosity/Thickness (Pa S)	Strain Amplitude Sweep (Pa)
0	151 - 200	151000 – 200000	<0.200
1	101 – 150	101000 – 150000	0.201 - 0.400
2	51 - 100	51000 – 100000	0.401 – 0.600
3	0 - 50	<50000	0.601 – 0.800

Figure 5.2 reveals that all cream models exhibited non-Newtonian behavior, shear-thinning with increasing stress or applied force. In Table 5.5, model IIA was the most structurally robust, with the highest yield stress of 112/±22.3 Pa (i.e., model IIA requires a large amount of force to break its structure apart, allowing it to flow like a liquid) and the highest viscosity/thickness of 117302/±36498 PaS, therefore having the lowest pourability and spreadability scores of four and three, respectively. Model IIB had a low yield stress of 48/±15.2 Pa and a viscosity/thickness of 34358/±9249 PaS; this means that model IIB showed an increased spreadability and pourability score of seven, compared to model IIA. Model IA was the second most structurally robust, with a high yield stress of 79/±15.8 Pa, indicating that a large amount of force is needed to break its structure apart, with a viscosity/thickness of 53270/±3010 PaS, consequently possessing a pourability and spreadability score of six. Model IB had the lowest yield stress of 26/±15.5 Pa and the highest pourability score of eight compared to other creams, i.e., it requires the least force to break its structure apart, and a viscosity/thickness of 21590/±10090 PaS, with a high spreadability score of eight.
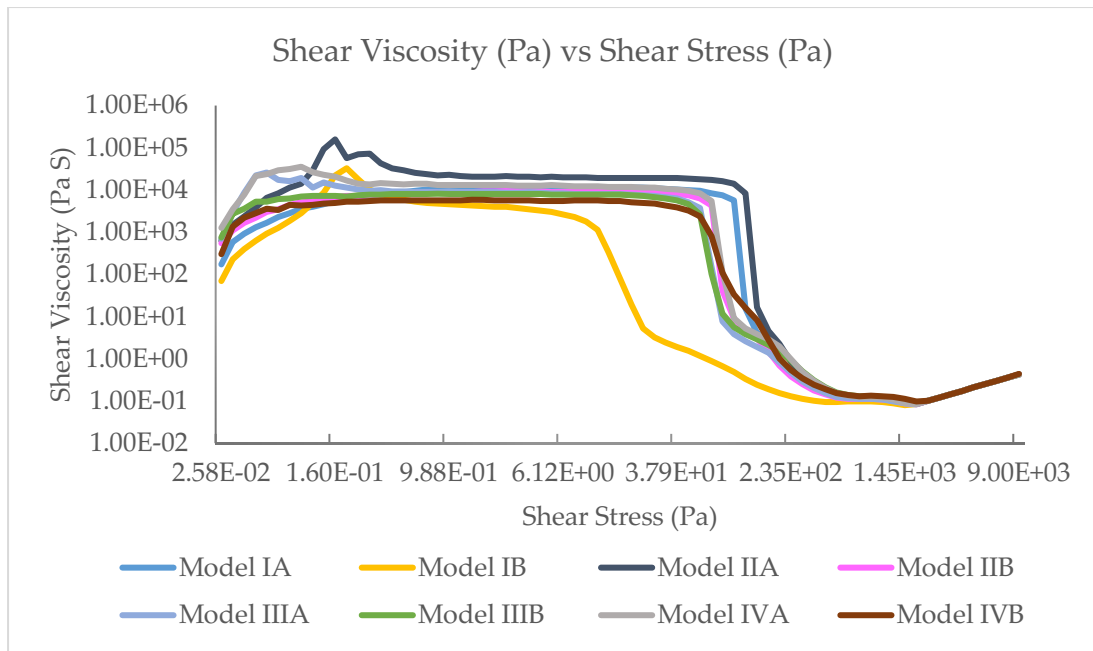
Figure 5.2. Viscosity (Pa S) of sample against applied stress (Pa).

Table 5.5. Mean and standard deviation of yield stress and viscosity/thickness values. (n=3).

Model	Mean Yield Stress (Pa)	Pourabili ty Score	Mean Viscosity/Thickness (PaS)	Spreadability Score	Mean Shear Strain within the LVR	Firmness Score
IA	79 ± 15.8	6	53270 ± 3010	6	9.755E-002 ± 6.028E-003	5
IB	26 ± 15.5	8	21590 ± 1090	8	7.206E-002 ± 6.513E-003	4
IIA	112 ± 22.3	4	117302 ± 36498	3	7.268E-002 ± 6.628E-003	4
IIB	48 ± 15.2	7	34358 ± 9249	7	5.077E-002 ± 2.341E-002	3
IIIA	66 ± 10.5	6	20100 ± 3874	8	1.022E-001 ± 9.295E-003	6
IIIB	67 ± 10.5	6	8085 ± 15	9	6.844E-002 ± 2.498E-002	4
IVA	75 ± 7.5	6	38050 ± 4550	7	4.910E-002 ± 1.007E-002	3
IVB	46 ± 9.2	7	4767 ± 1067	9	1.272E-001 ± 1.905E-003	6

Model IVA also had a yield stress of 75/±7.5 Pa, with a viscosity/thickness of 38050/±4550 PaS, and a decreased pourability and spreadability score of six and seven, respectively when compared to its pair. Model IVB had a low yield stress of 46/±9.2 Pa (pourability score of seven), and the lowest viscosity/thickness of 4767/±1067 PaS, providing the highest spreadability score of nine. Model IIIB had a yield stress of 67/±10.5 Pa (pourability score of six), with the second lowest viscosity/thickness of 8085/±15 PaS compared to others, showing an increased spreadability score of nine, while model IIIA had a similar yield stress of 66/±10.5 Pa (pourability score of six) but a higher viscosity/thickness of

20100/±3874 PaS (spreadability score of eight), when compared to its pair. Models IB and IVB appeared to be the best creams in terms of pourability and spreadability scores, with eight, seven and nine, respectively. The largest difference is seen between the following pairs: IA and IB, IIA and IIB, and IVA and IVB, and could be a result of the presence of active niosomes contained in the former (IA, IIA and IVA).

Generally, it was observed that all model creams without niosomes exhibited higher pourability and spreadability scores, with a lower firmness score, when compared to their niosome-containing counterparts, which could be attributed to their higher water content. This shows the sensitivity of the method in detecting the effect of niosome vesicles on the overall sensorial perception of the creams in terms of pourability, spreadability and firmness.

Pearson Chi-Square test showed a statistical correlation between viscosity and yield stress values for all eight samples with p values < 0.001.

5.3.1.2. Stress (Strain) Amplitude Sweep with LVR Determination: Firmness

An oscillatory test that measures the degree of linearity of the formulation is the strain or stress amplitude sweep test, a good first step in determining the viscoelastic characteristics of the cream. As shown on Figure 5.3, the linear viscoelastic region, LVR, gives information on how stable/firm/structured the cream is, i.e., the longer the LVR, the more structured the cream, while the shorter the LVR, the less structured it is. Other information, such as the position of the LVR, illustrates how well the cream is able to resist stress [19]. As reported in Table 5.3, score 0 signifies the least firm/structured cream while the most firm/structured product was allocated score 9.
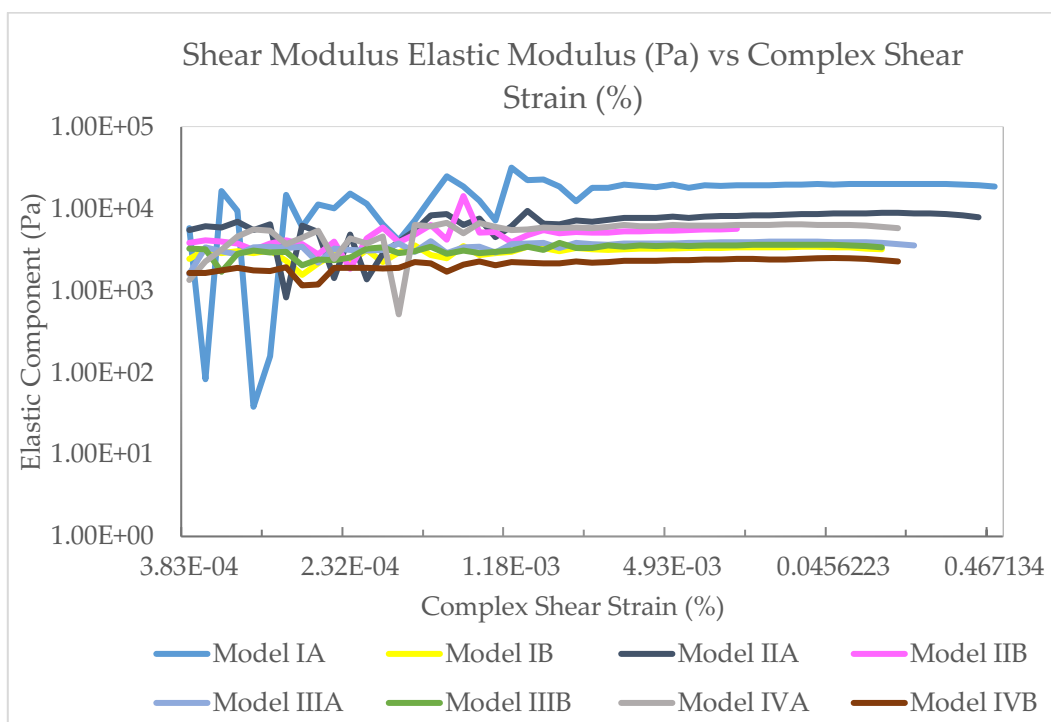

Figure 5.3. Elastic modulus, G' (Pa) plotted against complex strain (%).

Table 5.5 above showed the highest firmness was observed in creams containing coconut oil: model IVB (coconut and baobab oil) and IIIA (jojoba and coconut oil)—0.13 and 0.10, respectively. The least firmness was seen in model IVA and IIB—0.049 and 0.051, respectively. Therefore, the method was sensitive enough to differentiate between the effect of the fatty-acids characteristics of the oils (with coconut oil is made up of 95% saturated FA) on the overall texture of the formulation. These results complied with the frequency data, showing the two models to be more elastic compared to models IA, IB, IIA, IIB IIIB and IVA, because IVB and IIIA are more firm and are capable of resisting the action of any external force longer than others, maintaining their structure.

5.3.1.3. Frequency Sweep; Stickiness and Elasticity or Stretchability

The frequency sweep test is also an oscillatory rheology test that gives information on the structure (elastic/bouncy, just like a solid, or viscous like thin oils or water) or identity of the cream at a strain below the critical strain. Therefore, allowing for the assessment of the effect of colloidal forces as well as particles and droplets interaction, the dispersed particles and/or globules are expected to float and not form sediment when G′ is greater than the viscous modulus, G″, at a low frequency, and vice-versa. A structured or solid-like cream shows an elastic modulus or component, with G′ nearly independent of frequency, while the more dependent G′ is on frequency, the more liquid the cream. The cream is said to be non-sticky when no crossover of the elastic and viscous modulus is observed, and sticky in nature when crossover occurs [21]. Score 0 represented a nonsticky or non-stretchy, while score 3 indicated a very sticky or very stretchy cream (Table 5.6).

Table 5.6. Correlation of Frequency Sweep Information to Stickiness and Elasticity/Stretchability Scores (0-3).

Score	Elasticity/Stretchability	Stickiness
0	Non-Stretchy	Non-Sticky
1	Moderately Stretchy	Moderately Sticky
2	Stretchy	Sticky
3	Very Stretchy	Very sticky

The graphs in Figure S1 show that all cream models were non-sticky in nature (i.e., no crossover was observed) and had their G′ component greater than G″ at a low frequency, indicating the stability of products, as all particles and globules did not sediment or separate. However, it was observed that models IB and IIB had their G′ component a lot higher than G″ at a low frequency compared to the pairs containing active niosome particles, models IA and IIA, whereas the opposite was seen when models IIIB and IVB were compared with IIIA and IVA. (See Supplementary Materials)

It was also observed that models IIIA IIIB, IVA and IVB showed their G′ to be more independent of frequency than models IA, IB, IIA and IIB, implying that models IIIA IIIB, IVA and IVB are more solid, therefore, more elastic or stretchy in nature, and had the highest elasticity score of 2 (Table 5.7)

compared to models IA, IB, IIA and IIB. Models IVB and IIIA also exhibited the highest firmness scores, showing similarities with the elasticity data. This could be the effect of the coconut oil's fatty-acid composition (95% saturated fatty acid), contained in models IIIA IIIB, IVA and IVB.

Table 5.7. Stickiness and Elasticity or Stretchability Scores for the eight O/W Creams.

Model	Stickiness	Score	Elasticity/Stretchability	Score
IA	Non-Sticky	0	Moderately Stretchy	1
IB	Non-Sticky	0	Moderately Stretchy	1
IIA	Non-Sticky	0	Moderately Stretchy	1
IIB	Non-Sticky	0	Moderately Stretchy	1
IIIA	Non-Sticky	0	Stretchy	2
IIIB	Non-Sticky	0	Stretchy	2
IVA	Non-Sticky	0	Stretchy	2
IVB	Non-Sticky	0	Stretchy	2

The sensorial properties of these formulations can be depicted in radar diagrams, as shown in Figures 5.4 and 5.5. These diagrams compare the sensorial properties of products and can be used as a marketing tool.
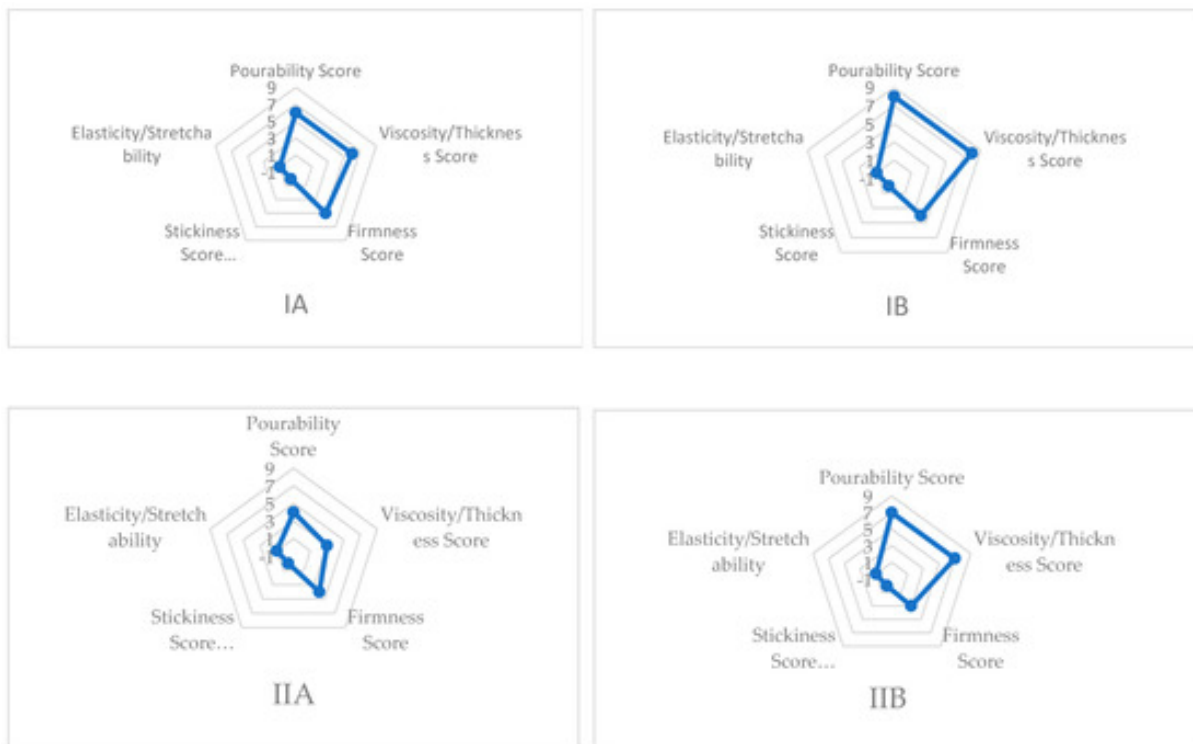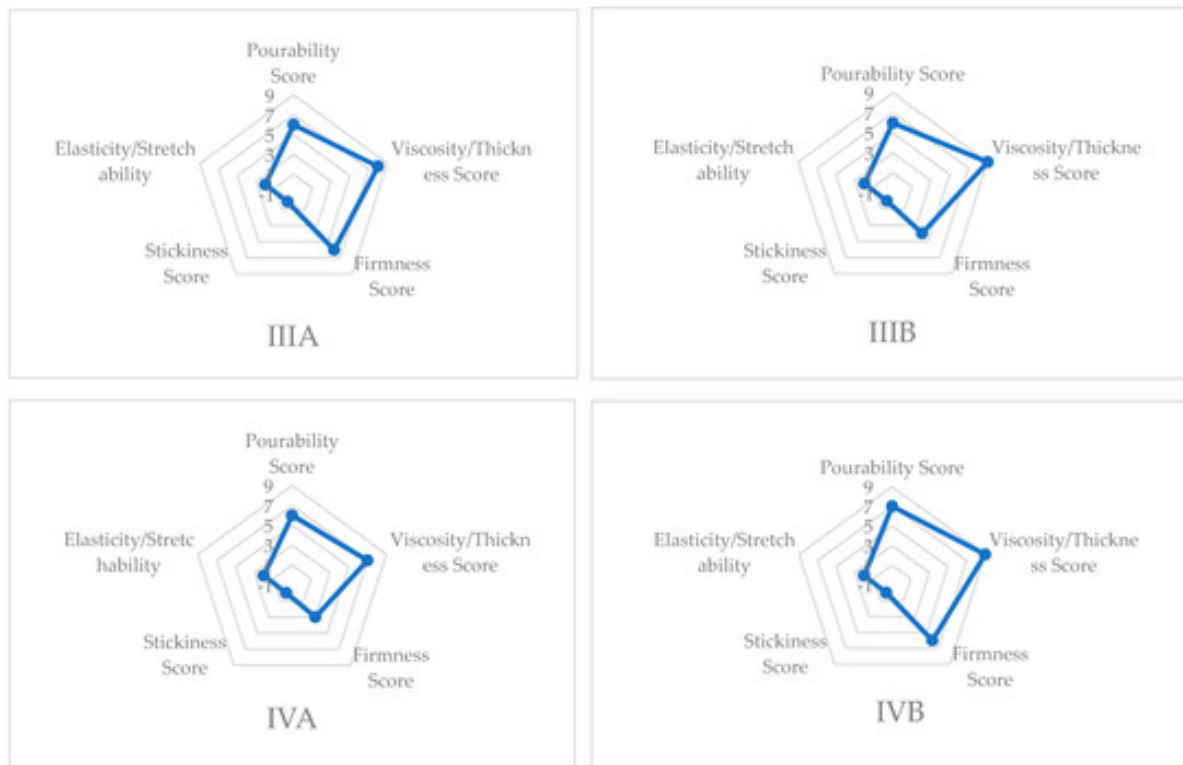
Figure 5.4. Radar diagrams of all eight oil-in-water cream model pairs (IA/IB, IIA/IIB, IIIA/IIIB, IVA/IVB) indicating Pourability, Spreadability, Firmness, Stickiness and Elasticity or Stretchability on a scale (0–9).
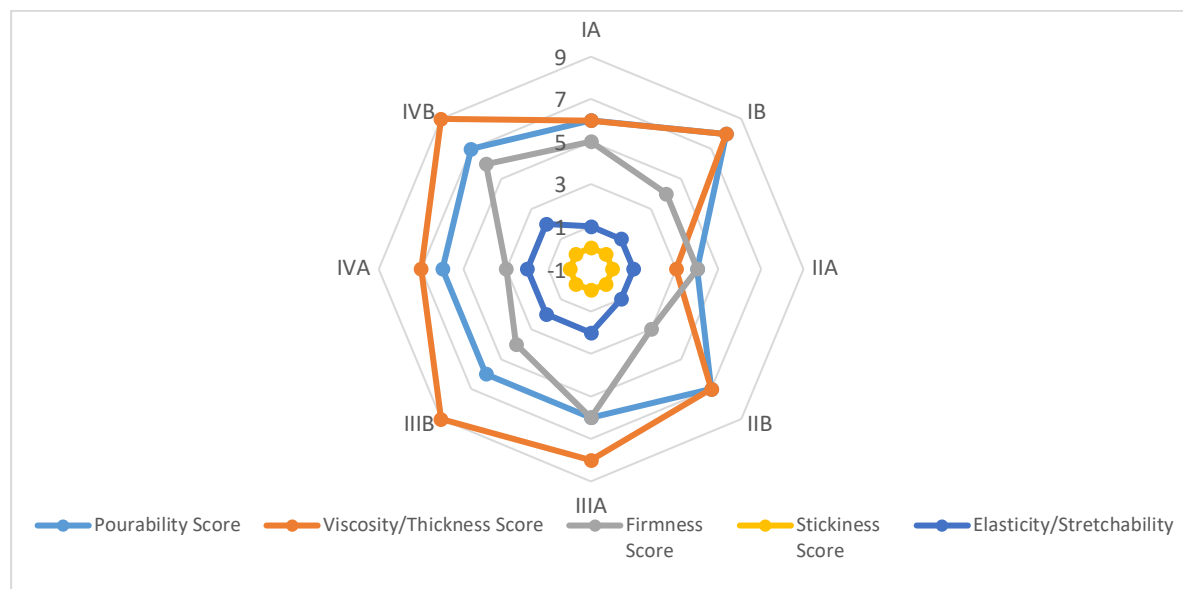
Figure 5.5. Radar diagram of the summary of all eight O/W creams indicating Pourability, Spreadability, Firmness, Stickiness and Elasticity or Stretchability on a scale (0–9).

5.4. CONCLUSIONS

As consumer perception of a cosmetic product an important determinant of market approval and success, sensory assessment is consequently a mandatory step in the claims substantiation stage of a product's launch to the market.

In this study, we report a new quantitative test protocol (in terms of application and interpretation), which correlates the rheological parameters of semisolid formulations (creams) with their sensorial characteristics such as pourability, firmness, elasticity and stickiness. This protocol avoids the time, costs and subjectivity associated with qualitative user-trials; it is a quantitative method that can be used for the creation of sensorial radar diagrams for cosmetic and personal care semisolid formulations.

One limitation of the protocol is the inability of rheological measurements to reveal sensory attributes like odour, color, glossiness and oiliness. This limitation can be compensated by using other relevant analytical laboratory meters in conjunction with the rheological measurements.

REFERENCE

1. Chang, W.C.;Wu, T.Y. Exploring types and characteristics of product forms. Int. J. Des. 2007, 1, 1–3.

2. Liao, S.H.; Hsieh, C.L.; Huang, S.P. Mining product maps for new product development. Expert Syst. Appl. 2008, 34, 1–50.

3. Durán, S.S.; Sánchez, J.S. Sensory Studies. In Bee Products-Chemical and Biological Properties; Springer: Berlin/Heidelberg, Germany, 2017; pp. 21–41.

4. Bonod, I.; Sandoz, J.C.; Loublier, Y.; Pham-Delègue, M.H. Learning and discrimination of honey odours by the honeybee. Apidologie 2003, 34, 2–147.

5. Galán-Soldevilla, H.; Ruiz-Pérez-Cacho, M.P.; Jimenez, S.S.; Villarejo, M.J.; Manzanares, A.B. Development of a preliminary sensory lexicon for floral honey. Food Qual. Prefer. 2005, 16, 1–71.

6. Serra Bonvehi, J.; Ventura Coll, F. Characterization of citrus honey (Citrus spp.) produced in Spain. J. Agric. Food Chem. 1995, 43, 2053–2057.

7. Piana, M.L.; Oddo, L.P.; Bentabol, A.; Bruneau, E.; Bogdanov, S.; Declerck, C.G. Sensory analysis applied to honey: State of the art. Apidologie 2004, 35, S26–S37.

8. ISO 6658:2017. Sensory Analysis—Methodology—General Guidance, International Organization for Standardization. ISO. 2019. Available online: https://www.iso.org/standard/65519.html (accessed on 20 September 2019).

9. Murray, J.M.; Delahunty, C.M.; Baxter, I.A. Descriptive sensory analysis: Past, present and future. Food Res. Int. 2001, 34, 6–461.

10. Pensé-Lhéritier, A.M. Recent developments in the sensorial assessment of cosmetic products: A review. Int. J. Cosmet. Sci. 2015, 37, 465–473.

11. Gilbert, L.; Savary, G.; Grisel, M.; Picard, C. Predicting sensory texture properties of cosmetic emulsions by physical measurements. Chemom. Intell. Lab. Syst. 2013, 124, 21–31.

12. Montenegro, L.; Rapisarda, L.; Ministeri, C.; Puglisi, G. E_ects of lipids and emulsifiers on the physicochemical and sensory properties of cosmetic emulsions containing vitamin E. Cosmetics 2015, 2, 35–47.

13. Varela, P.; Ares, G. Sensory profiling, the blurred line between sensory and consumer science. A review of novel methods for product characterization. Food Res. Int. 2012, 48, 2–893.

14. Tabilo-Munizaga, G.; Barbosa-Cánovas, G.V. Rheology for the food industry. J. Food Eng. 2005, 67, 147–156.

15. Cheng, D.C. Yield stress: A time-dependent property and how to measure it. Rheol. Acta 1986, 25, 5–542.

16. Barnes, H.A. The yield stress—A review or '_____ _"_'—Everything flows? J. Non-Newton. Fluid Mech. 1999, 81, 133–178.

17. Stokes, J.R.; Telford, J.H. Measuring the yield behaviour of structured fluids. J. Non-Newton. Fluid Mech. 2004, 124, 137–146.

18. Rueda, M.M.; Auscher, M.C.; Fulchiron, R.; Perie, T.; Martin, G.; Sonntag, P.; Cassagnau, P. Rheology and applications of highly filled polymers: A review of current understanding. Prog. Polym. Sci. 2017, 66, 22–53.

19. Ho, K.Y.; Dodou, K. Rheological studies on pressure-sensitive silicone adhesives and drug-in-adhesive layers as a means to characterise adhesive performance. Int. J. Pharm. 2007, 333, 24–33.

20. Souto, E.B.; Gohla, S.H.; Müller, R.H. Rheology of nanostructured lipid carriers (NLC®) suspended in a viscoelastic medium. Die Pharm. Int. J. Pharm. Sci. 2005, 60, 9–671.

21. Mason, T.G. New fundamental concepts in emulsion rheology. Curr. Opin. Colloid Interface Sci. 1999, 4, 231–238.

CHAPTER 6

A NOVEL METHOD FOR THE EVALUATION OF THE LONG-TERM STABILITY OF CREAM FORMULATIONS CONTAINING NATURAL OILS

AVAILABLE ONLINE:

https://www.mdpi.com/2079-9284/7/4/86/htm

6.1. INTRODUCTION

In recent times, the health and beauty industry has tended to lean towards the use of natural ingredients such as herbal or natural oils because of their low toxicity profile [1]. Some of these oils e.g., jojoba oil, are superior compared to others (e.g., castor, olive oil etc.) due to their structural and chemical similarity to the human skin's sebum [2,3]. Jojoba (pronunciation; hohoba) oil is extracted from the jojoba seed plant called *Simmondsia Chinensis*, also known as desert gold. It mostly comprises of straight-chain monoesters within the C20–C22 range, and at each end of the acidic and alcoholic ester bond, two double bonds exist. Jojoba plant originated from South-Western North America and the oil has found applications in food, pharmaceuticals, electrical insulators, lubricants, plasticizers, and cosmetics. This range of applications can be attributed to its unique properties [4]; in the medical and pharmaceutical industries, the oil is used for treating a wide range of skin diseases (e.g., eczema, seborrheic dermatitis, acne, sores and inflammation), as an anaesthetic for severe pain [5] and for the manufacture of penicillin-G.

When used on the skin, jojoba oil reduces the appearance of fine lines by inhibiting the aging process due to its antioxidant effect and promotes cutaneous healing or rejuvenation through the stimulation of collagen synthesis [2–8]. Jojoba oil has a refractive index of 1.46, is highly stable and resistant to oxidation both under normal and extreme temperature conditions [8,9].

Another natural seed oil that is unique and nontoxic in nature is the baobab oil. Baobab oil is derived from the baobab plant, also known as *Adansonia digitate*. It is largely distributed across the semi-arid and sub humid province of sub-Sahara Africa and Western Madagascar [10–12]. Baobab oil is composed of 0.2–3% of Omega 3 (linolenic acid), 25–37% of Omega 6 (linoleic acid), 23–44% of Omega 9 (oleic acid), 1.5–6.0% of Stearic acid and 18–30% of Palmitic acid [12]. In many African regions, the oil is used as an analgesic for the treatment of pain (e.g., toothache), as anti-inflammatory, antioxidant, immune-stimulant, insect repellent, for treating wounds, varicose veins, muscle spasm, dysentery and diarrhea [13,14]. When used with coconut oil, the mixture can be used for the production of antibacterial soap to be applied on skin lesions such as eczema, acne, rashes and sunburn. Baobab oil is a powerful emollient that nourishes, hydrates and conditions the skin, scalp and nails, it helps reduce stretchmarks and improves skin elasticity through the restoration of the skin and rejuvenation of the epithelial tissue. This explains why the oil is recommended during pregnancy [14–16]; the high concentrations of Omega 6 and 9 found in the oil stimulates synthesis of collagen and elastin fibers, promoting flexibility, firmness and smoothness while inhibiting inflammation [17,18]. Baobab oil has a strong oxidative stability and a long shelf life, its refractive index and iodine value range from 1.4596 to 1.4633 and 55 to 96 mg/100 g, respectively [17–19].

Coconut oil, extracted from coconut kernel also called the white endosperm, is obtained from *Cocos nucifera* of the family of *Arecaceae* and subfamily of *Cocoideae*. *Cocos nucifera* tree grows in tropical countries of Africa, Asia, South and Central America and the Pacific, [20,21]. It is composed of 95% saturated fatty acids, most of which are medium-chain fatty acids (MCFA), C8–C12 i.e., 44% lauric, 18% myristic, 11% palmitic, 6% capric and 6% caprylic acids, and 15% long-chain fatty acid (LCFA) i.e., 7% oleic, 6% stearic and 2% linoleic acids. MCFAs do not require the action of carnitine for mitochondrial transportation; instead, they are directly oxidized and thus decreasing cholesterol synthesis and fat deposition in the adipose tissue and other body organs [21–25]. MCFAs such as monoglyceride monolaurin largely make up human breast milk and function to protect infants from viral, bacterial and fungal infections, thereby, boosting the immune system. Monoglyceride monolaurin has also been seen to be effective in the reduction of degenerative diseases such as premature aging and skin inflammation, as well as increasing insulin secretion and blood glucose utilization [25,26]. Studies have revealed the oil's ability to heal the skin by elevating the levels of pepsin-soluble collagen and by increasing collagen cross-linking through glycohydrolase activity [27].

Testing of the physical and chemical stability of natural cosmetics is an essential quality control step due to their highly degradable nature [28]. Various analytical techniques can be used to determine product stability, such methods involve: (i) differential scanning calorimetry (DSC)—to detect changes in heat flow related to material changes (crystallization or melting); (ii) solution calorimetry (SC)—to detect changes in enthalpy dependent on the structure of solid and liquid and their interactions; (iii) HPLC—to measure residual content of specific compounds in a semisolid after extraction by an organic or inorganic solvent [29,30]. As water is ubiquitous in most semisolid cosmetic formulations, the dynamic vapor sorption (DVS) technique could be a useful technique for new product development and processing [31,32]. The DVS analyzer was first invented in the 1990s [33]. It is a computer-automated gravimetric method, i.e., measures mass changes that translate to water vapour sorption isotherms—a phase change of H_2O molecules from vapour to condensed phase, involving the production or interruption of strong intermolecular bonds between the H_2O molecule and solids or other H_2O molecules in the sample. Sorption occurs in two ways; adsorption (water interaction only with molecules at the surface) and absorption (interaction both within and on the surface of the sample); and desorption isotherms—involves the transition of moisture absorbed into the vapour phase, over a wide variety of temperatures (5–85 °C) and humidity (0–98% RH) against time [34–36].

In contrast to the aforementioned techniques, the DVS is a multifaceted system due to its ability to provide long-term temperature stability and maximum level of humidity precision and accuracy; allowing generated and delivered vapour to occur typically within ±0.02 °C and ±0.1% RH of target temperature and humidity, respectively. It has a highly-sensitive microbalance that measures mass

changes at 0.1 µg resolution, with sample size ranging from 1 mg to 1.5 g [36,37] alongside a unified resolution for generating and capturing Raman spectra in sorption analysis. This combination allows for a thorough comprehension of the chemical and structural properties of materials in relation to their vapour–solid interaction. It also provides an optional vapour permeability measurement and moisture vapour transmission rates via porous elements; microscopic visualization at 200× zoom lens, 5 megapixel camera for well-defined images; and an analysis software that generates a single key result from over 20 various models for stability prediction, surface characterization, and understanding hysteresis (difference in H_2O vapor uptake between the isotherms) and solvent interaction [36–38].

The focus of this work is to prepare four novel, active oil-in-water creams and their controls (without active) from 100% naturally sourced oil ingredients, and to compare their effects on the physico-chemical properties of creams over short- and long-term storage. All short-term stability assessment was carried out in agreement with the ICH guideline over a period of 28 days. The long-term stability assessment involved the development of a novel method, using the Dynamic Vapor Sorption system to help provide information on the percentage change in mass, in a cycle of drying and sorption. In a previous paper, we demonstrated that stability can be measured using the oscillatory amplitude sweep rheological test, showing changes in the Linear Viscosity Region, LVR (where the complex modulus is independent of stress applied i.e., the longer the LVR, the more stable the structure) [39].

6.2. MATERIALS AND METHODS

6.2.1. Materials

The active ingredient (X), cholesterol, span65 and solutol HS-15 were obtained from Sigma-Aldrich, Inc. (Gillingham, UK). Baobab oil was purchased from Aromatic Natural Skin Care (Forres, UK), Jojoba and Coconut oil from SouthernCross Botanicals (Knockrow, Australia). The Emulsifying Wax was obtained from CRODA International Plc (Goole, East Yorkshire, UK). Other excipients of the cream and Tris buffer solutions were of analytical grade.

6.2.2. Methods

6.2.2.1. Preparation of Creams

The formulation of the creams was according to the method described in our previous paper [39]. Four novel active oil-in-water creams and their controls (without active) were prepared. Each model cream contained oils combined as follows: I (1:1 of 8% jojoba and baobab oils)—water phase (85%), oil phase (10%) and emulsifier (5%); II (1:1 of 10% jojoba and baobab oil), III (1:1 of 10% jojoba

oil and coconut oil) and IV (1:1 of 10% baobab and coconut oil)—water phase (83%), oil phase (12%) and emulsifier (5%). All models were formulated within the standard concentration range for a cream formulation.

6.2.2.2. Short-Term Stability Studies

The short-term stability assessment was carried out in agreement with the ICH guideline. Creams with actives (model IA-IVA) and without actives (model IB-IVB) were roughly divided into 3 equal portions in similar glass jars and stored at 4 ± 1 °C in the refrigerator, 25 ± 1 °C ambient room temperature and 40 ± 1 °C in an incubator. Physical (appearance, odor, color, phase separation resistance, globule size), chemical (pH, zeta potential measurement) and microbial changes were assessed after 8 , 14 and 28 days. The creams were made to acclimatize at room temperature 2 h before assessment.

Cream Separation Resistance

This experiment was conducted using an automated centrifuge after 8 days of product formulation at an rpm of 3000 for 15 min to assess the physical stability of the formulations. The study was repeated after 14 and 28 days. All measurements were conducted at room temperature.

pH Determination

The determination of pH value for each formulated cream model was performed using a benchtop pH meter with a single electrode, measuring temperature and pH, constantly stored in 0.1 M HCl solution. After 8 days of product preparation, the measurement was attained by rinsing the probe with deionized H_2O after it was removed from the 0.1 M HCl storage solution and placed into the diluted test sample (0.05 mL of cream, using a 1 mL graduated syringe, was dissolved in 5 mL deionized H_2O). The probe was kept in place until a steady pH value was reached. All measurements were done in triplicate, taken at a temperature of 23 °C and repeated after 14 and 28 days of storage.

Microscopic Size Examination

Globule size analysis was conducted using the Olympus microscope, AxioVision® Rel. software version 4.4. This was done by placing a dot of each product on a glass slide and viewed in nonpolarized light (angle 90), 40× magnification. All measurements were carried out at room temperature, 25 ± 1 °C and humidity of 33%, and repeated after 14 and 28 days.

Globule Size and Zeta Potential Measurement

Globule size analysis was performed after 8 days of product preparation using the photon correlation principle of the Malvern® ZETASIZER NANO Instrument (Malvern, UK) by dissolving 10 µL of each cream in 990 µL of distilled H_2O (100× dilution) in a cuvette cell. Globule charge analysis was also performed using the same instrument by mixing 10 µL of each cream with 990 µL of distilled H_2O and injecting the mix into a double folded capillary cell. All measurements were done in triplicate, at 25 ± 1 °C, a humidity of 33% and repeated after 14 and 28 days.

Microbial Challenge Test

The microbial challenge test was performed using Schulke+ mikrocount® duo dipslides containing two agar surfaces (the yellow agar surface promotes bacteria growth, i.e., *Staphylococcus spp* and *Escherichia coli*, while the pink agar surface promotes yeast and fungi growth).

The test sample was transferred onto the yellow agar surface via a wet swab in a unidirectional motion and a different swab was used the same way for the pink agar surface. The slides were then enclosed and left for 72 h to allow optimum fungi growth. The products were made to acclimatize at room temperature 2 h before assessment. All measurements were done at room temperature 25 ± 1 °C and a humidity of 33%.

6.2.2.3. Long-Term Stability Study

The Dynamic Vapour Sorption (DVS) analyser was used to determine the long-term stability of the creams, by measuring changes in sample mass by uptake (sorption) and loss (desorption) of moisture content, at 25 °C constant temperature. The instrument was initially calibrated, the device preheated, and a new method was created as follows—the nitrogen tank was set at a constant pressure of 2 mbar, a full cycle (sorption and desorption) was selected on the software, at 200 sccm gas flow, dm/dt was 0.0005 for 100 mg sample weight (DMDT% mass change of rate in time, to determine equilibrium) and a pair of 9 mm glass pans were used. The sample was exposed to an increasing and decreasing step size of 10 in humidity ranging from 0% up to 90% RH, and 90% down to 0% RH. Following the short-term stability studies, the test samples initially stored at 25 °C room temperature was used to perform this study.

6.2.2.4. Statistical Analysis

Statistical evaluation of results obtained for all formulated creams was carried out using the IBM SPSS software. Analysis of variance (one-way ANOVA) was conducted to observe differences between attributes of the O/W creams stored under 4, 25 and 40 °C, after 8, 14 and 28 days, where $p < 0.05$ indicates a significant difference between the emulsions stored under the three different storage conditions.

6.3. RESULTS AND DISCUSSION

6.3.1. Short-Term Stability Studies

6.3.1.1. Cream Separation Resistance

The centrifuge test showed that all models remained completely intact without separating into different layers, i.e., no phase separation was observed in the formulations (Figure 6.1). This implies that all products (with equal ratio oil combinations jojoba and baobab oil; jojoba and coconut oil; and baobab and coconut oils) were physically stable in terms of macroscopic stability.

(a)   (b)
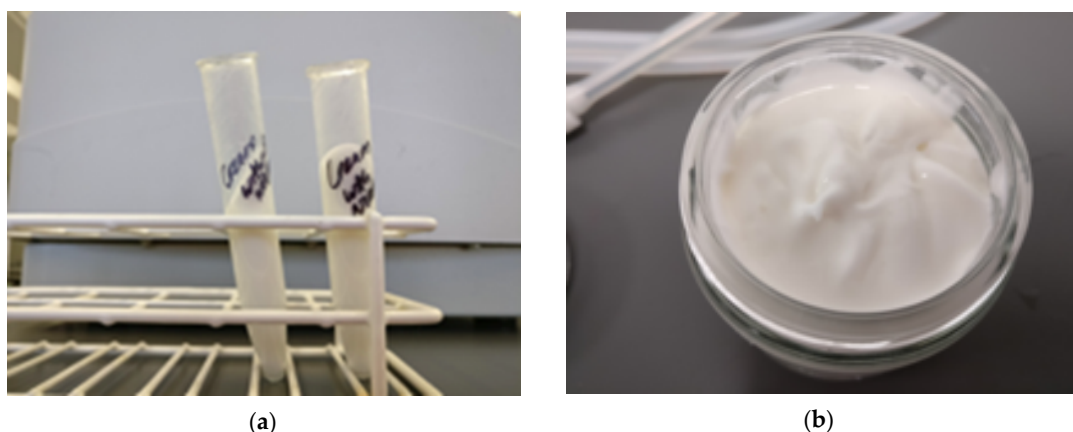
Figure 6.1. (a) Image of newly prepared oil-in-water cream formulation. **(b)** An active model and its baseline after centrifuging for 15 min at 3000 rpm.

6.3.1.2. pH Determination

The surface of human integument has a slightly acidic pH ranging from 4.0 to 5.5 [40,41], this value is said to be slightly higher in old age (i.e., >80 years) [41]. An acidic pH range of 4.0 to 5.5 on the surface of the skin is essential for colonizing microbiota metabolites, i.e., *Propioni, Staphylococcus epidermidis and Corynebacteria*, which have no harmful effect but serve to inhibit non-resident bacteria and fungi growth, ultimately acting as a biological barrier. Constant use of cosmetic products that are alkaline in nature tamper with the acidic mantle, allowing multiplication of non-resident bacteria and fungi on the surface [42,43]. These microorganisms can then penetrate the surface of the skin and become harmful or toxic to human health; therefore, the formulation of cosmetic products between pH 4.0/±0.10 and 5.5/±0.10 could help maintain the acidic barrier and prevent toxic reactions [43].

Nearly all products containing actives showed higher pH values in comparison to their baseline (Table 6.1, Figure 6.2); this difference in pH could be attributed to the basic nature of the active vehicle. Models stored under 4 °C, at the end of 28 days were observed to have the highest pH increase than those stored at 25 and 40 °C. This shows that the products are not suitable for prolonged storage under

4 °C. Model IVA stored at 25 °C had high pH values after 14 days of 5.66 and after 28 days, the pH value was 5.78; however, pH remained low at 40 °C storage, i.e., 5.02 and 5.16 after 14 days and 28 days, respectively.

Model			8 Days			14 Days			28 Days
	4 °C	25 °C	40 °C	4 °C	25 °C	40 °C	4 °C	25 °C	40 °C
IA	5.17/±0.3	5.19/±0.02	5.50/±0.2	5.46/±0.1	5.22/±0.01	5.31/±0.1	5.70/±0.1	5.14/±0.1	5.18/±0.04
IB	4.55/±0.2	4.84/±0.1	4.73/±0.1	5.15/±0.3	4.98/±0.03	5.00/±0.2	5.70/±0.1	4.91/±0.1	4.85/±0.04
IIA	5.33/±0.1	5.29/±0.1	4.82/±0.1	5.35/±0.1	5.33/±0.1	5.28/±0.2	5.73/±0.04	5.21/±0.1	5.66/±0.1
IIB	5.17/±0.2	4.84/±0.1	4.88/±0.1	5.37/±0.2	4.83/±0.1	5.37/±0.03	5.49/±0.04	5.28/±0.1	5.54/±0.01
IIIA	5.11/±0.1	5.32/±0.1	4.87/±0.04	5.23/±0.1	5.35/±0.1	5.34/±0.1	5.75/±0.2	5.50/±0.1	5.44/±0.03
IIIB	5.20/±0.02	5.27/±0.1	4.77/±0.1	5.31/±0.2	5.25/±0.1	5.22/±0.1	5.44/±0.1	4.97/±0.1	5.03/±0.2
IVA	5.47/±0.2	5.55/±0.04	4.88/±0.1	5.62/±0.1	5.66/±0.04	5.02/±0.2	5.82/±0.1	5.78/±0.1	5.16/±0.02
IVB	5.35/±0.04	5.50/±0.1	4.81/±0.2	5.45/±0.04	5.53/±0.04	4.96/±0.3	5.55/±0.1	5.51/±0.1	5.15/±0.1

Table 6.2 shows the average cumulative pH values and/or standard deviation of 8, 14, 28 days measurements for each cream under the different storage conditions. Nearly all creams stored at 25 °C room temperature, exhibited very low changes in pH < 0.1, and only products IIB and IVB showed low changes in pH after 28 days. However, all products stored at 40 °C after the end of the 4 weeks' measurement showed variations in pH > 0.1. This implies that all products stored at room temperature had very good shelf-life or stability and could be safe for use. On the contrary, products stored at 4 °C (except for model IIIB and IVB) and 40 °C did not exhibit good shelf-life due to large variations in average pH values after 4 weeks. This may mean that the control creams containing coconut oil (models IIIB and IVB) are suitable for low-temperature storage but, the differences observed in their active-containing pairs (model IIIA and IVA), under the same storage temperature, could be attributed to the effect of the active ingredient on the overall stability of the products after 28 days.

Model	Mean/SD at 4 °C	Mean/SD at 25 °C	Mean/SD at 40 °C
IA	5.44/±0.22	5.18/±0.03	5.33/±0.13
IB	5.13/±0.47	4.91/±0.06	4.89/±0.11
IIA	5.47/±0.18	5.27/±0.05	5.25/±0.34
IIB	5.34/±0.13	4.98/±0.21	5.26/±0.28

IIIA	5.36/±0.28	5.39/±0.08	5.22/±0.25
IIIB	5.32/±0.10	5.16/±0.14	5.01/±0.18
IVA	5.64/±0.14	5.66/±0.09	5.02/±0.11
IVB	5.45/±0.08	5.51/±0.01	4.97/±0.14

6.3.1.3. Microscopic Size Examination

Overall, from the microscopic data obtained, models IIA and IIB (containing 1:1 of 10% jojoba and baobab oils) appeared to have the highest stability under low, normal or high temperatures, followed by models IA and IB (1:1 of 8% jojoba and baobab oils), and IVA and IVB (1:1 of 10% baobab and coconut oils), while models IIIA and IIIB (containing 1:1 of 10% jojoba and coconut oils) showed the least stability. The increase in temperature presumably led to the swelling, and eventually rupturing, of the niosome vesicles causing the active drug (methylene blue) to leak out into the cream base. An increase in temperature resulted in an increase in thermal energy, allowing the globules and niosome particles to move faster, colliding with each other and thereby coalescing.

6.3.1.4. Globule Size and Zeta Potential Measurement

In an oil-in-water emulsion, oil globule sizes range from 100 to 15,000 nm [44,45]. Globule size and zeta potential of the prepared oil-in-water cream models were performed to assess their stability [46,47]. Zeta potential value is influenced by the pH of the test sample, i.e., an addition of alkali medium to a negative zeta potential causes the negative charge to increase, while the addition of an acidic medium to a negative zeta potential causes a reduction in the negative charge until a neutral state is obtained, and additional acid will result in a positive charge [48].

An increase in globule size, i.e., a globule size approaching 10,000 nm is due to coalescence [49–51]. In this study, an emulsion with average globule size ≥6000 nm was classified as having poor stability. Charges > −25 were termed poor stability, −25 to −29.9 as average stability, −30 to −44.9 were said to have good stability and ≤−45 indicated excellent stability.

Overall, the oil-in-water creams demonstrated positive but weak conductivity values, which was expected as water (the dispersion medium) is a good conductor of electricity. The size and zeta measurement revealed all formulations, i.e., model IA, IB, IIA, IIB, IIIA and IIIB showed physical and chemical stability or shelf-life when stored at 25 °C, with the exception of models IVA and IVB which showed good stability only at storage conditions of 4 °C. The average size and zeta potential result (Figure 6.4) revealed that models IA, IB, IIA, IIB and IIIB were the most stable in comparison to other cream models. This result also correlates with the pH and globule size analysis.

The one-way ANOVA test revealed a statistically significant difference in globule size between samples stored under the different temperature conditions, i.e., 4 °C, 25 °C and 40 °C after 8, 14 and 28 days. The total highest change was observed after 28 days measurement. At the end of the first week

of measurement, 8 days, a significant difference in globule size of p value = 0.03 between 4 °C and 25 °C was seen, samples in 4 °C and 40 °C, and 40 °C and 25 °C had p values of <0.001. After 14 days measurement, samples stored under 40 °C and 25 °C showed a significant difference in globule size of p value = 0.033. A p value of 0.034 was observed between those stored under 40 °C and 25 °C, after 28 days measurement. However, there was no statistically significant difference in charge.

Based on the results from the short-term stability tests, creams IA, IB, IIA and IIB (1:1 jojoba and baobab oil) and IIIB (1:1 jojoba and coconut oil) all had good shelf-life or stability, particularly with samples stored at room temperature, with cream IA, IB and IIA showing little to no changes in all parameters compared to creams IIIA, IVA and IVB, over the period of evaluation. The variations observed in the short-term stability data of cream IIIA and IIIB with the same oil combination formulation, under the same storage temperatures (4 °C, 25 °C and 40 °C after 8, 14 and 28 days) could be attributed to the effect of the active ingredient on the overall stability of the product IIIA. This implies that the 1:1 of jojoba and baobab oil combinations (regardless of the amount used in formulation i.e., 8% or 10%) appeared to be the best oil combinations in terms of short-term stability compared to 1:1 of jojoba and coconut oil or baobab and coconut oil combinations.
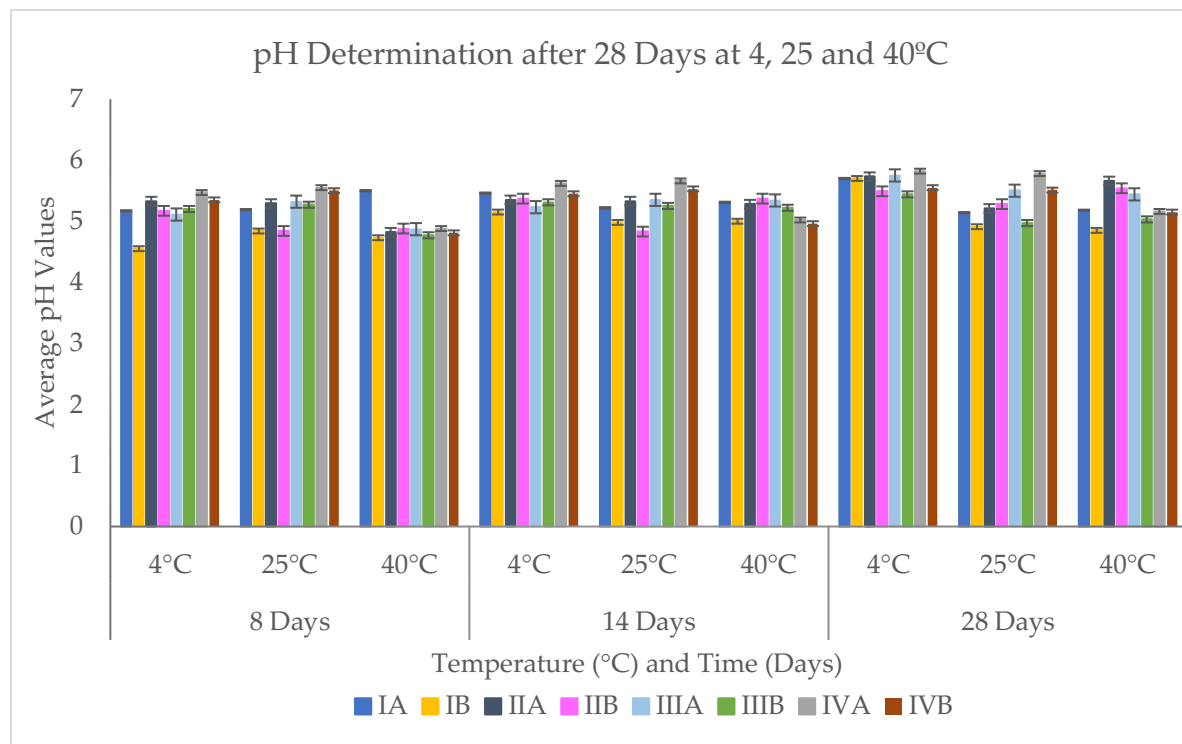
Figure 6.2. A graphical representation of the average pH values after 8, 14, 28 days measurements.

Table 6.3. Globule size and zeta values of model IA to IVA and their controls at 4 °C, 25 °C and 40 °C after 8 days.

Model	Average Size/±SD (d.nm)	Zeta Potential (mV)	Conductive (mS/cm)	Storage Temperature (°C)	Report Quality

91

Model	Average Size/±SD (d.nm)	Zeta Potential (mV)	Conductive (mS/cm)	Storage Temperature (°C)	Report Quality
IA	1500/±408	−44.2	0.021	4	Good
	1257.3/±80.7	−39.3	0.015	25	Good
	4964/±2770.9	−43.6	0.033	40	Good
IB	1298/±395.5	−40.4	0.017	4	Good
	1798/±7.8	−40.2	0.069	25	Good
	3487.6/±486.8	−43.2	0.042	40	Good
IIA	939.3/±38	−39.6	0.121	4	Good
	2755.6/±51.5	−40.1	0.040	25	Good
	3488/±480	−41.6	0.334	40	Good
IIB	891.6/±61.7	−17.9	0.037	4	Poor
	2181/±359	−40.0	0.109	25	Good
	3470.6/±298.6	−28.7	0.028	40	Average
IIIA	800/±112.9	−44.7	0.022	4	Good
	1530/±287	−41.3	0.049	25	Good
	3879/±584	−39.7	0.045	40	Good
IIIB	1579/±237	-46.9	0.017	4	Excellent
	2213/±252.7	−52.5	0.022	25	Excellent
	6184/±1651.9	−47.1	0.027	40	Excellent
IVA	872.9/±276	−47.0	0.023	4	Excellent
	1859/±71.8	−45.4	0.034	25	Excellent
	3674/±173	−38.1	0.068	40	Good
IVB	831/±87.7	−53.0	0.021	4	Excellent
	2344.6/±129	−33.6	0.030	25	Good
	3674/±173	−38.1	0.068	40	Good

Table 6.4. Globule size and zeta values of model IA to IVA and their controls at 4 °C, 25 °C and 40 °C after 14 days.

Model	Average Size/±SD (d.nm)	Zeta Potential (mV)	Conductive (mS/cm)	Storage Temperature (°C)	Report Quality
IA	2434.6/±203	−45.9	0.036	4	Excellent
	3233/±1269.5	−48	0.030	25	Excellent
	4353/±1682.6	−45	0.049	40	Excellent
IB	3417/±917	−41.1	0.024	4	Good
	1419.7/±64.7	−47.7	0.013	25	Excellent
	2164/±86	−37.6	0.083	40	Good
IIA	3056/±28.8	−36.3	0.023	4	Good
	3129/±120	−44.1	0.025	25	Good
	3045/±186.6	−39	0.065	40	Good
IIB	2706/±317.5	−26.9	0.023	4	Average
	1472/±167	-41.3	0.015	25	Good
	3001.6/±111.5	−28.5	0.026	40	Average
IIIA	2889.6/±149.9	−43.5	0.048	4	Good
	2007.6/±26.5	−42.8	0.034	25	Good
	7103/±2447.7	−38.8	0.045	40	Poor
IIIB	2691/±53.6	−30.7	0.039	4	Good
	1157/±62.6	−46.6	0.022	25	Excellent
	3932/±440	−39.6	0.023	40	Good
IVA	5059/±499.8	−41.9	0.044	4	Good
	1509/±675	−37.6	0.058	25	Good
	3220.6/±331.8	−39.1	0.032	40	Good
IVB	4291/±34.5	−36.9	0.023	4	Good
	2083/±247.6	−31.5	0.047	25	Good
	1922/±130.6	−37.9	0.029	40	Good

Table 6.5. Globule size and zeta values of model IA to IVA and their controls at 4 °C, 25 °C and 40 °C after 28 days.

| Model	Average Size/±SD (d.nm)	Zeta Potential (mV)	Conductive (mS/cm)	Storage Temperature (°C)	Report Quality
	3754/±926.6	−38.3	0.027	4	Good
IA	2760/±254.6	−48.1	0.027	25	Excellent
	3826/±994.7	−29.9	0.069	40	Average
	3037.6/±768.6	−40.2	0.053	4	Good
IB	3998.6/±655.5	−40.6	0.022	25	Good
	4176/±771.8	−29.5	0.051	40	Average
	3635/±329	−25.7	0.035	4	Average
IIA	3129/±120	−38.8	0.041	25	Good
	4176/±771.8	−35.8	0.038	40	Good
	4156/±169.5	−23.2	0.034	4	Poor
IIB	1928/±322	−34.5	0.018	25	Good
	6190/±837.8	−25.0	0.037	40	Average
	7152.6/±1350.9	−36.7	0.066	4	Poor
IIIA	2054/±260	−38.7	0.026	25	Good
	6729/±1596	−20.4	0.091	40	Poor
	2781.6/±385	−37.8	0.025	4	Good
IIIB	2768/±194.5	−40.5	0.027	25	Good
	5014/±1070.5	−38.6	0.031	40	Good
	2174.6/±150.9	−46.0	0.051	4	Excellent
IVA	3003.6/±408	−23.0	0.066	25	Poor
	5781/±381.6	−23.2	0.091	40	Poor
	3657.6/±1134	−29.2	0.035	4	Average
IVB	7157/±1839	−18.7	0.048	25	Poor
	6756.6/±1205	−18.1	0.065	40	Poor
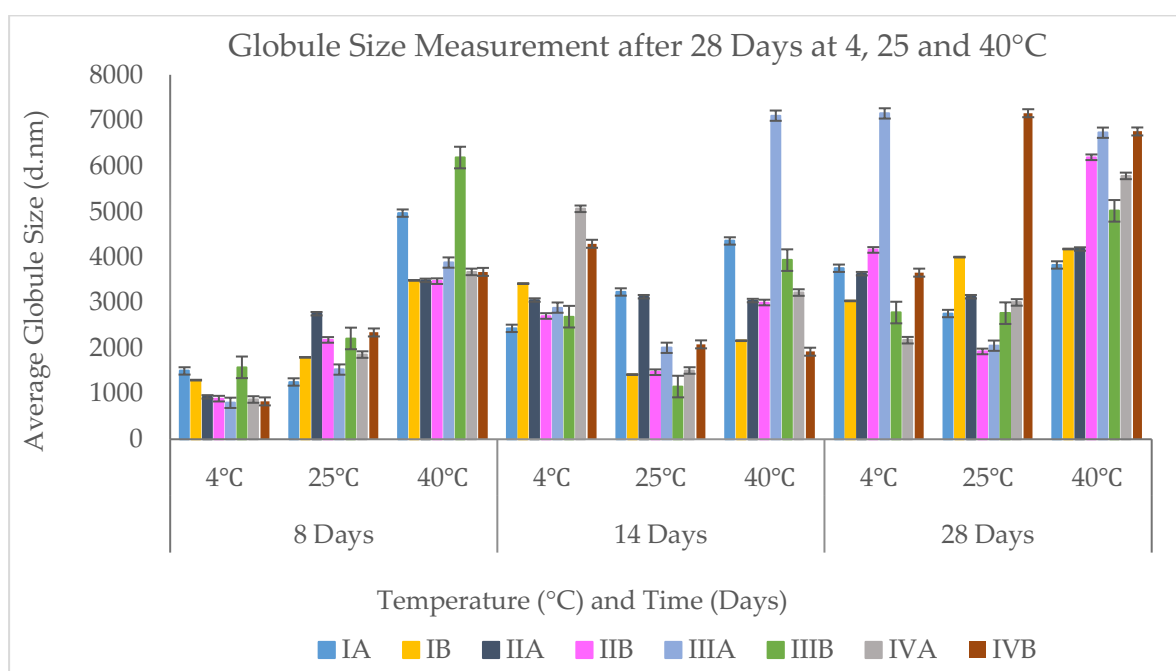
Figure 6.3. Globule size measurement after 8, 14 and 28 days at 4, 25 and 40 °C.

6.3.1.5. Microbial Challenge Evaluation

Microbial challenge test is a safety assessment of formulated products, indicating the ability of the product to promote or inhibit bacteria and fungi growth. In other words, it determines the effectiveness or efficiency of the preservative and the compatibility of the preservative with the other ingredients in the creams [52]. The challenge test performed using Schulke+ mikrocount® duo dipslides containing two agar surfaces (the yellow agar surface promotes bacteria growth, i.e., *Staphylococcus* spp. and *Escherichia coli* while the pink agar surface promotes yeast and fungi growth).

The density and type of colony formed on the nutrient plate is determined using the colony density charts specified by Schulke+. After 72 h, there was an absence of microbial growth in all formulations. Model IVA stored at 25 °C room temperature, in reference to the colony density charts, as shown in Figure 6.5, had <1 CFU/cm^2 total plate count (TPC) on the bottom of the yellow agar surface after 28 days of evaluation, indicating bacteria contamination, although, the preservative was effective against yeast or fungi growth. It is important that the preservative is capable of inhibiting microbial growth as this may cause changes in the product, i.e., color, smell, viscosity and stability, and acne, desquamation or infections to the skin [52,53]. The bacteria contamination observed in model IVA, in contrast to the absence of bacterial growth in model IVB, could be attributed to the packing material, as no sterilization of the containers were done prior to packaging.

(**a**)   (**b**)
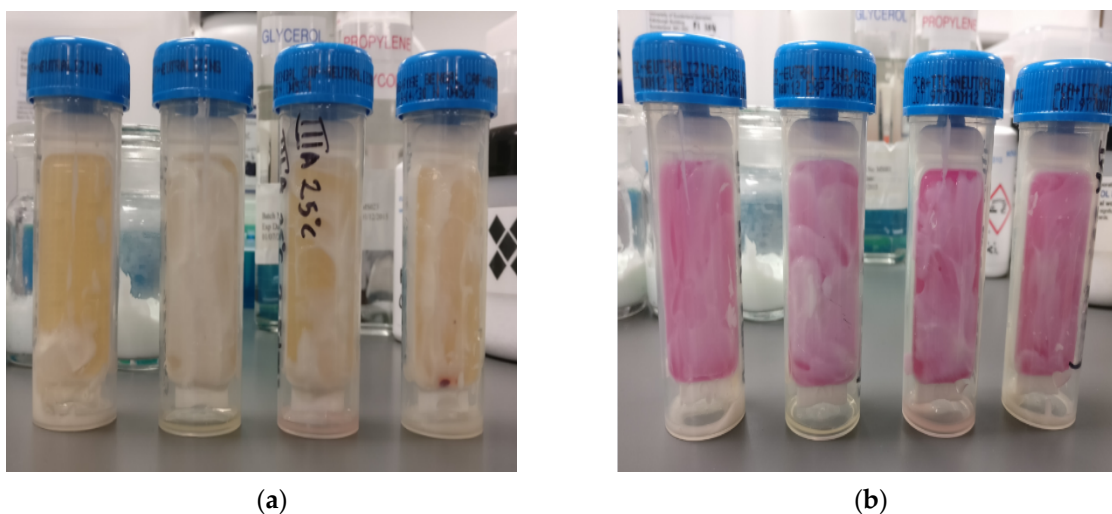
Figure 6.4. Model IVA under 25 °C storage temperature after 28 days evaluation showing (**a**) TPC of bacteria <1 CFU/cm^2 (**b**) TCP of yeast or fungi, no colonies formed.

6.3.2. Long-Term Stability Studies

The Dynamic Vapour Sorption (DVS) analyser was evaluated as a potential technique for the determination of the long-term stability of the creams (Figure 6.5). Using the DVS-Advantage-1 system, the percentage change in sample mass was achieved by measuring sample uptake (sorption or

absorption) and loss (desorption or drying) of moisture content, at % RH ranging from 0 to 90, at 25 °C constant temperature.

(**a**)   (**b**)
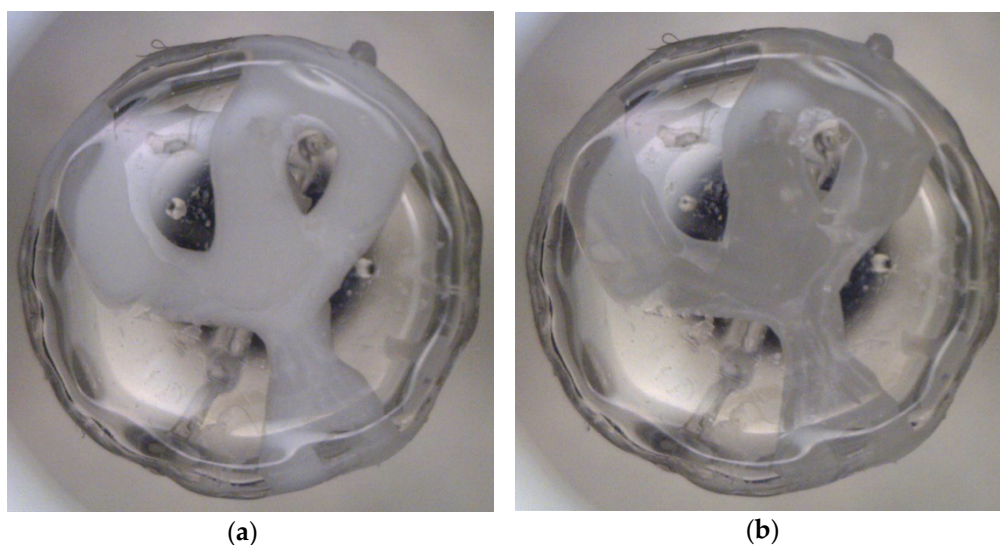
Figure 6.5. Images produced by the dynamic vapour sorption system of sample on 9 mm glass pan after **(a)** moisture content uptake or absorption and **(b)** drying phase, at 90% RH and 25 °C steady temperature.

The uptake and loss of moisture content (and organic vapour) data of all eight creams were derived from the DVS software and analysed using Microsoft Excel® (Figure 6.6) Although moisture (and organic vapour) was absorbed in the hydration phase by each test cream (Table 6.6), a reduction in moisture (mass) at the end of the analysis compared to their initial moisture content (%) was observed i.e., IA, IB, IIA, IIB, IIIA, IIIB, IVA and IVB had a % moisture content decrease of 37.37%, 27.04%, 52.75%, 37.08%, 72.75%, 74.09%, 56.25% and 56.41%, respectively, at the end of the analysis. This could be as a result of the cream becoming too saturated, making the test sample very runny that it flows over the 9 mm measuring pan, rendering the sorption (uptake) method of the DVS for semi-solid materials less valid. However, the method can be applied to a more structured material (e.g., lipsticks, patches and solid dosage forms) to observe changes in swelling or expansion of the solid material during moisture uptake.

Table 6.6. Target relative humidity (increasing steps) and % change in sample mass through moisture content uptake (sorption).

Target RH (%)	Change in Mass (%)—Sorption							
	IA	**IB**	**IIA**	**IIB**	**IIIA**	**IIIB**	**IVA**	**IVB**
Initial	83.65	89.67	105.21	80.87	92.60	98.65	102.72	109.03
0.0	83.49	89.42	105.04	80.67	92.42	98.43	102.46	108.74
10.0	63.69	62.36	83.42	58.55	67.15	70.62	70.54	74.27
20.0	52.64	52.55	71.44	48.65	51.31	53.98	53.43	57.51

30.0	45.91	48.99	64.07	43.57	40.49	42.81	44.23	48.99
40.0	41.65	47.76	59.33	40.77	32.77	35.96	39.43	44.68
50.0	39.08	47.82	55.98	39.18	27.15	29.36	37.14	42.88
60.0	39.06	48.66	53.63	38.25	23.15	25.45	37.01	42.89
70.0	39.20	50.85	53.62	38.28	20.08	22.53	37.4	43.62
80.0	40.71	54.65	52.41	39.18	19.24	22.28	40.27	46.46
90.0	46.28	62.63	52.46	43.79	19.85	24.56	46.47	52.62

The desorption (drying) method of the DVS in Table 6.7 revealed more reliable data for the long-term stability analysis of semi-solid formulations. Models IA, IB, IIA, IIB, IIIA, IIIB, IVA and IVB showed a decrease in moisture content (mass change) % by 51.52%, 45.34%, 58.60%, 47.91%, 80.06%, 85.73%, 71.53% and 71.68%, respectively, as shown in Figure 6.6. This means that the moisture content at equilibrium is greater for the creams in the following order IB, IIB, IA and IIA; therefore, they have the ability to retain more moisture and for an extended period. Models IIIB, IIIA, IVB and IVA were unable to retain more moisture when compared to IB, IIB, IA and IIA. The cream IVB and IVA initially contained the highest amount of moisture 109.03% and 102.72%, respectively, compared to other cream models (except for IIA, 105.21%) but as humidity decreased, <90% over time, both samples experienced a high loss of moisture content. Therefore, creams IB, IIB, IA and IIA—1:1 jojoba and baobab oil combinations showed good long-term stability compared to IIIB and IIIA—1:1 jojoba and coconut oil combinations; and IVB and IVA—1:1 of baobab and coconut oil. This result correlates with the short-term stability studies where, creams IA, IB, IIA and IIB all had good shelf-life or stability based on the data derived from the phase separation resistance, pH, microscopic size analysis, globule size, zeta potential, and conductivity measurements.

Table 6.7. Target relative humidity (decreasing steps) and % change in sample mass through moisture content loss (desorption).

Target RH (%)	Change in Mass (%)—Desorption							
	IA	IB	IIA	IIB	IIIA	IIIB	IVA	IVB
Initial	83.65	89.67	105.21	80.87	92.60	98.65	102.72	109.03
90.0	46.28	62.63	52.46	43.79	19.85	24.56	46.47	52.62
80.0	42.66	57.32	51.39	45.02	19.84	20.4	45.39	49.88
70.0	39.3	52.56	50.40	37.43	18.49	19.22	40.37	44.36
60.0	36.96	49.71	49.38	35.09	15.63	17.82	37.25	43.04
50.0	35.26	47.82	48.71	33.67	13.90	16.56	35.16	41.65
40.0	34.02	46.47	47.83	33.76	12.49	15.4	33.68	39.95
30.0	33.15	45.71	47.20	33.75	12.57	14.35	32.57	38.89
20.0	32.72	45.11	46.98	33.00	12.56	13.51	31.87	38.09
10.0	32.39	44.64	46.77	32.98	12.55	13.12	31.51	37.65
0.0	32.13	44.33	46.61	32.96	12.54	12.92	31.19	37.35

The chemical structure of jojoba oil inhibits free radical buildup, because its double bonds are not in close proximity to each other. Formulations containing jojoba oil have extensive storage life even in

the absence of preservative resulting in no color change and odor development of the product, making the oil highly suitable for use in the cosmetic industry [54,55].

The ability of creams containing a mixture of jojoba and baobab oil to exhibit good short- and long-term stability can be attributed to the strong oxidative stability of the individual oils, i.e., both jojoba and baobab oils are less prone to photooxidation (a common cause of degradation in oil quality) during manufacturing and storage, due to the presence of high amounts of monounsaturated fatty acids (FA) chains in them. Coconut oil is made up of 95% saturated FA, which allows it to absorb light and become more susceptible to deterioration by photooxidation during processing or storage [56]. Therefore, the validity of the DVS method in determining long-term stability was proven as all products formulated with jojoba and baobab oil combination showed extensive stability compared to those containing coconut oil.
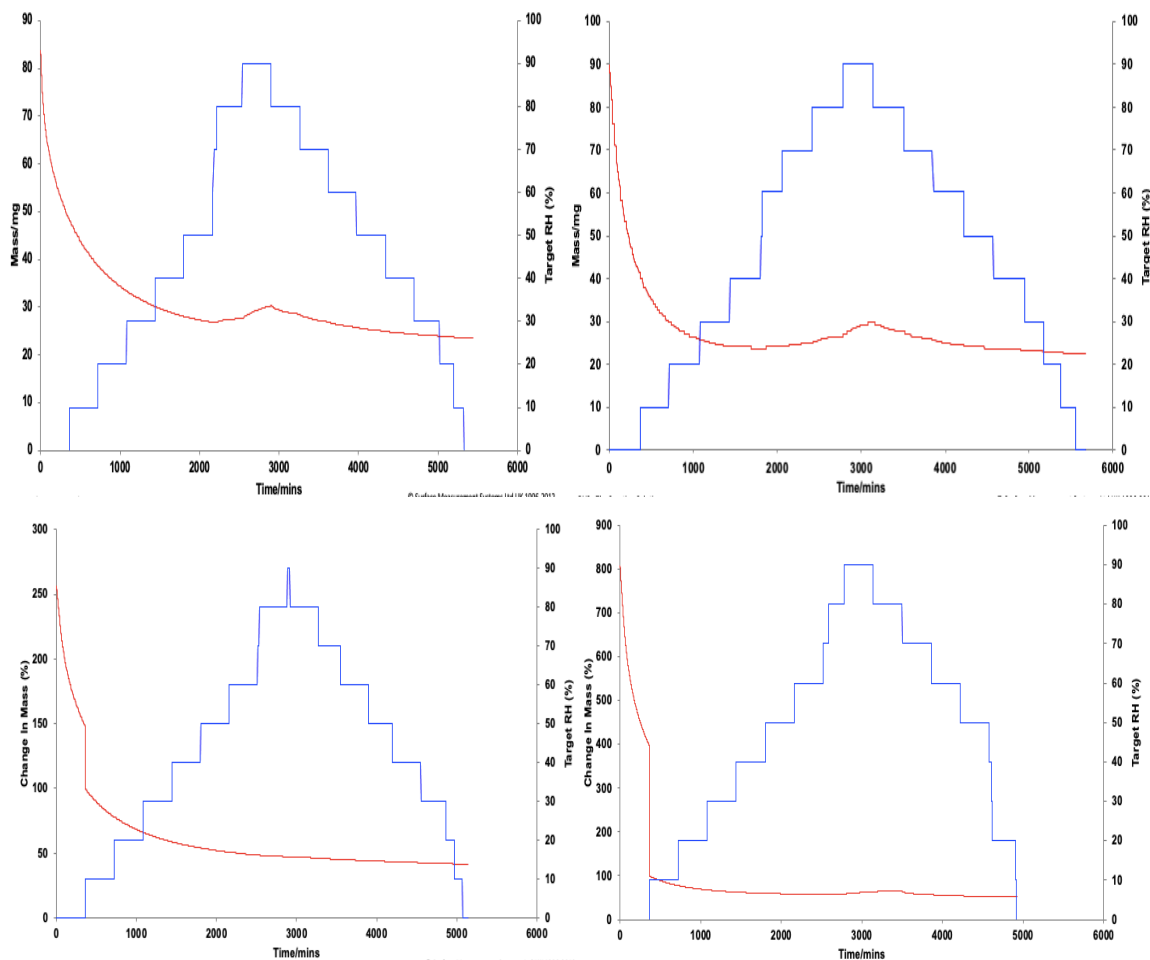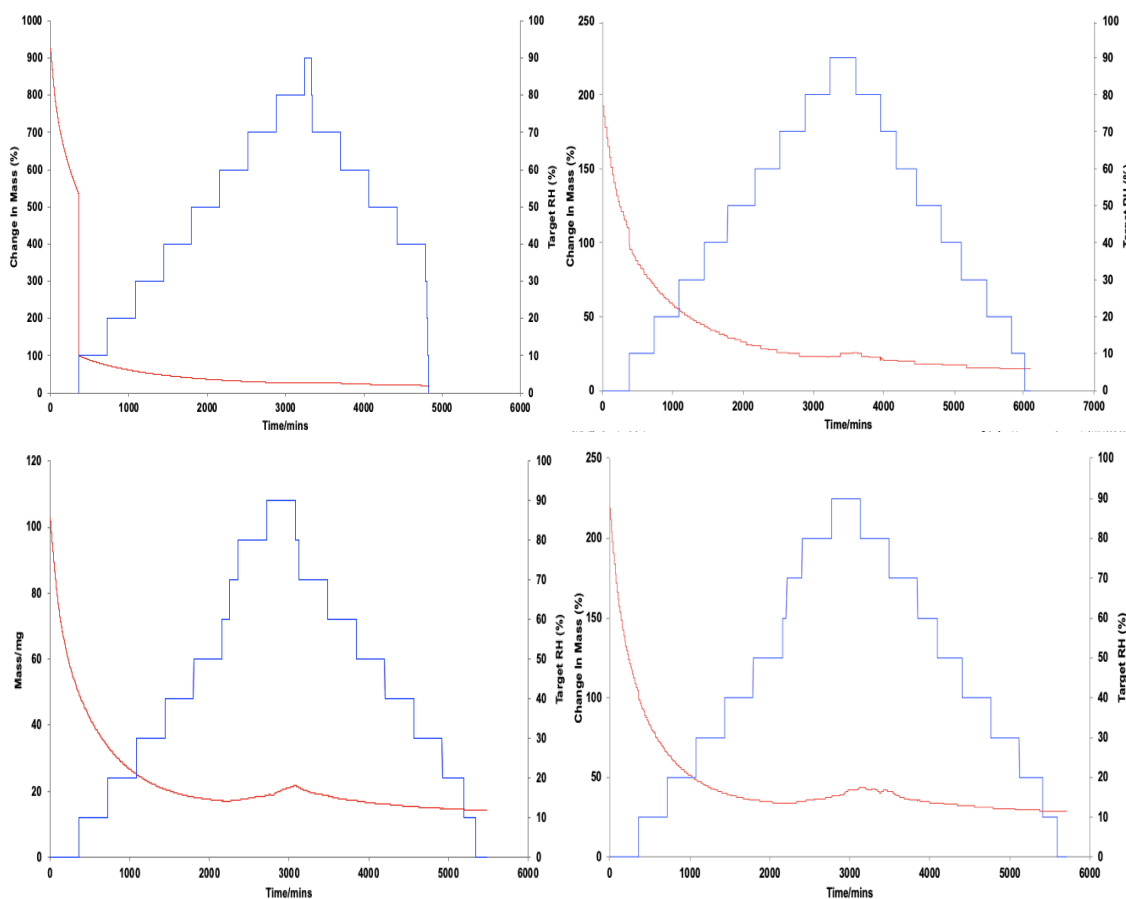
Figure 6.6. Graphical illustrations of moisture sorption and desorption kinetics at constant temperature of 25 °C, showing change in mass, DM (red) and % relative humidity, RH (blue) plotted against time/min, DT, of all model creams.

In this study, the long-term stability evaluation performed using the DVS desorption method proved to be very effective. The procedure has high accuracy due to the ability to detect mass changes of <1 part in 10 million. The method was time consuming as it took a period of 5 days to run a full cycle (both sorption and desorption process), see Figure 6.7. However, this can be overcome when a smaller sample size is applied because the equipment is capable of determining percentage mass changes in samples as small as 1 mg to 1.5 g, and when a half cycle procedure is selected (either, desorption for the accurate determination of mass change in a semi-solid material, or sorption for a more structured test sample). These attributes make the technique highly economical, reliable and less complex than other techniques (e.g., HPLC, DSC and SC).

4. Conclusions

As consumers begin to become increasingly aware of the harsh chemicals contained in commercially available products, there has been a recent surge for natural and organic ingredients [57].

98

Four novel cream formulas with natural oils, containing actives (model IA-IVA) and their controls (model IB-IVB) were evaluated for safety and quality in accordance with the ICH guideline.

The microbial challenge result revealed the products were capable of inhibiting bacterial, yeast and fungal growth; therefore, there was no color change or odor development over the period of storage. The phase separation resistance, pH, microscopic size analysis, globule size, charge, conductivity data revealed creams containing 1:1 jojoba and baobab oil, and 1:1 jojoba and coconut oil all had good shelf-life, especially with samples stored at 25 °C.

The proposed long-term stability test using the DVS system, desorption method, demonstrated a more comprehensive stability profile by indicating the ability of the creams to retain moisture.

In conclusion, Models IA, IB and IIA containing 1:1 of jojoba and baobab oil mix, were stable over short-term storage at 4 °C, 25 °C and 40 °C. Their stability was validated after long-term storage at 0 to 90 %RH using the proposed DVS method. Whereas, the creams containing coconut oil (IIIA and IVA) were less stable. The proposed DVS method was, therefore, reliable and can be universally applied in the food, cosmetic and pharmaceutical industries to determine the long-term stability of semi-solids.

REFERENCE

1. Chanchal, D.; Swarnlata, S. Novel approaches in herbal cosmetics. *J. Cosmet. Dermatol.* **2008**, *7*, 89–95, doi:10.1111/j.1473-2165.2008.00369.x.
2. Harsh LN, Tewari JC, Patwal DS, Menna GL. Package of practices for cultivation of jojoba (Simmondsia chinensis) in arid zone.
3. What You Need to Know about Jojoba Oil-Health Benefits. Available online: http://thejojobaoil.com/(accessed on 1 December 2017).

4. Abu-Arabi, M.; Allawzi, M.; Al-Zoubi, H.; Tamimi, A.; Abu-Arabi, M.; Al-Zoubi, H.S. Extraction of jojoba oil by pressing and leaching. *Chem. Eng. J.* **2000**, *76*, 61–65, doi:10.1016/s1385-8947(99)00119-9.

5. Kim, Y.-J.; Lee, M.S.; Yang, Y.S.; Hur, M.-H. Self-aromatherapy massage of the abdomen for the reduction of menstrual pain and anxiety during menstruation in nurses: A placebo-controlled clinical trial. *Eur. J. Integr. Med.* **2011**, *3*, e165–e168, doi:10.1016/j.eujim.2011.08.007.

6. Ruggeri, C. Jojoba Oil-Skin & Hair Healer and Moisturizer-Dr. Axe, 2016. Available online: https://draxe.com/jojoba-oil/(accessed on 29 March 2019).

7. Kubitschek-KM, A.R.; Zero, J.M. Development of jojoba oil (*Simmondsia chinensis* (Link) CK Schneid.) based nanoemulsions. *Lat. Am. J. Pharm.* **2014**, *33*, 459–463.

8. Arya, D.; Khan, S. A Review of *Simmondsia chinensis* (Jojoba)" The Desert gold": A multipurpose oil seed crop for industrial uses. *J. Pharm. Sci. Res.* **2016**, *8*, 381.

9. Knoepfler, N.B.; Vix, H.L.E. Vegetable oils, review of chemistry and research potential of *Simmondsia Chinensis* (Jojoba) Oil. *J. Agric. Food Chem.* **1958**, *6*, 118–121, doi:10.1021/jf60084a005.

10. Adenekan, M.K.; Fadimu, G.J.; Odunmbaku, L.A.; Nupo, S.S.; Oguntoyinbo, S.I.; Oke, E.K. Chemical and functional characterization of baobab (*Adansonia Digitata*, L.) seed protein concentrate using alcohol extraction method. *Int. J. Environ. Agric. Biotechnol.* **2017**, *2*, 2554–2558, doi:10.22161/ijeab/2.5.36.

11. Abubakar, S.; Etim, V.; Bwai, D.; Afolayan, M. Nutraceutical evaluation of baobab (Adansonia digitata L.) seeds and physicochemical properties of its oil. *Ann. Biol. Sci.* **2015**, *3*, 13–19.

12. Organic Baobab Oil Nourishing Skin Naturally. Available online: https://protecbotanica.com/downloads/baobab.pdf (accessed on 7 March 2019).

13. Kamatou, G.; Vermaak, I.; Viljoen, A.M. An updated review of *Adansonia digitata*: A commercially important African tree. *South Afr. J. Bot.* **2011**, *77*, 908–919, doi:10.1016/j.sajb.2011.08.010.

14. Cissé, M.; Sow, A.; Poucheret, P.; Margout, D.; Ayessou, N.C.; Faye, P.G.; Sakho, M.; Diop, C.M.G. Impact of extraction method on physicochemical characteristics and antioxidant potential of *Adansonia digitata* oil. *Food Nutr. Sci.* **2018**, *9*, 937–955, doi:10.4236/fns.2018.98069.

15. Komane, B.M.; Vermaak, I.; Kamatou, G.P.; Summers, B.; Viljoen, A.M. Beauty in Baobab: A pilot study of the safety and efficacy of *Adansonia digitata* seed oil. *Rev. Bras. de Farm.* **2017**, *27*, 1–8, doi:10.1016/j.bjp.2016.07.001.

16. Baobab Oil. Available online: https://slichemicals.com/wp-content/uploads/sites/2/2015/02/BAOBAB-OIL-Mail.pdf (accessed on 7 March 2019).

17. Babiker, S.; Mirghani, M.E.; Matar, S.M.; Kabbashi, N.A.; Alam, M.Z.; Marikkar, J.M. Evaluation of antioxidant capacity and physicochemical properties of Sudanese Baobab (*Adansonia digitata*) seed-oil. *Int. Food Res. J.* **2017**, *24*.

18. Osman, M.A. Chemical and nutrient analysis of Baobab (*Adansonia digitata*) fruit and seed protein solubility. *Plant Foods Hum. Nutr.* **2004**, *59*, 29–33, doi:10.1007/s11130-004-0034-1.

19. Zahra'u, B.; Mohammed, A.S.; Ghazali, H.M.; Karim, R. Baobab tree (*Adansonia digitata* L) parts: Nutrition, applications in food and uses in ethno-medicine-A review. *Ann Nutr Disord Ther.* **2014**, *1*, 1011.

20. Resende, N.M.; Félix, H.R.; Soré, M.R.; Neto, A.M.M.; Campos, K.E.; Volpato, G.T. The effects of coconut oil supplementation on the body composition and lipid profile of rats submitted to physical exercise. *Anais Acad. Bras. Ciênc.* **2016**, *88*, 933–940, doi:10.1590/0001-3765201620150302.

21. Bawalan, D.D.; Chapman, K.R. Virgin coconut oil production manual for micro-and village-scale processing.

22. Buderwitz, P. Health risks and benefits of coconut oil. *Pharm. Today* **2013**, *19*, 27, doi:10.1016/s1042-0991(15)31095-1.

23. Boemeke, L.; Marcadenti, A.; Busnello, F.M.; Gottschall, C.B.A. Effects of coconut oil on human health. *Open J. Endocr. Metab. Dis.* **2015**, *5*, 84–87, doi:10.4236/ojemd.2015.57011.

24. Lockyer, S.; Stanner, S. Coconut oil-A nutty idea? *Nutr. Bull.* **2016**, *41*, 42–45.

25. Mikołajczak, N. Coconut oil in human diet-nutrition value and potential health benefits. *J. Educ. Health Sport.* **2017**, *7*, 307–319.

26. Rethinam, P. Health and nutritional aspects of coconut oil. *Inform.* **2002**, *13*.

27. Kappally S, Shirwaikar A, Shirwaikar, A. Coconut oil-A review of potential applications. *Hygeia JD Med.* **2015**, *7*, 34–41.

28. Bloomfield, S. *Microbial Contamination. Guide to Microbiological Control. in Pharmaceuticals and Medical Devices*; 2nd edition; 2016, doi:10.1201/9781420021622.ch2.

29. Sheokand, S.; Modi, S.R.; Bansal, A.K. Dynamic vapor sorption as a tool for characterization and quantification of amorphous content in predominantly crystalline materials. *J. Pharm. Sci.* **2014**, *103*, 3364–3376, doi:10.1002/jps.24160.

30. Bilia, A.R.; Bergonzi, M.C.; Mazzi, G.; Vincieri, F.F. Development and stability of semisolid preparations based on a supercritical CO_2 Arnica extract. *J. Pharm. Biomed. Anal.* **2006**, *41*, 449–454, doi:10.1016/j.jpba.2005.12.024.

31. Penner, E. Comparison of the New Vapor Sorption Analyzer to the Traditional Saturated Salt Slurry Method and the Dynamic Vapor Sorption Instrument; 2013.

32. Driemeier, C.; Mendes, F.M.; Oliveira, M.M. Dynamic vapor sorption and thermoporometry to probe water in celluloses. *Cellulose* **2012**, *19*, 1051–1063, doi:10.1007/s10570-012-9727-z.

33. Wimmer, R.; Schmid, T. *Dynamic Vapor Sorption of Analyses of Wood-A New Approach to Classical Problems*; 2010.

34. Thybring, E.E.; Glass, S.V.; Zelinka, S.L. Kinetics of water vapor sorption in wood cell walls: State of the art and research needs. *Forests* **2019**, *10*, 704, doi:10.3390/f10080704.

35. Sheokand, S.; Modi, S.R.; Bansal, A.K. Quantification of low levels of amorphous content in crystalline celecoxib using dynamic vapor sorption (DVS). *Eur. J. Pharm. Biopharm.* **2016**, *102*, 77–86, doi:10.1016/j.ejpb.2016.03.006.

36. Automated Multi-Vapor Gravimetric Sorption Analyzer for Advanced Research Applications. Available online: https://www.micromeritics.com/Repository/Files/DVS_Advantage_Brochure.pdf (accessed on 23 October 2020).

37. Galdeano, M.C.; Tonon, R.V.; Carvalho, C.W.P.; Menezes, N.S.; Nogueira, R.I.; Leal-Junior, W.F.; Minguita, A.P.S. Moisture sorption isotherms of raw and extruded wholemeal sorghum flours studied by the dynamic and salt slurry methods. *Braz. J. Food Technol.* **2018**, *21*, doi:10.1590/1981-6723.20717.

38. Glass, S.V.; Boardman, C.R.; Zelinka, S.L. Short hold times in dynamic vapor sorption measurements mischaracterize the equilibrium moisture content of wood. *Wood Sci. Technol.* **2016**, *51*, 243–260, doi:10.1007/s00226-016-0883-4.

39. Adejokun, D.A.; Dodou, K. Quantitative sensory interpretation of rheological parameters of a cream formulation. *Cosmetics* **2019**, *7*, 2, doi:10.3390/cosmetics7010002.

40. Dikstein, S.; Zlotogorski, A. Measurement of skin pH. *Acta Derm. -Venereol. Suppl.* **1994**, *185*, 18–20.

41. Zlotogorski, A. Distribution of skin surface pH on the forehead and cheek of adults. *Arch. Dermatol. Res.* **1987**, *279*, 398–401, doi:10.1007/bf00412626.

42. Fluhr, J.W.; Elias, P.M. Stratum corneum pH: Formation and function of the 'acid mantle'. *Exog. Dermatol.* **2002**, *1*, 163–175, doi:10.1159/000066140.

43. Lambers, H.; Piessens, S.; Bloem, A.; Pronk, H.; Finkel, P. Natural skin surface pH is on average below 5, which is beneficial for its resident flora. *Int. J. Cosmet. Sci.* **2006**, *28*, 359–370, doi:10.1111/j.1467-2494.2006.00344.x.

44. Argov, N.; Lemay, D.G.; German, J.B. Milk fat globule structure and function: Nanoscience comes to milk production. *Trends Food Sci. Technol.* **2008**, *19*, 617–623, doi:10.1016/j.tifs.2008.07.006.

45. Michalski, M.-C.; Camier, B.; Briard, V.; Leconte, N.; Gassi, J.-Y.; Goudédranche, H.; Michel, F.; Fauquant, J. The size of native milk fat globules affects physico-chemical and functional properties of Emmental cheese. *Le Lait* **2004**, *84*, 343–358, doi:10.1051/lait:2004012.

46. Instruments M. Zeta potential: An Introduction in 30 minutes. *Zetasizer Nano Serles Tech. Note. MRK654.* **2011**, *1*, 1–6.

47. Seleci, D.A.; Seleci, M.; Walter, J.-G.; Stahl, F.; Scheper, T. Niosomes as nanoparticular drug carriers: Fundamentals and recent applications. *J. Nanomater.* **2016**, *2016*, 1–13, doi:10.1155/2016/7372306.

48. Clogston, J.D.; Patri, A.K. Zeta Potential Measurement. In Characterization of Nanoparticles Intended for Drug Delivery; Humana Press: 2011; pp. 63–70.

49. Milk Homogenization-HORIBA. Available online: http://www.horiba.com/uk/scientific/products/particle-characterization/applications/milk-homogenization/(accessed on 31 January 2019).

50. Walstra, P.; Geurts, T.J.; Noomen, A.; Jellema, A.; van Boekel, M.A.J.S. Dairy Technology: Principles of Milk Properties and Processes. Marcel Dekker, Inc.: New York, NY, USA, 1999.

51. Walstra, P.; Jenness, R. Dairy Chemistry and Physics; John Wiley & Sons: New York: NY, USA, 1984.

52. Orús, P.; Leranoz, S. Current trends in cosmetic microbiology. *Int. Microbiol.* **2005**, *8*, 77–79.

53. Budecka A, Kunicka-Styczyńska A. Microbiological contaminants in cosmetics–isolation and characterization. 2014

54. Chemistry-Jojoba Naturals. Available online: https://www.jojobanaturals.com/learn/jojoba-chemistry/(accessed on 7 August 2020).

55. Jojoba Oil: Boosting Stability, Advancing the Beauty Business. Available online: https://www.personalcaremagazine.com/story/30658/jojoba-oil-boosting-stability-advancing-the-beauty-business (accessed on 7 August 2020).

56. Madhujith, T.; Sivakanthan, S. Oxidative stability of edible plant oils. *Ref. Series Phytochem.* **2018**, 1–23.

57. Vermaak, I.; Kamatou, G.; Komane-Mofokeng, B.; Viljoen, A.; Beckett, K. African seed oils of commercial importance-Cosmetic applications. *South. Afr. J. Bot.* **2011**, *77*, 920–933, doi:10.1016/j.sajb.2011.07.003.

CHAPTER 7

EFFICACY STUDY OF NOVEL ANTI-CELLULITE CREAM AND ALTERNATIVE METHODS TO QUANTITATIVE SENSORY EVALUATION

7.1. INTRODUCTION

Gynoid lipodystrophy or cellulite is considered a multifactorial skin condition, although not entirely clear, inducing fatty tissue breakdown via modification steps in the interstitial matrix, micro-circulatory harmony, adipose cell hypertrophy and hyperplasia, thereby, resulting to blood and lymphatic vessel restriction and also the disruption of elastin and collagen network [1][2]. Cellulite can advance into a more severe condition, when left untreated and may give rise to edema, and eventually fibrosis [2]. In addition, cellulite encourages feelings of insecurity and low self-esteem due to its unappealing nature, reducing patient's life quality [3][4]. Despite the market availability of numerous anti-cellulite medical devices and cosmetic products, they appear to produce little to no clinical evidence to support their claims and none has been seen to demonstrate long-term effect or adequately manage the condition [4].

Elastin and collagen fiber network give the skin its viscoelastic or biomechanical properties [5][6]. Skin elasticity is the ability of the skin to deform in the presence of a mechanical force and return to its original state when the force is removed, because skin is not 100% elastic and neither is it 100% plastic, it deforms more or less according to the firmness (ability of the skin to resist further deformation by the negative pressure). When this mechanical force is removed, there is a delay in the skin to return to its original position, this is known as viscoelasticity. Skin viscoelastic property can be influenced by several extrinsic and intrinsic factors [7][8]. The cutometer is a dermal elasticity meter that determine the degree of skin firmness and elasticity. It is also used in efficacy testing, providing claim support for a wide range of cosmetic products [8].

Another device evaluating cutaneous biomechanical changes is the visiometer, it uses a blue silicone dye to produce skin replicas for surface texture measurements via image analysis [9]. The visioscan also measures skin surface texture (roughness and micro-relief), however the visioscan uses a high-resolution video sensor camera to provide a direct measurement. The two devices find their application in dermatological documentation, efficacy testing of cosmetic products and raw materials [9][10]. User perceptions (i.e. feel, appearance and efficacy), although not a biomechanical process, is a very useful tool in the cosmetic industry as it assesses sensory attributes of a cosmetic formulation from the user point of view, predicting market success [11][12][13].

In a previous study, we demonstrated how sensory attributes, like pourability, firmness, elasticity, spreadability and stickiness, can be accurately quantified in the laboratory using a rheometer to measure flow and deformation behavior of a formulation [14]. However, we failed to quantitatively determine other relevant attributes like skin hydration and turbity/opaqueness. Refractive Index (RI) of a given cream sample is a measure of the velocity of light in the cream divided by the velocity of light in vacuum. RI has a wide range of information from drug concentration present in a sample to

106

permeability to opaqueness or turbidity of the sample [15]. Also, RI has been shown to measure skin hydration after successive application of a moisturizer [16]. RI is said to increase with increased turbidity and decreased skin hydration and vice-versa [17][18]. A UV spectrophotometer is generally used to measure the RI of a material however, this would produce inaccurate results because of the extremely turbid nature of the test creams [19][20]. Therefore, the need for a highly sensitive device to measure the refractive index of an extremely turbid sample is important.

The present study aims to provide alternative quantitative method for sensory evaluation by directly investigating the RI of creams through a newly developed method, without cream dilution. *In vivo* efficacy study of the lead active anti-cellulite cream was also assessed, using both quantitative (the cutometer, visiometer and visioscan) and qualitative method (user perception of cream efficacy and quality through questionnaire study), in comparison to its baseline and a popular, market available anti-cellulite cream, providing the following claims "2-IN-1 BODY MOISTURISER + TONING CREAM" formulated with green coffee and Indian forskolin to inhibit lipogenesis and promote lipolysis.

7.2. MATERIALS AND METHODS

7.2.1. Participants/Volunteers

A total of twelve (n = 12) healthy female participants with varying cellulite grade (I-III) were enrolled into this randomized single blinded study. Their age, height and weight range were between 22 to 57 years, 155.4 to 179.8 cm and 54 to 112 Kg, respectively. The inclusion criteria used was the presence of cellulite, no history of related surgical procedure and absence of pregnancy or any disease or other existing skin condition. Prior to the investigation, all 12 participants were well informed about the procedures involved and signed a consent form (please see appendix section for additional information).

7.2.2. Study Design

All participants were assigned into 3 groups based on their arrival. Group 1 was given the novel active anti-cellulite cream, group 2 baseline/control cream (without the active ingredient) and finally, group 3 was appointed a best seller cream, available on the market.

Theory of Interventions

- The novel active anti-cellulite cream – (a) The active (methylene blue) contained in the cream is thought to demonstrate antioxidant and free radical scavenging activities by targeting cellular mitochondria [21]. Free radicals are responsible for increasing collagen and elastin degradation while decreasing its synthesis by promoting matrix metalloproteinase (MMP) expression (also called collagenases – they cleave or digest collagen), and eventually result to dermal network alteration. In order to reverse this process, localized application of

107

antioxidants to the skin surface can help reduce the production or accumulation of free radicals or neutralize its effect [22][23]. This active was entrapped in niosomal vesicles for delivering a much higher concentration to the site of action. (b) The cream was formulated using jojoba and baobab oil possessing antioxidant properties that helps reduce fine lines and wrinkles, stimulating collagen synthesis and eventually skin healing and rejuvenation of epithelial cells [24]. This sample was labelled cream A, the participants in the first group were assigned this intervention for a period of 4 months, to be applied daily on the right posterior lateral thighs.

- The novel anti-cellulite cream without the active ingredient - This cream contained only the antioxidant properties from the jojoba and baobab oil attributable to their omega 6 and omega 9 composition [24]. They mediate keratinocytes, endothelial cells and fibroblasts (collagen producing cells), migration, proliferation and differentiation, forming new vessels to encourage epithelialization through the release of growth factors and cytokines. This results to collagen fiber production and accumulation, restoring cutaneous tensile strength and structure. Additionally, omega 6 and 9 improves cutaneous hydration by lowering transepidermal water loss, mediating the regeneration of damaged epidermal lipid barrier and skin metabolism stabilization [25][26]. This sample was labelled cream B and assigned to participants in the second group.

- Market available cream. Participants in the third group were assigned a best seller anti-cellulite cream - an anti-cellulite cream containing 2 active ingredients, (a) Indian Forskolin. The principal mode of action is elevating intracellular assembly of cyclic adenosine monophosphate (cAMP) and its associated functions by activating the enzyme adenylate cyclase [27]. High assembly of cAMP results in the activation of protein kinase enzyme. Ultimately, active protein kinase (PKA) enzyme stimulates another enzyme known as the hormone sensitive lipase, resulting in the disintegration of triglycerides (TG - the building block of adipose tissue) - causing fat burn in the subcutis [27][28]. (b) Caffeine. This also elevates cellular level of cAMP through the inhibition of the enzyme phosphodiesterase (which degrades intracellular cAMP) in the subcutis and skeletal muscles, in turn activating hormone sensitive lipase resulting in lipolysis [29][30].

The study was carried out over a period of 4 months, during which the participants were asked not to apply any other moisturizer or cellulite reducing products, except for the assigned test creams, to their right posterior lateral thigh (beneath the buttocks). The first measurement was taken at the start of the experiment (where all participants were asked to come bare skin), time zero (t_0) before any intervention was employed. The second measurement was unable to be collected at the end of the

108

experiment, 4 months (t_4) due to COVID-19. In which case, a questionnaire study was performed to assess user perception of products efficacy.

7.2.3. Measurement of Skin Elasticity and Firmness

The Cutometer® dual MPA 580, (Courage - Khazaka electronics, Cologne, Germany) is a dermal elasticity meter that determine the degree of skin firmness and elasticity. It is also used in efficacy testing, providing claim support for a wide range of cosmetic products. The principle of operation of the Cutometer is based on suction, whereby, the device produces a negative pressure and an area of the skin in which the probe is placed is pulled into the small circular opening. As an optical measuring system, it is equipped with a light source, two prisms opposite one another that project the light generated to a receiver. The distance (mm) of skin penetration determines the brightness of the light, allowing the assessment of the following parameters,

- R0 (mm) – The lower the value (<0.5), the firmer the skin and vice versa

  R0 = Uf,   Where R0 is firmness and Uf is the complete elastic curve or the highest point (maximum amplitude) of the curve.

- R2 (%) – The adjacent the value is to 1 or 100% (>0.9 or 90%), the more elastic the skin.

R2 = Ua/Uf,   Where R2 is the gross elasticity, Uf the maximum amplitude and Ua the relaxation distance.

- R5 (%) – The adjacent the value is to 1 or 100% (>0.9 or 90%), the more elastic the skin.

R5 = Ur/Ue,   Where R5 is net elasticity, Ur is the elastic portion of the suction phase and Ue the elastic portion of the relaxation phase.

- R7 (%) – The adjacent the value is to 1 or 100% (>0.9 or 90%), the more elastic the skin.

R7 = Ur/Uf,   Where R7 is the elastic portion, Ur is the elastic portion of the suction phase and Uf is the complete elastic curve.

- R9 (mm) - The adjacent the value is to 0, the firmer the skin (measured in mm).

R9 = R3 – R0,   Where R9 is the fatigue or tiring effect, R3 is the maximum amplitude of the final curve and R0 is the maximum amplitude of the initial curve.

7.2.4. Measurement of Skin Surface Texture Parameters

7.2.4.1. Visioscan

To evaluate skin surface texture (roughness and micro-relief), the Visioscan was used - A black and white high resolution video sensor camera with a UVA light generator, illuminating the skin. The device which uses an arbitrary unit, produces an explicit assessment of the stratum corneum without protruding into the deeper layers of the epidermis based on the following,

- SE_R – The smaller the value (<5.0), the rougher the skin.

$SE_R = 10 \times Linf / [(Fax + Fay)/2]$, Where SE_R is the roughness, Linf is the number of pixels, Fax and Fay is the average number of horizontal and vertical wrinkles, respectively.

- SE_{SM} - The smaller the value, the smoother the skin (<100).

$SE_{SM} = 100/ [(Co - Cu)^x(Fmx + Fmy)]$, Where SE_{SM} is the Smoothness, Co – Cu is the average width of the histogram, Fmx is the average width of wrinkles in x direction and Fmy is the average width of wrinkles in y direction.

- Desquamation, SE_{SC} (%) – The smaller the value, the more the scaling of the stratum corneum (<0.5). It corresponds to skin moisture.
- Wrinkles, SE_W – The higher the value, the more apparent the wrinkles (>70).

$SE_W = (Fmx + Fmy) \times 100/ (Fax + Fay)$, Where Fmx is the average width of wrinkles in x direction, Fmy is the average width of wrinkles in y direction, Fax and Fay is the average number of horizontal and vertical wrinkles, respectively.

7.2.4.2. Visiometer

The Visiometer is more or less like the Visioscan, except that it uses a blue silicone dye to produce skin replicas for surface texture measurements. It is based on the principle of Lambert's and Beer law where, the amount of light absorbed is equivalent to the thickness of replica produced. To assess the skin surface texture, the following parameters (measured in μm) are important,

- Energy – Young, elastic and hydrated skin shows increased energy value (>0.1) than a rough or aged skin.
- Variance – Highly rough skin gives elevated variance values.
- Contrast – A smooth or even skin gives a low contrast value (<0.5) compared to a rough skin.
- Entropy – A smooth or even skin gives low entropy value (<0.5) than rough skin.
- Homogeneity – An elastic and hydrated skin gives an elevated homogeneity value (>2.0).

7.2.5. Photonumeric Assessment of Cellulite Severity

High-definition photographs of the women's thigh area were taken before, t_0 and after treatment, t_5 at the medical photography unit at the SRH. The number of bulging and depressions was inspected and scored by 2 independent health professionals, after which a comparison of pre- and post-photographs for each volunteer was made. The criteria used in scoring cellulite severity were developed and validated by Hexsel Table 7.1, (please see appendix for full details) [31].

Table 7.1. Cellulite Severity Scoring and Classification.

Score	Severity Scale	Classification
0	0	Absent
1	1-5	Mild
2	6-10	Moderate
3	11-15	Severe

7.2.6.   Quantitative Depictive Sensory Evaluation

Quantitative depictive sensory evaluation i.e. Skin Hydration and Viscosity/Opaqueness was performed on the formulated oil-in-water products using a new and originally devised method, without dilution to directly investigate the refractive index, RI, to help provide information on the identity and quality of the test products. All evaluations were carried out at room temperature, 25±1°C and a humidity of 33%.

7.2.7.   Refractive Index

RI is said to increase with increased turbidity and decreased skin hydration and vice-versa [17] [18]. This experiment was done in triplicate and performed at room temperature. In order to eliminate the inaccuracy of the UV spectrophotometer in RI measurement of an extremely turbid sample, we aim to directly investigate the RI (without any dilution), using the Sun Protective Factor – 290 Automated System (SPF-290AS) technique and the below Sellmeier equation showing the relationship between RI and critical wavelength of the sample was applied;

$$n^2 (\lambda) = 1 + (B_1\lambda^2/\lambda^2 – C_1) + (B_2\lambda^2/\lambda^2 – C_2) + (B_3\lambda^2/\lambda^2 – C_3)$$

Where,

n = Refractive Index (RI),

λ = Wavelength of Test Sample Determined by SPF Meter,

And the coefficients of Sellmeier equation for fused silica/silicon substrate are as follows.

$B_1 = 0.696166300$ $C_1 = 4.67914826 \times 10^{-3}$

$B_2 = 0.407942600$ $C_2 = 1.35120631 \times 10^{-2}$

$B_3 = 0.897479400$ $C_3 = 97.9340025$

The RI measurement in this study was used to demonstrate the opaqueness/turbidity of the formulated products and hydration of the skin after product application using the Sun Protective Factor – 290 Automated System (SPF-290AS) technique, to obtain the individual transmittance wavelength of the samples and then calculated using the above equation. Wavelength measurement on the SPF-290 meter was made by initially placing an empty transpore tape (the transpore tape was applied as it imitates the surface of the biological skin) in the optical path to acquire a reference scan. The tape was

111

loaded with the test sample at 2.0μL/cm^2, spread out in a unidirectional motion, allowed to dry for 15mins and returned to the optical path. Six different scans were taken by the monochromator over the wavelength region 380-500nm and an average scan was produced. Then the SPF software factors out the reference scan data resulting in the transmittance of only the measured sample. This experiment was done in triplicate and performed at room temperature.

7.2.8. Skin Hydration

This is a quantitative sensory analysis performed to evaluate the hydration or moisturizing effect of the creams, using the skin hydration meter, Delfin MOISTUREMETERSC COMPACT, producing measurement in percentage (%). Hands were washed with soap and dried, after a 5 minutes wait, the moisture meter was placed on the back of the hand, held in a steady position until a measurement was taken, T0 and the value recorded. A small amount of each product was applied in a circular motion to the same location of the original reading, after another 5 minutes wait, a second measurement was taken, T5. This process was repeated thrice for each formulation.

7.2.9. Statistical Analysis

Statistical evaluation of results obtained for all formulated creams were achieved using the IBM SPSS software. To indicate whether any significant difference ($p < 0.05$) exist in the skin hydration after cream application, a paired sample t-test was used to compare the before and after measurement.

7.3. RESULTS AND DISCUSSION

7.3.1. Participants/Volunteers

On the day of the study, only 7 participants showed up for the study. The characteristics of the 7 healthy female participants from different backgrounds and ethnic groups were summarized in Table 7.2. Their mean age, height, weight and BMI were 32.7 years, 166.9 cm, 76.5 Kg and 27.2 Kg/m², respectively. At the end of the 4 months treatment, the mean weight did not change.

Table 7.2. Participant's Information

Volunteer No	Age	Height (cm)	Weight (Kg)	Body Mass Index (Kg/m²)	Ethnicity	Cream
1	22	167.6	61.0	21.7	White	Active
2	28	173.7	100.0	33.1	Black	Active
3	33	155.4	85.0	35.2	Black	Active
4	31	179.8	112.0	34.6	Black	Control
5	28	160.0	54.0	21.1	Asian	Control
6	30	176.8	65.6	21.0	Black	Best Seller
7	57	155.4	57.9	24.0	White	Best seller

7.3.2. Measurement of Firmness, Elasticity and Skin Topography

The measurement of average skin firmness, elasticity, roughness and smoothness was performed in triplicate (n = 3) for each participant and their individual mean was taken. In Table 7.3, all participants showed good skin firmness (R0 < 0.5), with the exception of volunteer 4 who showed a firmness value of 1.1963. This means the skin has a decreased resistance to mechanical force. Generally, dermal elasticity was observed to be low.

Table 7.3. Pre-Treatment (t_0) Measurement of Mean Firmness, Elasticity, Skin Roughness and Smoothness.
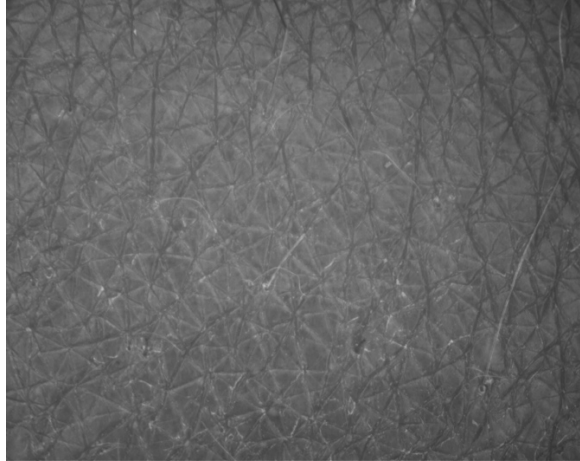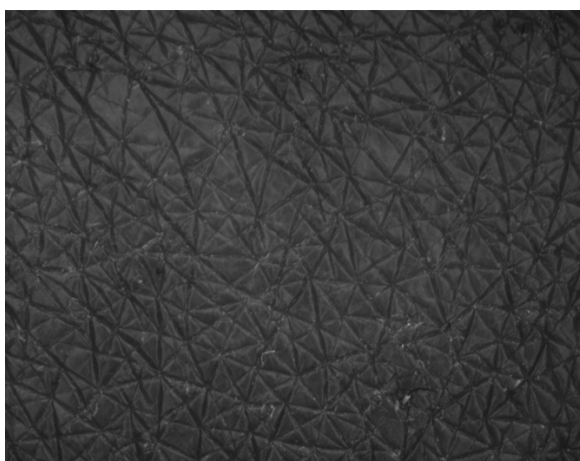
Volunteer No	R0 (mm)	R2	R5	R7	SE_R %	SE_{sm} (%)	SE_{Sc} (%)	SE_W (%)	Cream
1	0.2900	0.9035	0.9191	0.8325	1.8533	143.2267	0.8667	51.5420	Active
2	0.4107	0.8909	0.7644	0.7032	0.1833	82.5400	0.2200	40.2016	Active
3	0.2036	0.9166	0.8212	0.7072	0.7033	70.1067	0.6733	55.9683	Active
4	1.1963	0.6870	0.7333	0.6527	1.7100	116.9300	0.7367	66.6253	Control
5	0.3787	0.8721	0.7155	0.6394	2.8200	329.7833	0.2367	126.0133	Control
6	0.4183	0.9029	0.8239	0.7734	0.8467	107.7633	0.7767	43.8960	Best Seller
7	0.2400	0.8635	0.8447	0.7362	1.5000	161.0600	1.4567	43.9293	Best seller

Table 7.4 below revealed skin energy was observed to be low and the entropy was very high in all individuals, this means a reduction in dermal elasticity, hydration and smoothness. This is also visible in the visioscan images in Figure 7.1, the images also revealed the outer skin (stratum corneum) integrity was more compact in black individuals than in the whites and Asian participants. However, this cannot be scaled up to the entire world population due to the small number of volunteers present in this study.

The post-treatment measurement of dermal firmness, elasticity, roughness and micro-relief is unavailable, as a result of the COVID-19 pandemic.

Table 7.4. Pre-Treatment (t_0) Measurement of Skin Energy, Contrast, Variance and Entropy.

Volunteer No	Energy	Contrast	Variance	Entropy	Cream
1	0.062	0.376	2.103	1.671	Active
2	0.056	0.407	2.250	1.607	Active
3	0.041	0.398	2.175	1.618	Active
4	0.022	0.414	2.132	1.533	Control
5	0.050	0.290	1.670	1.635	Control
6	0.074	0.319	1.867	1.688	Best Seller
7	0.099	0.326	1.886	1.723	Best seller

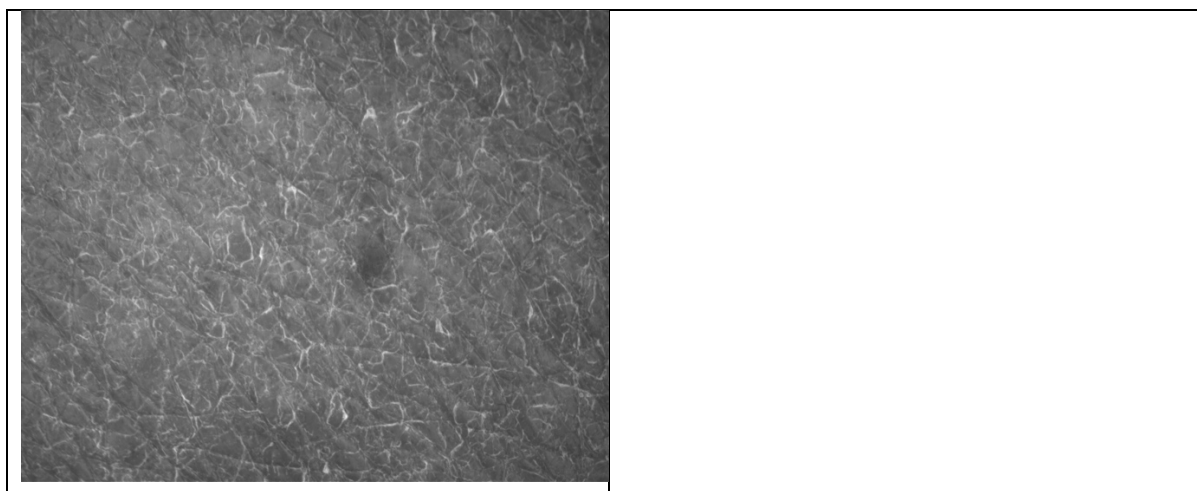| VOLUNTEER 1	VOLUNTEER 2
VOLUNTEER 3	VOLUNTEER 4
VOLUNTEER 5	VOLUNTEER 6
VOLUNTEER 7	

114

Figure 7.1. Pre-Treatment Skin-Visioscan images for all Cream groups. When comparing each photograph, some images appeared to have fewer fine lines than others and visible white residues or patches illustrating dry skin was observed to be higher in whites and Asian than the black participants.

7.3.3. User Perception/Questionnaire Study

According to the participants who used the test creams for 4 months, Table 7.5 shows the active anticellulite cream was more solid-like and hydrating effect (average cream firmness and hydration was 7±0.0 and 8±0.0, respectively) when compared to the control cream (4±2.8 and 7.5±2.1, respectively) and best seller (4.5±0.7 and 7±1.4, respectively). Average transcutaneous absorption or penetration was seen to be slowest in the market available cream.

Table 7.5. Questionnaire Study of Cream Quality Based on Volunteer Perception.

Cream Quality According to Volunteer Perception	Scale		
	Active	Control	Best Seller
On a scale of 0-9, How thick was the cream sample you were assigned? With 0 being more liquid-like or runny, and 9 having a more solid or firmer appearance.	7 7 7	6 2	4 5
On a scale of 0-9, How fast did the cream absorbed into the skin and was no longer visible on the area of application? With 0 being delayed absorption, and 9 having very fast absorption.	7 8 9	8 8	6 6
On a scale of 0-9, How hydrating was your assigned cream to the skin?	8 8 8	9 6	8 6

With 0 having no hydration effect,
and 9 being very hydrating.

Also, the volunteers in the active novel cream group were of the opinion that their right posterior lateral thigh (beneath the buttocks) enhanced in smoothness, hydration and dermal softness and eventually reducing cellulite appearance, at least to an extent. Generally, the volunteers in the market available cream group did not record a similar improvement in skin condition, when compared to the novel active cream or the control group, Table 7.6.

Table 7.6. Questionnaire Study of Cream Quality and Cellulite Improvement Based on the Volunteer's Perception.

Cream Quality and Cellulite Improvement According to Volunteer Perception	Individual Score		
	Active	Control	Best Seller
Do you think your cellulite appearance influences the way you dress?	3 3 2	1 2	1 2
Have you ever purchased any anti-cellulite or skin firming cream?	2 1 2	1 2	2 2
Have you ever purchased any anti-cellulite or skin firming products other than creams?	2 2 2	2 2	2 2
Did you observe any irritable or adverse reaction while using the test product?	2 2 2	2 2	2 2
Did you notice a reduction in cellulite appearance after product application?	3 1 3	3 2	2 2
Did you observe any increase in skin smoothness?	1 1 1	3 1	2 2
Did you observe any increase in skin softness after application?	1 1 1	3 3	3 2
Did you observe any reduction in skin dryness on the test area?	1 1	1 2	1 2

	1		
Did your skin appear firmer after application?	3 1 1	3 2	2 2
Would you choose to use the test product again?	1 3 1	3 1	3 2

<div align="center">Where Score 1 = YES, 2 = NO, and 3 = SOMEWHAT/MAYBE</div>

7.3.4. Refractive Index

A typical full cream milk has an RI of 1.38810 [32]. In order to directly investigate the RI of a test sample, an original means was devised in this study using the Sun Protective Factor – 290 Automated System (SPF-290AS) technique and *Sellmeier* equation showing the relationship between RI and wavelength of the sample was applied.

Table 7.7. The Critical Wavelength of all Models Taken in Triplicate and their Refractive Index Values.

Model	Wavelength 1	Wavelength 2	Wavelength 3	Mean Wavelength(μm)	± STDEV	Wavelength (nm)	RI Value
IA	387.7	387.8	387.8	387.8	0.06	0.3878	2.12377
IB	387.7	387.7	387.8	387.7	0.06	0.3877	2.12378
IIA	385.0	384.9	385.0	385.0	0.06	0.3850	2.12397
IIB	385.1	385.0	385.0	385.0	0.06	0.3850	2.12397
IIIA	385.4	385.4	385.4	385.4	0	0.3854	2.12393
IIIB	385.5	385.6	385.5	385.5	0.06	0.3855	2.12393
IVA	385.9	385.5	385.9	385.8	0.23	0.3858	2.12391
IVB	385.9	385.9	385.9	385.9	0	0.3859	2.12392

In Table 7.7, all cream models were seen to be extremely opaque or turbid with RI values greater than full cream milk, 1.38810. The least turbid was model IA having an RI of 2.12377, proving to have a more hydrating effect to the skin. Model IA was also seen to have a low turbidity and higher hydration compared to model IIA, IIB, IIIA, IIIB, IVA and IVB. Model IIA and IIB showed the highest RI value of 2.12397, indicating model IIA and IIB to be the most turbid and had the least skin hydration compared to model IA, IB, IIIA, IIIB, IVA and IVB. Model IIIA and IIIB showed the second highest RI value of 2.12393, followed by model IVB and IVA with 2.12392 and 2.12391, respectively.

The hydration effect seen in model IA and IB can be attributed to a higher water percentage in its composition i.e. 78.8% compared to model IIA, IIB, IIIA, IIIB, IVA and IVB formulated using 76.7% of water. This effect can also be attributed to the humectant used and its compatibility with jojoba and

baobab oil contained in the cream formulations [33]. The extreme turbid nature of model IIA and IIB could be the effect of propylene glycol used in its preparation in comparison to the glycerine present in model IA, IB, IIIA, IIIB, IVA and IVB.

7.3.5. Skin Hydration

This is a quantitative sensory analysis performed to evaluate the moisturising effect of the creams, using the skin hydration meter, Delfin MOISTUREMETERSC COMPACT, which produces measurement in percentage (%). This process was repeated thrice for each formulation before a product is applied (T_0) and after a product was applied (T_5), their means were determined. Table 7.8 below showed an increase in skin hydration after every application of product and even on bare skin i.e. after skin was washed with soap, dried and allowed to stand for 5 minutes. This means the formulated products were capable of retaining or locking in moisture, enhancing skin hydration even after soap wash. This effect can be attributed to the humectant used and its compatibility with jojoba, baobab and coconut oil contained in the oil in water formulations [33].

Table 7.8. Before (T_0) and After (T_5) Measurement Values of Skin Hydration in Percentage (%).

| Model	1		2		3		Mean	
Interval	Before, T_0	After, T_5	Before, T_0	After, T_5	Before, T_0	After, T_5	Before, $T_0/\pm SD$	After, $T_5/\pm SD$
IA	51.2	59.4	29.6	55.9	59.5	59.8	46.8/±15.4	58.4/±2.1
IB	36.4	52.3	59.8	67.2	51.7	65.3	49.3/±11.9	61.6/±8.1
IIA	58.7	62.4	58.0	67.4	51.5	55.6	56.1/±4.0	61.8/±5.9
IIB	44.5	57.1	67.2	66.8	48.0	58.7	53.2/±12.2	60.9/±5.2
IIIA	67.4	72.0	60.3	68.6	54.9	63.8	60.9/±6.3	68.1/±4.1
IIIB	65.7	65.2	70.5	77.1	62.1	73.0	66.1/±4.2	71.8/±6.0
IVA	58.2	64.7	55.6	60.8	65.9	70.5	59.9/±5.4	65.3/±4.9
IVB	61.0	74.1	66.4	73.9	59.4	66.5	62.3/±3.7	71.5/±4.3
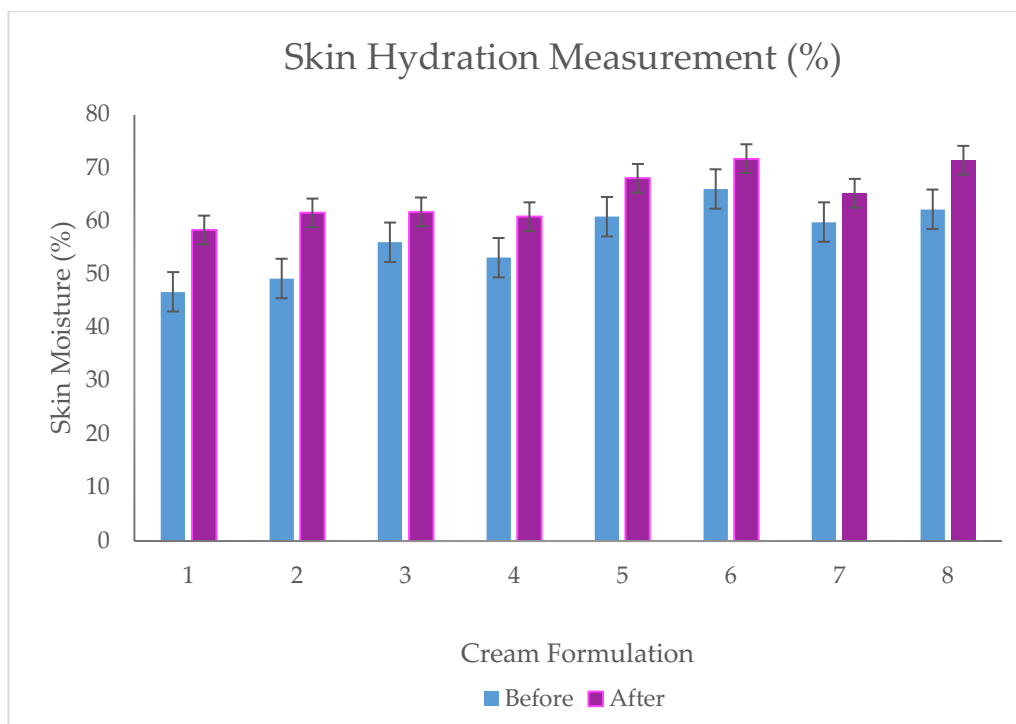
Figure 7.2. Before and After Skin Hydration Measurement of all Cream Formulation.

As seen in Figure 7.2 above model IA and IB showed the highest skin moisture or hydration, which confirms the novel refractive index result using Sun Protective Factor – 290 Automated System (SPF-290AS) technique and *Sellmeier* equation,

The paired sample t-test revealed there was a statistically significant difference, *p value* < 0.001, between the before and after measurement of skin hydration.

7.4. CONCLUSION

Cellulite affects most of the entire female population, it is said to be a multifactorial condition caused by stages of morphological, inflammatory, structural and biochemical changes, making it difficult to abolish [34]. The present study aims to provide alternative quantitative method for sensory evaluation by directly investigating the RI of creams through a newly developed method, without cream dilution. The result showed cream IA and its baseline was the most hydrating compared to other creams. Model IIA and its baseline appeared to be the least hydrating when compared. Another method for determining skin hydration using the moisture meter was also employed, the results confirmed the RI data, indicating cream IA and IB having higher hydrating values, and IIA and IIB showed the least hydrating when compared to other creams. This proved the novel combination technique to be effective in the direct determination of the RI value of an extremely turbid sample.

In vivo efficacy study of the lead active anti-cellulite cream was also assessed, using a qualitative method (user perception of cream efficacy and quality through questionnaire study), in comparison to its baseline and a popular, market available anti-cellulite cream. The best cream in terms of quality and efficacy, as chosen by the volunteers, was the novel active anti-cellulite cream. Presumably, the cream

improved skin elasticity through elastin fibre synthesis and reconstruction, since the appearance of cellulite is said to cause a reduction or breakdown of elastin and collagen network [1][2].

REFERENCE

1. Soares IJ, Cristina doAmaral T, Miranda deAraújo DD, Sales deMelo V, Valentim daSilva RM, Meyer PF. Effects of combined therapy in celullitis: controlled clinical trial, randomized and blind. Manual Therapy, Posturology & Rehabilitation Journal= Revista Manual Therapy. 2016;14.

2. Naves JM, Soares C, Svezzia VD, Cussolim FD, Mendonça AC. Correlation between pelvic alignment and cellulitis. Fisioterapia e Pesquisa. 2017 Mar;24(1):40-5.

3. Purim KS, Titski AC, and Leite N. Dermatological aspects influencing the practice of physical activities by obese individuals. Fisioterapia em Movement. 2015 Dec;28(4):837-50.

4. Costa A, Alves RT, Pegas Pereira ES, Martins Cruz FA, Fidelis MC, Marega Frigerio R, Montagner S, de Medeiros VL. Gynoid Lipodystrophy and clinical therapy: critical analysis of available scientific publications. Surgical & Cosmetic Dermatology. 2012; 4 (1).

5. Diridollou S, Patat F, Gens F, Vaillant L, Black D, Lagarde JM, Gall Y, Berson M. In vivo model of the mechanical properties of the human skin under suction. Skin Research and technology. 2000 Nov;6(4):214-21.

6. Cua AB, Wilhelm KP, Maibach HI. Elastic properties of human skin: relation to age, sex, and anatomical region. Archives of Dermatological Research. 1990 Aug 1;282(5):283-8.

7. Everett JS, Sommers MS. Skin viscoelasticity: physiologic mechanisms, measurement issues, and application to nursing science. Biological research for nursing. 2013 Jul;15(3):338-46.

8. Courage + Khazaka Electronic, Köln - Brochure Cutometer® Dual MPA 580 [Internet]. Courage-khazaka.de. 2020 [cited 21 December 2020]. Available from: https://www.courage-khazaka.de/en/downloads-en/item/prospekt-cuto-dual-e

9. Cosmeticsonline.com.br. 2020 [cited 22 December 2020]. Available from: https://www.cosmeticsonline.com.br/produtos/arquivos/A43_instructions_sv600_fw.pdf

10. Bauer H. Courage + Khazaka Electronic, Köln - Visioscan® VC 20plus (E) [Internet]. Courage-khazaka.de. 2020 [cited 22 December 2020]. Available from: https://www.courage-khazaka.de/en/scientific-products/all-products/imaging/16-wissenschaftliche-produkte/alle-produkte/150-visioscan-e

11. Chang WC, Wu TY. Exploring types and characteristics of product forms. International journal of design. 2007 Mar 30;1(1).

12. Liao SH, Hsieh CL, Huang SP. Mining product maps for new product development. Expert Systems with Applications. 2008 Jan 1;34(1):50-62.

13. Murray JM, Delahunty CM, Baxter IA. Descriptive sensory analysis: past, present and future. Food research international. 2001 Jan 1;34(6):461-71.

14. Adejokun DA, Dodou K. Quantitative Sensory Interpretation of Rheological Parameters of a Cream Formulation. Cosmetics. 2020 Mar;7(1):2.

15. Singh S. Refractive index measurement and its applications. Physica Scripta. 2002;65(2):167.

16. Sand M, Gambichler T, Moussa G, Bechara FG, Sand D, Altmeyer P, Hoffmann K. Evaluation of the epidermal refractive index measured by optical coherence tomography. Skin Research and Technology. 2006 May;12(2):114-8.

17. Chadwick AC, Kentridge RW. The perception of gloss: a review. Vision research. 2015 Apr 1;109:221-35.

18. Ezerskaia A, Ras A, Bloemen P, Pereira SF, Urbach HP, Varghese B. High sensitivity optical measurement of skin gloss. Biomedical optics express. 2017 Sep 1;8(9):3981-92.

19. Calhoun WR, Maeta H, Roy S, Bali LM, Bali S. Sensitive real-time measurement of the refractive index and attenuation coefficient of milk and milk-cream mixtures. Journal of dairy science. 2010 Aug 1;93(8):3497-504.

20. Walstra P. Dairy technology: principles of milk properties and processes. CRC Press; 1999 Apr 23.

21. Marimuthu M, Praveen Kumar B, Mariya Salomi L, Veerapandian M, Balamurugan K. Methylene blue-fortified molybdenum trioxide nanoparticles: harnessing radical scavenging property. ACS applied materials & interfaces. 2018; 10(50):43429-38.

22. Rinnerthaler M, Bischof J, Streubel MK, Trost A, Richter K. Oxidative stress in aging human skin. Biomolecules. 2015; 5(2):545-89.

23. Masaki H. Role of antioxidants in the skin: anti-aging effects. Journal of dermatological science. 2010; 58(2):85-90.

24. Adejokun DA, Dodou K. A Novel Method for the Evaluation of the Long-Term Stability of Cream Formulations Containing Natural Oils. Cosmetics. 2020 Dec;7(4):86.

25. Ishak WM, Katas H, Yuen NP, Abdullah MA, Zulfakar MH. Topical application of omega-3-, omega-6-, and omega-9-rich oil emulsions for cutaneous wound healing in rats. Drug delivery and translational research. 2019 Apr 15;9(2):418-33.

26. Silva JR, Burger B, Kühl C, Candreva T, dos Anjos MB, Rodrigues HG. Wound healing and omega-6 fatty acids: From inflammation to repair. Mediators of inflammation. 2018 Jan 1;2018.

27. Wagh VD, Patil PN, Surana SJ, Wagh KV. Forskolin: upcoming antiglaucoma molecule. Journal of postgraduate medicine. 2012 Jul 1;58(3):199.

28. Ding X, Staudinger JL. Induction of drug metabolism by forskolin: the role of the pregnane X receptor and the protein kinase a signal transduction pathway. Journal of Pharmacology and Experimental Therapeutics. 2005 Feb 1;312(2):849-56.

29. Dulloo AG, Seydoux J, Girardier L, Chantre P, Vandermander J. Green tea and thermogenesis: interactions between catechin-polyphenols, caffeine and sympathetic activity. International journal of obesity. 2000 Feb;24(2):252.

30. Dulloo AG, Duret C, Rohrer D, Girardier L, Mensi N, Fathi M, Chantre P, Vandermander J. Efficacy of a green tea extract rich in catechin polyphenols and caffeine in increasing 24-h energy expenditure and fat oxidation in humans–. The American journal of clinical nutrition. 1999 Dec 1;70(6):1040-5.

31. Hexsel DM, Dal'Forno T, Hexsel CL. A validated photonumeric cellulite severity scale. Journal of the European Academy of Dermatology and Venereology. 2009 May 1;23(5):523-8.

32. Calhoun WR, Maeta H, Roy S, Bali LM, Bali S. Sensitive real-time measurement of the refractive index and attenuation coefficient of milk and milk-cream mixtures. Journal of dairy science. 2010 Aug 1;93(8):3497-504.

33. Sagiv AE, Dikstein S, Ingber A. The efficiency of humectants as skin moisturizers in the presence of oil. Skin Research and Technology. 2001 Feb;7(1):32-5.

34. Schonvvetter B, Soares JL, Bagatin E. Longitudinal evaluation of manual lymphatic drainage for the treatment of gynoid lipodystrophy. Anais brasileiros de dermatologia. 2014 Oct;89(5):712-8.

CHAPTER 8

CONCLUSION AND FUTURE WORK

8.1. CONCLUSION

In this study, we investigated the best intervention for cellulite (dry brushing, exercise and cream) based on efficacy studies involving 9 adult female volunteers, encapsulation of the new active ingredient into niosome vesicles using the thin-film hydration technique, and characterisation studies such as microscopic examination, size and zeta measurement, separation and entrapment efficiency studies, determined the lead niosomal formulation and incorporated the vesicles into the cream base. Designed a novel oil in water cream formulation and investigated the safety and quality. The criteria for progression were based on short- to long-term stability and resistance to microbial contamination (safety evaluation), flow behavior and sensory profile or attributes (quality evaluation). Lastly, an efficacy study involving 12 adult female volunteers was performed using subject perception, the cutometer, visioscan and the visiometer to evaluate changes in skin topography after cream application.

The preliminary study investigates the best method of eliminating cellulite in a group of female volunteers for a period of 5 weeks. The elasticity data from this study proved dry brushing to be the best treatment for cellulite among the 3 interventions evaluated presumably improved skin elasticity through elastin fibre synthesis and reconstruction, since the appearance of cellulite is said to cause a reduction or breakdown of elastin and collagen integrity. All 3 interventions brought about skin firmness, although exercise proved to be the best among the three treatments for skin firmness. The post-treatment photographs of the thigh area presented decreased number of visible bulging and depressions on the surface in all groups, with dry brushing proving to be the best anti-cellulite treatment (Figure 2.5). Although exercise significantly reduced body fat (as it demonstrated the highest total percentage improvement in body fat by 5.5% among the 3 interventions), it does not effectively improve cellulite. The body fat measurement proved that the action of Indian forskolin and caffeine to burn fat was very low, however, improved cellulite appearance. The development of a novel formulation that would help transport these actives through the tough barrier of the stratum corneum, delivered to the targeted site, would lead to a better management of cellulite.

The niosomal formulation study revealed model A had visible levels of aggregation and model E had slight irregularities when observed under the microscope. Model B, C, D and E proved to have a monodisperse or more uniform niosomal dispersion size compared to model A. Model C and D showed stability against the formation of aggregates, rapid coagulation or flocculation, showing very low toxicity due to their strongly anionic nature. Model A, B and E had neutral zeta values of -4.94, -3.53 and -3.64, respectively, indicating electrostatic instability. Therefore, the lead active niosomal formulations (model C and D) were incorporated into the cream base in 4 equal parts (5 mL). The cream was formulated as follows; model I (1:1 of jojoba and baobab oil) contained a water phase of 80%, oil phase (10%), emulsifier (5%) and active (5%) while the remaining three had an equal % composition of

water phase (78%), oil phase (12%), emulsifier (5%) and active (5%), labelled II (1:1 of jojoba and baobab oil), III (1:1 of jojoba and coconut oil) and IV (1:1 of baobab and coconut oil), then stored in separate jars. Characterization studies using both pre-existing and novel methods for the determination of short- to long-term stability for safety and quality assessment. Also, qualitative sensory analysis was performed using a novel technique involving rheological parameters. These information are openly available online at;

https://www.mdpi.com/2079-9284/7/1/2/htm

https://www.mdpi.com/2079-9284/7/4/86/htm

Alternative quantitative method for skin hydration and turbidity determination was successfully performed by direct investigation of the RI of the 8 cream models through a newly developed method, without cream dilution. Finally, *In vivo* efficacy study of the lead active anti-cellulite cream (model IA) was also assessed, using a qualitative method (user perception of cream efficacy and quality through questionnaire study), in comparison to its baseline (model IB) and a popular, market available anti-cellulite cream - providing the following claims "2-IN-1 BODY MOISTURISER + TONING CREAM" formulated with green coffee and Indian forskolin to inhibit lipogenesis and promote lipolysis. The lead active anti-cellulite cream is said to demonstrate antioxidant and free radical scavenging activities by targeting cellular mitochondrial, therefore promoting elastin fiber and collagen network repair, improving skin biomechanical strength and skin surface topography. The best cream in terms of quality and efficacy, as chosen by the volunteers, was the novel active anti-cellulite cream. The users believed the cream was capable of improving skin elasticity through elastin fibre synthesis and reconstruction, since the appearance of cellulite is said to cause a reduction or breakdown of elastin and collagen network, therefore supporting the active claim.

8.2. FUTURE WORK

Future work directions could involve the investigation into the pathophysiology of cellulite using biochemical techniques to better understand the condition. Also, more efficacy study of the active should be performed using a larger population size i.e. 50 or 100 healthy female volunteers, skin viscoelastic properties and surface topography measurement, fatty tissue quantification using an ultrasound system to observe changes in body fat. Furthermore, a follow up study on the same female volunteers should be carried out to observe if the skin condition remained the same or worsened after the product was discontinued.

Scoring form for cellulite severity

Name/Number of volunteer: _____

Before or After intervention? _____

Photonumeric Cellulite Severity Scale

	Score (0 - 3)
A	
B	
C	
D	
E	
Total	

Grade of Cellulite (0 – III)

_____

Name of assessor:_____

Where; A = "No of evident depressions", B = "Depth of depressions", C = "Morphological appearance of skin surface alterations", D = "Grade of laxity, flaccidity or sagging skin", and E = "Classification scale by NÜRNBERGER and MÜLLER"

Appendix B

Appendix C

Appendix D

Calculations

- **Amount of each excipients (mg) required for the preparation of 300µmol of niosomal vesicles.**

  (a) Required amount of 45% of cholesterol in mg

   (45/100) x 300 = 135µmol

   Converting to M, divide by 1,000,000

   135/1000000 = 0.000135M

   Multiply by the molecular weight of cholesterol

   0.000135 x 387g/mol = 0.052245g

Therefore, amount of cholesterol to be measured for the manufacture of 300µmol of niosomal vesicles is 0.05g

  (b) Required amount of 10 % of solutol HS-15 in mg

   (10/100) x 300 = 30µmol

   Converting to M, divide by 1,000,000

   30/1000000 = 0.00003M

   Multiply by the molecular weight of solutol HS-15

   0.00003 x 1069g/mol = 0.03207g

Therefore, amount of solutol HS-15 to be measured for the manufacture of 300µmol of niosomal vesicles is 0.03g

  (c) Required amount of 45% of span 65 in mg

   (45/100) x 300 = 135µmol

   Converting to M, divide by 1,000,000

   135/1000000 = 0.000135M

   Multiply by the molecular weight of span 65

   0.000135 x 964g/mol = 0.13014g

Therefore, amount of span 65 to be measured for the manufacture of 300µmol of niosomal vesicles is 0.130g

- **Dilution concentration calculation**

Stock Solution – A 1000X dilution of methylene blue was made to enable absorbance reading at various concentrations.

Amount of active (g) = Amount of solvent/No of dilution times

Amount of active = 10/1000 = 0.01g

0.01g of the entrapped active was added to 10mL of trizma buffer pH 7.4 and isopropanol (1:1 mixture i.e. 5mL of triz and 5mL of IPA).

<div align="center">

Same as 10mg of active in 10mL of solvent

Or 10000µg of active in 10mL of solvent,

10000µg/10mL = 1000µg/mL

</div>

Therefore, the prepared stock solution of 1000µg/mL was used to make up the following calibration standards;

(a) For 0.100µg/mL, 10µL (0.01mL) of stock solution was added to 100mL of trizma buffer pH 7.4 and isopropanol (1:1 mixture i.e. 50mL of triz and 50mL of IPA).

(b) 0.250µg/mL, 25µL (0.025mL) of stock solution was added to 100mL of trizma buffer pH 7.4 and isopropanol.

(c) 0.375µg/mL, 37.5µL (0.0375mL) of stock solution was added to 100mL of trizma buffer pH 7.4 and isopropanol.

(d) 0.500µg/mL, 50µL (0.050mL) of stock solution was added to 100mL of trizma buffer pH 7.4 and isopropanol.

(e) 0.750µg/mL, 75µL (0.075mL) of stock solution was added to 100mL of trizma buffer pH 7.4 and isopropanol.

(f) 1.000µg/mL, 100µL (0.1mL) of stock solution was added to 100mL of trizma buffer pH 7.4 and isopropanol. Another way to do this is to add 1mL of stock solution in 1L of 1:1 mixture of trizma buffer pH 7.4 and isopropanol. Or 0.5mL of stock solution in 500mL of 1:1 mixture of trizma buffer pH 7.4 and isopropanol. However, the best dilution is 100µL (0.1mL) of stock solution was added to 100mL of trizma buffer pH 7.4 and isopropanol as this helps minimize waste.

(g) 1.250µg/mL, 125µL (0.125mL) of stock solution was added to 100mL of trizma buffer pH 7.4 and isopropanol.

(h) 1.500µg/mL, 150µL (0.150mL) of stock solution was added to 100mL of trizma buffer pH 7.4 and isopropanol.

(i) 1.750µg/mL, 175µL (0.175mL) of stock solution was added to 100mL of trizma buffer pH 7.4 and isopropanol.

Appendix E

Deborah Adejokun
School of Pharmacy and Pharmaceutical Sciences

Dear Deborah

PROJECT TITLE: Design of a Novel Anti-Cellulite Treatment - An Evidence Based Approach
APPLICATION: Reference Number 006180

On behalf of the University ethics reviewers who reviewed your project, I am pleased to inform you that on 20/02/2020 the above-named project was **approved** on ethics grounds, on the basis that you will adhere to the following documentation that you submitted for ethics review:

- University research ethics application form 006180 (form submission date: 18/02/2020); (expected project end date: 27/03/2020).
- Participant information sheet 1011402 version 2 (18/02/2020).
- Participant consent form 1011403 version 3 (18/02/2020).

The following optional amendments were suggested:

Add a clause about retroactive withdrawal (even if it is not possible) to PI Sheet and Consent Form Say on PI Sheet when data will be destroyed

If during the course of the project you need to deviate significantly from the above-approved documentation please email ethics.review@sunderland.ac.uk

For more information please visit: https://www.sunderland.ac.uk/research/governance/researchethics/

Yours sincerely

Veronique Laniel
Ethics Administrator
University of Sunderland

Appendix F

CONSENT FORM

Study Title: *In Vivo* Efficacy Studies of Novel Anti-cellulite Cream on Healthy Participants

	Please initial box	
I confirm that I am over the age of 16 years.	□	
I have read and understood the information sheet for the above study and have had the opportunity to ask questions.	□	
I understand that my participation is voluntary and that I am free to withdraw at any time, without giving reason.	□	
I agree to take part in the above study.	□	
	Yes	No
I agree to the use of anonymised quotes in publications.	□	□
I agree that my data gathered in this study may be shared (after it has been anonymised) with other researchers.	□	□
I agree that my data gathered in this study may be shared (after it has been anonymised) may be used for teaching purposes.	□	□

Name of Participant	Date	Signature
Deborah Adefunke Adejokun	18/02/2020	DEBORAH ADEJOKUN
Name of Researcher	Date	Signature

Retroactive Withdrawal

As stated in the participant information sheet, if you wish to withdraw or discontinue your involvement in this study, before data analysis, all data pertaining to you will be deleted from our system as soon as we've been notified. However, in the case of withdrawal after the data analysis stage, your information will still be retained and used for the purpose of research, after it has been anonymised.

Consent Form 3.0. 20 February, 2020

Appendix G

University of Sunderland

PARTICIPANT INFORMATION SHEET

You are being invited to take part in a research study. Before you decide whether or not to take part, it is important for you to understand why the research is being done and what it will involve. Please take time to read the following information carefully.

Study Title:
In Vivo Efficacy Studies of Novel Anti-cellulite Cream on Healthy Participants

What is the purpose of the study?

Background

Cellulite affects 80-90% of the total female population worldwide, from puberty onset and increases during menstruation, pregnancy, and nursing. It is believed to be a multifactorial condition, although not entirely understood, causes fatty tissue, elastin and collagen network breakdown. In some cases, cellulite can progress into a more severe form and may result in oedema, and eventually fibrosis. It also causes feelings of insecurities and low self-esteem due to its unattractive nature, reducing the quality of life of patients. Although numerous medical devices and cosmetic products targeted at treating cellulite are on the market today, however, they seem to provide little to no clinical evidence to support their claims and none has been seen to produce a long-term effect or effectively manage the condition.

Objective

To assess the *in vivo* efficacy of the novel anti-cellulite cream on 12 healthy female (adult) participants.

This study is conducted as part of the student research, Deborah Adefunke Adejokun of the PhD programme in Pharmacy Health and Wellbeing at the University of Sunderland.

Why have I been approached?

The current research is based on a newly prepared, all natural, anti-cellulite cream product. To be eligible for this user-trial, you need to have met the following criteria;

- **Adult female** between the ages of 18 and 60
- Healthy **without** a history of disease(s) or skin condition(s)
- **Have** existing cellulite (to some degree)
- **Not** involved in a similar trial and,
- **Not** using other cellulite reducing interventions

Thus, you have been selected to take part in this study because you, along with 11 others have met the above criteria.

Also, if you are already taking part in a different consumer-trial, please be sure to inform a member of the research team to avoid any inconveniencies or undesired effects.

Do I have to take part?

Your involvement in this project is completely voluntary so, please take time to read and digest this participant information sheet before you decide whether or not to accept the invitation to participate. An informed consent form will be attached to this document, where your signature on this form will indicate your agreement to voluntarily participate in this trial.

What will happen if I don't want to carry on with the study?

Participation is entirely voluntary so, if you change your mind about taking part in the study, **you can withdraw at any point in time up until data analysis without giving a reason and without penalty**.

In the case of withdrawal, all data collected before the analysis stage will be immediately destroyed.

Retroactive Withdrawal

As stated above, if you wish to withdraw or discontinue your involvement in this study, before data analysis, all data pertaining to you will be deleted from our system as soon as we've been notified. However, in the case of withdrawal after the data analysis stage, your information will still be retained and used for the purpose of research, after it has been anonymised.

What will happen to me if I take part?

The research in question will involve the use of a natural newly formulated cosmetic cream on the thighs of 12 healthy female participants, at T_0 (before skin application) and T_4 (after 4 months of skin application), to assess the efficacy or ability of the cream to bring about the reduction of cellulite appearance. Participants will be divided into 3 groups, the first group will be given the novel product, second will be given the novel cream without the active ingredient (a baseline) and the third group is a popular anti cellulite cream obtained from boots. Efficacy studies would be carried out using the Cutometer, Skin Visioscan and Visiometer, to measure skin surface area both directly and indirectly (using a blue silica dye to produce replica of the skin test area), respectively. Also, a photonumeric assessment of cellulite severity, involving high-definition photographs of participants thighs taken at T0 and T4 will be performed to count the number of skin bulging and depression. All testing methods are completely safe and non-invasive, causing no harm or whatsoever to the participants or researcher.

At the end of the study, you will receive a £20 reimbursement for feeding and travel expenses.

What are the possible disadvantages and risks of taking part?

A COSHH risk assessment has been carried out to evaluate the safety of ingredients contained in the product and the cream was seen to pose no potential threat to users. However, if a reaction or an irritation occurs, the user is advised to immediately rinse the product off with cold water and to discontinue use. Furthermore, the product should not be applied in the eyes, mouth, to opened or broken skin, if this occurs, please rinse off under cold running water.

What are the possible benefits of taking part?

Reduction in cellulite appearance on the measured skin area.

What if something goes wrong?

If you change your mind or are unhappy with the conduct of this study, please contact myself, Deborah Adejokun, or my supervisor Dr Kalliopi Dodou, or the Chair of the University of Sunderland Research Ethics Group, Dr John Fulton. Contact details listed below.

How will my information be kept confidential?

All participant information (data) will be treated in accordance with the terms of the Data Protection Act (2018).

The use of participants names would be eliminated from the experiment, personal data would be stored as Participant 1 to 12 consecutively so, participants will remain completely anonymous. Data obtained would be collected one after the other to prevent a participant gaining access to another participant's data. The computer used in data analysis of the cutometer, visioscan, visiometer and photonumeric studies would be password protected and only accessible by the researcher.

What will happen to the results of this study?

If possible, the results may also be presented at academic conferences and/or written up for publication in peer reviewed academic journals. All personal information will however be preserved with great confidentiality as a participant code will be allocated at the start of the study and used wherever appropriate as far as the study is concerned.

Who is organising and funding the research?

The research is organised by Deborah Adejokun who is a research student at the University of Sunderland, Faculty of Pharmacy Health and Wellbeing, School of Pharmacy and Pharmaceutical Sciences.

The project is not externally funded.

Who has reviewed the study?

The study has been reviewed and approved by the University of Sunderland Research Ethics Group. Please see details below

Contact Details

Deborah Adejokun (Research Student)

Email: bg69bo@research.sunderland.ac.uk

Phone: 07448517611

Dr Kalliopi Dodou (Supervisor of Study)

Email: Kalliopi.dodou@sunderland.ac.uk

Phone: +44(0)191-515-2503

Dr John Fulton (Chair of the University of Sunderland Research Ethics Group)
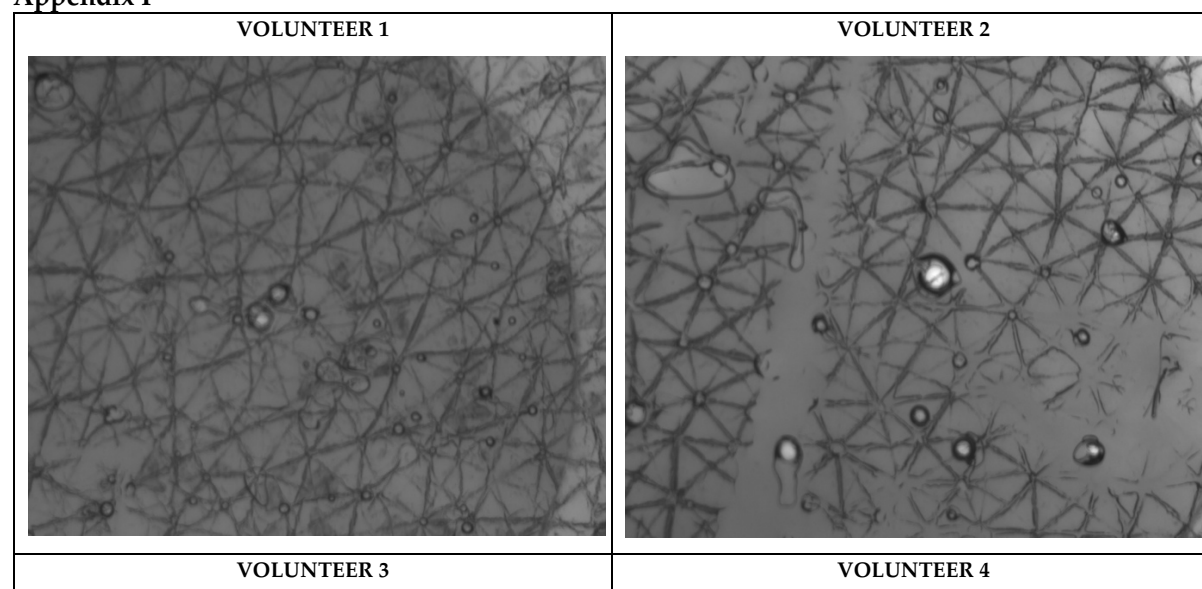
Email: john.fulton@sunderland.ac.uk
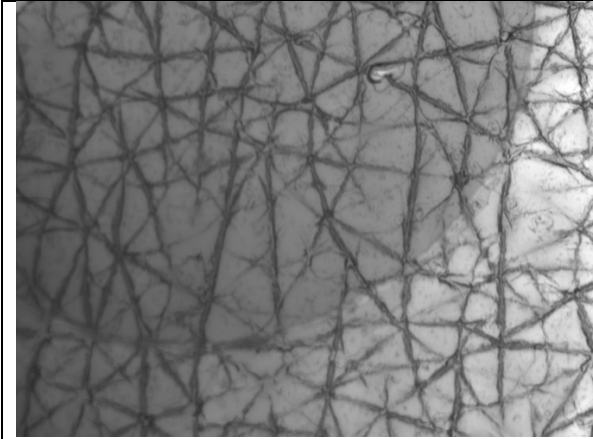
Phone: 0191 515 2529

Appendix H

Pre-Treatment Measurement for Firmness, Elasticity, Skin Roughness and Smoothness.

Volunteer No	R0	R2	R5	R7	SE_R %	SE_{sm} %	SE_{Sc} %	SE_w %	Cream
1	0.3150	0.8476	0.9029	0.7968	1.92	123.97	0.85	59.601	Active
	0.2760	0.9275	0.9209	0.8442	1.33	159.21	0.76	43.130	
	0.2790	0.9355	0.9336	0.8566	2.31	146.50	0.99	51.895	
2	0.4170	0.8849	0.7579	0.6906	0.42	80.27	0.17	46.944	Active
	0.3970	0.9169	0.7688	0.7204	0.08	80.28	0.23	37.338	
	0.4180	0.8708	0.7664	0.6986	0.05	87.07	0.26	36.323	
3	0.2070	0.9179	0.8182	0.6957	0.55	67.08	0.61	56.415	Active
	0.2070	0.9130	0.8258	0.7101	0.85	63.11	0.72	51.310	
	0.1970	0.9188	0.8198	0.7157	0.71	80.13	0.69	60.180	
4	1.1970	0.7382	0.6640	0.6066	1.84	109.19	0.66	55.481	Control
	1.4367	0.6722	0.7728	0.6344	1.30	114.88	0.75	70.890	
	0.9551	0.6505	0.7631	0.7171	1.99	126.72	0.80	73.505	
5	0.4120	0.8204	0.7179	0.6117	3.07	317.23	0.00	111.62	Control
	0.3700	0.8892	0.7224	0.6541	2.38	342.79	0.44	147.44	
	0.3540	0.9068	0.7064	0.6525	3.01	329.33	0.27	118.98	
6	0.4570	0.8490	0.8005	0.7287	0.60	94.28	0.61	39.269	Best Seller
	0.4050	0.9210	0.8312	0.7901	1.09	110.56	0.92	38.309	
	0.3930	0.9389	0.8400	0.8015	0.85	118.45	0.80	54.110	
7	0.2370	0.8469	0.8469	0.7468	1.25	144.74	1.53	45.948	Best seller
	0.2240	0.9018	0.8241	0.7321	1.36	171.21	1.86	46.336	
	0.2590	0.8417	0.8630	0.7297	1.89	167.23	0.98	39.504	

Appendix I

VOLUNTEER 1	VOLUNTEER 2
VOLUNTEER 3	**VOLUNTEER 4**

VOLUNTEER 5	VOLUNTEER 6

VOLUNTEER 7